RELATIONSHIP BETWEEN SUCTION AND SHEAR STRENGTH PARAMETERS OF COMPACTED METU CAMPUS CLAY

A THESIS SUBMITTED TO
THE GRADUATE SCHOOL OF NATURAL AND APPLIED SCIENCES OF
THE MIDDLE EAST TECHNICAL UNIVERSITY

BY

HÜSEYİN PARS TİLGEN

IN PARTIAL FULLFILLMENT OF THE REQUIREMENTS FOR THE
DEGREE OF
MASTER OF SCIENCE
IN
THE DEPARTMENT OF CIVIL ENGINEERING

SEPTEMBER 2003

Approval of Graduate School of Natuaral and Approved Sciences

Prof. Dr. Canan ÖZGEN
Director

I certify that this thesis satisfies all the requirements as a thesis for the degree of Master of Science.

Prof. Dr. Mustafa TOKYAY
Head of Department

This is to certify that we have read this thesis and in our opinion it is full adequate, in scope and in quality, as a thesis for the degree of Master of Science.

Prof. Dr. Erdal ÇOKÇA
Supervisor

Examining Committee Members

Prof. Dr. A. Orhan EROL

Prof. Dr. Erdal ÇOKÇA

Assit. Prof. Dr. K. Önder ÇETİN

Dr. Mutlu AKDOĞAN

Dr. Oğuz ÇALIŞAN

ABSTRACT

RELATIONSHIP BETWEEN SUCTION AND SHEAR STRENGTH

PARAMETERS OF COMPACTED METU CAMPUS CLAY

Tilgen, Hüseyin Pars

M.S., Department of Civil Engineering

Supervisor: Prof. Dr. Erdal ÇOKÇA

September 2003, 120 pages

In this study, the relationship between soil suction and shear strength parameters of compacted METU campus clay were investigated at different moisture contents. Soil samples were tested at optimum moisture content (i.e. w=20.8%), at dry side of optimum moisture content (i.e. w=14.8%, 16.8%, 18.8%) and at wet side of optimum moisture content (i.e. w=22.8%, 24.8%, 26.8%). Direct shear tests were performed to measure shear strength parameters (c', Φ') and soil suctions were measured by filter paper method after direct shear tests. These relationships were also investigated on soaked samples. The trends for suction, angle of internal friction and cohesion, which change on the dry side and wet side of optimum moisture content, were analyzed. The compacted METU campus clay gains granular soil fabric at the dry side of optimum moisture content. As moisture content increases, cohesion increases up to optimum moisture content and then decreases. But angle of internal friction decreases as moisture content increases. Soaking affects the samples more which are

on the dry side of optimum moisture content. The soil suction (total suction and matric suction) affects the shear strength, and an increase in soil suction increases the shear strength.

Keywords: Clay, compaction, expansive soil, filter paper, moisture content, shear strength, suction, standard proctor energy.

ÖZ

SIKIŞTIRILMIŞ ODTÜ KAMPUS KİLİNDE EMME BASINCI İLE KAYMA DAYANIMI PARAMETRELERİ ARASINDAKİ BAĞINTI

Tilgen, Hüseyin Pars
Yüksek Lisans, İnşaat Mühendisliği Bölümü
Tez Yöneticisi: Prof. Dr. Erdal ÇOKÇA

Eylül 2003, 120 sayfa

Bu çalışmada çeşitli su muhtevalarında sıkıştırılmış ODTÜ kampus kili numunelerinin emme basıncı ile direkt kayma dayanımı parametreleri arasındaki ilişki araştırılmıştır. Numuneler optimum su muhtevasında (w=%20.8), optimum su muhtevasının kuru tarafında (w=%14.8, %16.8, %18.8) ve optimum su muhtevasının yaş tarafında (w=%22.8, %24.8, %26.8) test edilmiştir. Kayma dayanımı parametreleri (c', Φ') direkt kesme deneyleri yapılarak elde edilmiş ve emme basınçları filtre kağıdı yöntemiyle kesme deneylerinden sonra ölçülmüştür. Ayrıca bu ilişki suya boğulmuş numuneler üzerinde de araştırılmıştır.Emme basıncı, içsel sürtünme açısı ve kohezyon optimum su muhtevasının kuru ve yaş kısmında ayrı ayrı analiz edilmiştir. Sıkıştırılmış ODTÜ kampus kili optimum su muhtevasının kuru tarafında granuler bir yapı kazanmaktadır. Su muhtevası arttıkça

kohezyon optimum su muhtevası seviyesine kadar artmakta ardından azalmaktadır. Fakat su muhtevası arttıkça içsel sürtünme açısı azalmaktadır. Numuneleri suya boğma optimum su muhtevasının kuru tarafındaki numuneleri daha çok etkilemektedir. Zeminin emme basıncı (toplam basınç ve matrik basınç) kayma mukavemetini etkilemektedir, emme basıncı arttıkça kayma mukavemeti artmaktadır.

Anahtar Kelimeler: Kil, sıkıştırma, şişen zemin, filtre kağıdı, su muhtevası, kayma dayanımı, emme basıncı, standart proktor enerjisi.

To my family

ACKNOWLEDGEMENTS

I express sincere appreciation to Prof. Dr. Erdal ÇOKCA for his guidance throughout the research and preparation of the thesis. I would like to thank him for his helpful comments, suggestions and giving me chance to work together. Also I would like to thank M.E.T.U. soil mechanics laboratory staff Mr. Ali Bal, Mr. Mehmet Ekinci and Chemical Engineering laboratory staff Mr. Turgut Aksakal for their valuable helps during testing period. I gladly acknowledge my father, mother and sister for their endless support. Finally, I wish to gratefully acknowledge my friends, Gülşah Yeşilbaş and Burak Sapaz for believing me starting from the first step.

TABLE OF CONTENTS

LIST OF FIGURES

FIGURE

LIST OF TABLES

TABLE

CHAPTER 1

INTRODUCTION

Compacted soils are the part of many earth structures. Therefore their shear strength parameters (cohesion and angle of internal friction) are very important in geotechnical problems like, bearing capacity, slope stability, lateral earth pressures. To determine these parameters usually laboratory samples are tested which have the same moisture content and dry density with the fill.

The fill can be wetted, the source wetting is primarily by rainfall. Rising groundwater may be a source of wetting. In addition, broken utility lines, utilty trenches, street subgrades, permeable layers, gravel packed subdrains, all acts as subsurface conduits that lead water to fill (Croney et al., 1958).

Fredlund (1997) states the following shear strength problems about the unsaturated compacted soils:

1. The stability of loosely compacted fills can result in high velocity mass movements upon approaching saturation.
2. The backfill material for an earth retaining structure should be a cohesionless material. However, many retaining structures are backfilled with cohesive materials which change shear strength in response to the intake of water. The lateral pressures against the wall are a function of the shear strength of the unsaturated soil and extent of wetting.

3. The bearing capacity of shallow footings on compacted fills is commonly based on the compressive strength of the unsaturated soil. The strength measurements are often performed on soil specimens which has negative pore water pressures. The assumption is then made for design purposes that conditions in the future will remain similar. This may not be a realistic assumption.

In this study, suction and shear strength parameters of an unsaturated compacted METU campus clay were measured. The soil suction was measured by filter paper method and direct shear testing method was used to measure shear strength parameters. Additional direct shear tests were performed where the compacted samples were soaked and consolidated prior to shearing. The relationships between moisture content, suction and shear strength parameters were found.

CHAPTER 2

LITERATURE REVIEW

2.1 The Strength of Compacted Clays

Many researchers such as Rosenqvist (1959), Escario and Sáez (1986), Alonso et al. (1990), Fredlund and Rahardjo (1993), Wheeler and Sivakumar (1995), Leroueil and Barbosa (2000), Kong and Tan (2000), Kos et al. (2000) have studied the shear strength of unsaturated compacted soils.

The mechanical or physical component of shear strength is attributable primarily to the granular particles and, for a soil of a given composition, the magnitude of this component is essentially dependent on the effective normal pressure between particles (Rosenquist, 1959), and cohesion is taken to mean that part of the soil strength that is present independently of any applied pressures (i.e. the shear strength, τ - intercept of the failure envelope). Fredlund and Rahardjo (1993) states that the suction influences the shear strength of unsaturated compacted specimens.

There are certain limits of the water content for each compaction pressure within which the shear strength is maximal. The optimum water content decrease with the increasing compaction (consolidation) pressure. This is the result of two influences on the global effect of pore water suction: the force of adhesion between two soil particles and the relative amount of soil particles connected by capillary (contact) water. The first influence decreases with the increasing particle diameter, water content and water temperature. The second influence increases with the increasing water content (saturation ratio) and soil density. The increasing water content negatively influences the force of adhesion, but positively the total number of connected particles. It means that, as a compromise, there is an optimum water content (Kos et al. 2000).

2.2 The Influence of Fabric on the Shear Behavior of Unsaturated Compacted Soils

The interparticle forces, in conjunction with the external forces at the time of formation of the soil and the stress history, are resposible for the structure of a compacted cohesive soil (Seed et al., 1961). Leroueil and Vaughan (1990) states that "the effects of structure are as important in determining engineering bahaviour as are the effets of initial porosity and the stress history".

Much attention has been paid to the understanding of the structure of compacted soils and to the effects of water content changes on the structure. From a fundamental point of view, observations at a microstructural level involving elemental clay platelets and their aggregations are also important, since they should help further understanding of their structural levels (Delage et al. 1996).

Lambe and Whitman (1979) states that for a given compactive effort and dry density, the soil tends to be more flocculated for compaction on the dry side as compared to compaction on the wet side (i.e. on the wet side the soil is more dispersive).

In clays, the water content is important; it controls the ease with which particles and particle groups can be rearranged under the compactive effort (Mitchell, 1993). Increasing the moisture content tends to increase the interparticle repulsions, thereby permitting a more orderly arrangement of the soil particles to be obtained with a given amount of effort.

In general, an element of floculated soil has a higher strength than the same element of soil at the same void ratio put in a dispersed state (Lambe and Whitman, 1979).

Previous studies (Mitchaels , 1959; Daimond, 1970; Brackley, 1973, 1975; Zein, 1985; Delage et al., 1996; Kong and Tan, 2000; Toll, 2000) show the development of an aggregated fabric in materials compacted dry of optimum moisture content. This type of aggregation was not found to exist in the materials compacted on the wet side of optimum moisture content.

Mitchaels (1959) observed a reduction in the cohesion with decreasing moisture content below optimum moisture content (OMC) in unsaturated compacted clays. The lower magnitude of cohesion at dry side of optimum is attributed to the presence of clay aggregates that give rise to a granular character to the soil mass.

Diamond (1970) did manage to show the fundamental differences between the structures of soils compacted wet and dry side of optimum water content. On the dry side he showed the existence of aggregates or packets of platelets adhering to each other with a dimension of about 5 μm; between these aggregates, he found fairly large pores, well-defined in mercury porosimetry, with an average diameter of 0.5 μm. On the wet side, he found a much more compact structure, with no evidence of large pores. It is clear that capillary effects, which are much more on the dry side, favour the formation of aggregates by binding the platelets together.

Brackley (1973, 1975) proposed a model of unsaturated clay fabric in which the clay particles grouped together in 'packets'. The soil within the aggregation or 'packets' is held together by suction, and the packets act as individual particles. The larger effective particle size produces more frictional behavior and hence a higher angle of friction.

Zein (cited in Toll, 2000) showed that although compacted materials are highly aggregated on the dry side of optimum moisture content, aggregation does not exist on the wet side; Zein identified the degree of aggregation of a clayey soil for British Standard (BS) light (Proctor) compaction (2.5 kg rammer falling through 300mm, 62 blows/layer, 3 layers of soils). He noted that at optimum moisture content (and also wet of optimum) there were no aggregations and matrix material dominated. However the degree of aggregation increased as the water content reduced below optimum water content; at moisture contents below 70% of OMC the material was completely aggregated with no matrix material.

The effect of compaction water content (at three points of the Proctor curve, i.e. dry, OMC and wet) on the microstructure of Jossigny silt (the clay fraction is 34%) was studied by Delage et al. (1996); on the dry side: A well-developed granular aggregate structure with large interaggregate pores visible in porosimetry occured, due to high suction, compaction cannot entirely break them down. At optimum water content: A more massive structure with less obvious aggregates occured. The greater density is a result of lower resistance to deformation of the aggregates, which deform and break down more easly, reducing in particular the interaggreagate porosities. On the wet side, due to hydration, the clay volume is much larger and forms a clay paste surrounding the silt grains. Also, suction pressures probably reach null or positive values. Delage et al. (1996) state that "the results obtained on various clays by Ahmed et al. (1974) are similar to the ones of this study, the same conclusion should be valid for clays. In this case, the solid state would correspond to a microstructure composed of clayey aggregates, which behave like rather rigid grains.".

Kong and Tan (2000) have studies the shear strength characteristics of an expansive soil. The correlation between the shear strength parameters and initial water content of unsaturated compacted expansive soil was established. Two of the data points were at dry of optimum (i.e. 26.5%, 28.5%), two of them (i.e. 29.3% and 30.8%) were near OMC (i.e. 30%), five of them were at wet of optimum (i.e. 31.6%, 33.6%, 34.8%. 37.0%, 41.2%). They found that the cohesion reduces with the increase of water content, the friction angle decreases significantly in the range of water contents less than the plastic limit (34.7%), whereas as the water content is more than the plastic limit, the friction angle tends to a constant value.

According to Toll (2000) fabric plays a vital role in determining the engineering behavior of compacted soils. Clayey materials compacted dry of optimum moisture content develop an aggregated or 'packet' fabric. The presence of aggregations causes the soil to behave in a coarser fashion that would be justified by the grading. For soils compacted to degrees of saturation of 90% and over, the material would be expected to be non-aggregated. As the degree of saturation drops, the amount of aggregation increases rapidly and reaches a fully aggregated condition for degrees of saturation below 50%.

CHAPTER 3

UNSATURATED SOIL MECHANICS

The general field of soil mechanics can be subdivided into two portions dealing with saturated soils and dealing with unsaturated soils (Figure 3.1). The differentiation between saturated and unsaturated soils becomes necessary due to basic differences in their nature and engineering behavior. An unsaturated soil has more than two phases. As known from saturated soil mechanics, there are two phases; water and soil. But an unsaturated soil has four phases which are; solids, water, air and air-water interface which is called as contractile skin. And unsaturated soils' pore water pressure is negative relative to the pore-air pressure.

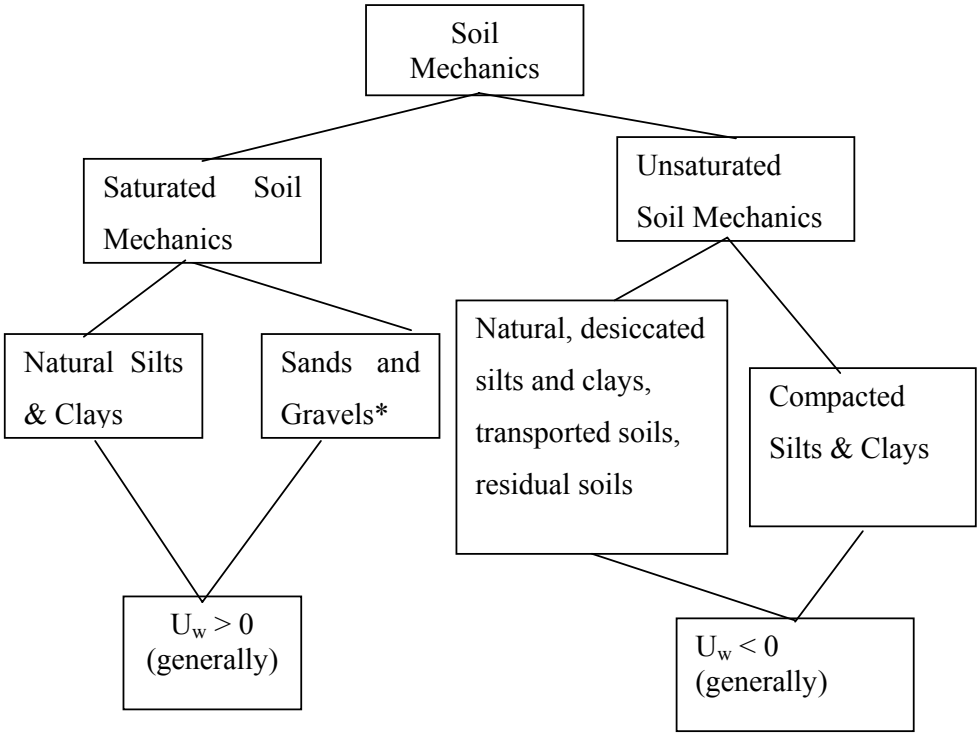

*may be saturated or dry

Figure 3.1 Categorization of soil mechanics (after Fredlund, 1993).

3.1 Types of Problems

The types of problems of interest in unsaturated soil mechanics are similar to those of interest in saturated soil mechanics. Common to all unsaturated soil situations are the negative pressures in the pore-water. These types of problems can be listed as;

- Construction and operation of a dam
- Natural slopes subjected to environmental changes
- Mounding below waste retention ponds
- Stability of vertical or near vertical excavations

- Lateral earth pressures
- Bearing capacity for shallow foundations
- Ground movements involving expansive soils
- Collapsing soils

3.2. Phases of an Unsaturated Soil

Saturated soils have phases of soil solids and water. However, unsaturated soils have soil solids, water, air and the fourth one air-water interface.

3.2.1 Air-Water Interface or Contractile Skin

The most distinctive property of the contractile skin is its ability to exert a tensile pull. It behaves like an elastic membrane under tension interwoven through soil structure.

It is advantageous to recognize an unsaturated soil as a four-phase when performing stress analysis on an element. An unsaturated soil can be visualized as a mixture with two phases that come to equilibrium under applied stress gradients; i.e., soil particles and contractile skin. And two phases that flow under applied stress gradients; i.e., air and water.

Consideration of the contractile skin as a fourth phase is later used in theoretical stress analysis for an unsaturated soil.

3.2.2 Surface Tension

The air-water interface possesses a property called surface tension. The phenomenon of surface tension results from the intermolecular forces acting on molecules in the contractile skin. These forces are different from those that act on molecules in the interior of the water (Figure 3.2.a).

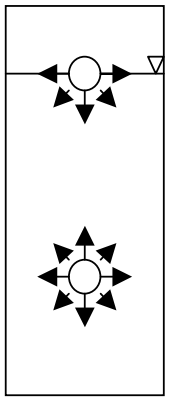

Molecule at the air-water interface.

Molecule in the interiour water.

(a)

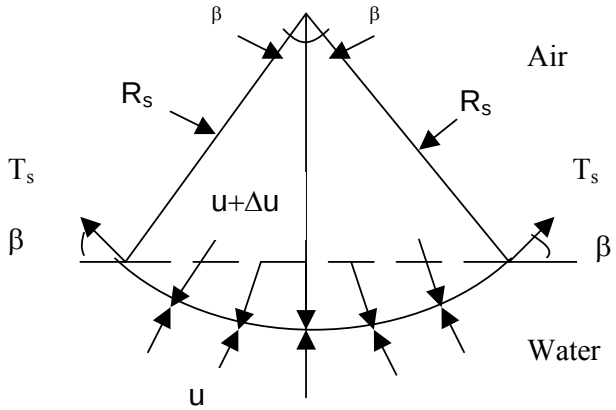

(b)

Figure 3.2 Surface tension phenomenon at the air-water interface. (a) Intermolecular forces on contractile skin and water; (b) Pressures and surface tension acting on a curved two-dimensional surface (after Fredlund, 1993).

A molecule in the interior of the water experiences equal forces in all directions, which means there is no unbalanced force. A water molecule within the contractile skin experiences an unbalanced force towards the interior of the water. In order for the contractile skin be in equilibrium, a tensile pull is generated along the contractile skin. The property of the contractile skin that allows it to exert a tensile pull is called a surface tension, T_s. Surface tension is measured as the tensile force per unit length of the contractile skin (N/m). Surface tension is tangential to the contractile skin surface. Its magnitude decreases as temperature increases. Table 3.1 gives surface tension values for contractile skin at different temperatures.

Table 3.1 Surface tension of the contractile skin (from Fredlund, 1993)

Temperature, t° (°C)	Surface Tension, T_s (mN/m)*
0	75.7
10	74.2
15	73.5
20	72.75
25	72.0
30	71.2
40	69.6
50	67.9
60	66.2
70	64.4
80	62.6
100	58.8
* Tensile force per unit length of the contractile skin - milli Newton per meter	

The surface tension causes the contractile skin to behave like an elastic membrane. This behavior is similar to inflated balloon, which has a greater pressure inside the balloon than outside. If a flexible two-dimensional membrane is subjected to different pressures on each side, the membrane must assume a concave curvature towards the larger pressure and exert a tension in the membrane in order to be in equilibrium. The pressure difference across the curved surface can be related to the surface tension and the radius of curvature of the surface by considering equilibrium across the membrane (Figure 3.2.b).

The pressure acting on the membrane are u and (u+Δu). The membrane has a radius of curvature of, R_s, and a surface tension T_s. The horizontal forces along the membrane balance each other. Force equilibrium in the vertical direction requires that

$$2\ T_s \sin\beta = 2\ \Delta u R_s \sin\beta \qquad (3.1)$$

Where,

$2\ R_s \sin\beta$ = length of the membrane projected onto the horizontal plane.

Rearranging Eq. (3.1) gives

$$\Delta u = T_s / R_s \qquad (3.2)$$

Equation (3.2) gives the pressure difference across a two-dimensional curved surface with a radius, R_s, and a surface tension, T_s. For a wrapped or saddle-shaped surface (i.e., three-dimensional membrane), Eq. (3.2) can be extended using Laplace equation (Fig. 3.3)

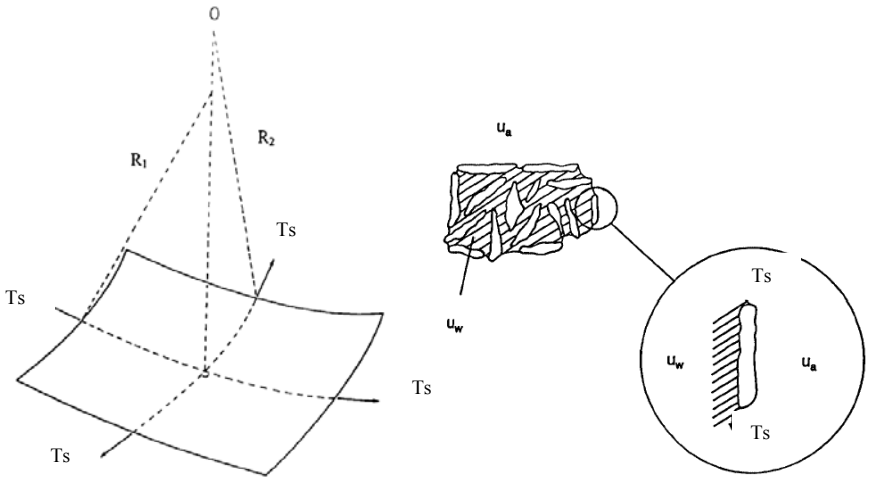

Figure 3.3 Surface Tension on wrapped membrane and surface tension on soil water particle (after Fredlund, 1993).

$$\Delta u = T_s / ((1/R_1)+(1/R_2)) \qquad (3.3)$$

Where,

R_1 and R_2 = radii of curvature of a wrapped membrane in two orthogonal principal planes.

If the radius of curvature is the same in all directions (i.e., R_1 and $R_2 = R_s$), Eq. (3.3) becomes

$$\Delta u = 2T_s / R_s \qquad (3.4)$$

In an unsaturated soil, the contractile skin would be subjected to an air pressure, u_a, which is greater than the water pressure, u_w. The pressure difference, $(u_a - u_w)$, is referred to as matric suction. The pressure difference causes the contractile skin to curve in accordance with Eq. (3.4):

$$(u_a - u_w) = 2T_s / R_s \quad (3.5)$$

Where,

$(u_a - u_w)$ = matric suction or the difference between pore-air and pore water pressures acting on the contractile skin.

Equation (3.5) is referred to as Kelvin's capillary model equation. As the matric suction of a soil increases, the radius of curvature of the contractile skin decreases. The curved contractile skin is often called a meniscus. When the pressure difference between the pore-air and pore-water goes to zero, the radius of curvature, R_s, goes to infinity. Therefore, a flat air-water interface exists when the matric suction goes to zero.

3.3 Theory of Soil Suction

Soil suction is commonly referred to as the free energy state of soil water. The free energy of the soil water can be measured in terms of the partial vapor pressure of the soil water. The thermodynamic relationship between soil suction (or the free energy of the soil water) and the partial pressure of the pore-water vapor can be written as follows:

$$\Psi = - (RT/(v_{w0}\omega_v)). \ln(u_v/u_{v0}) \quad (3.6)$$

Where,

ψ = soil suction or total suction (kPa)

R = universal molar gas constant [8.31432 J/(mol K)]

T = absolute temperature [T= (273.16 + t°) (K)]

t° = temperature (°C)

v_{w0} = specific volume of water or the inverse of the density of water $[1/\rho_w\ (m^3/kg)]$

ρ_w = density of water (998 kg/m^3 at t°=20°C)

ω_v = molecular mass of water vapor (18.016 kg/kmol)

u_v = partial pressure of pore water vapor

u_{v0} = saturation pressure of water vapor over a flat surface of pure water at the same temperature (kPa).

If select 20°C and put constant values we will get;

$$\Psi = - 135022 \ln(u_v/u_{v0}) \quad (3.7)$$

Here, u_v/u_{v0} is called as relative humidity, RH. The concentration of water vapor in the air is commonly expressed in terms of relative humidity. A RH value less than 100% indicates presence of suction in the soil.

$$RH= u_v(100)/u_{v0} \quad (3.8)$$

3.4 Components of Total Suction

The total suction,ψ, of a soil is made up of two components, namely, the matric suction, $(u_a - u_w)$, and the osmotic suction, π.

Figure 3.4 illustrates the concept of total suction and its component as related to the free energy of the soil water. The matric suction component is commonly associated with the capillary phenomenon arising from the surface tension of the water.

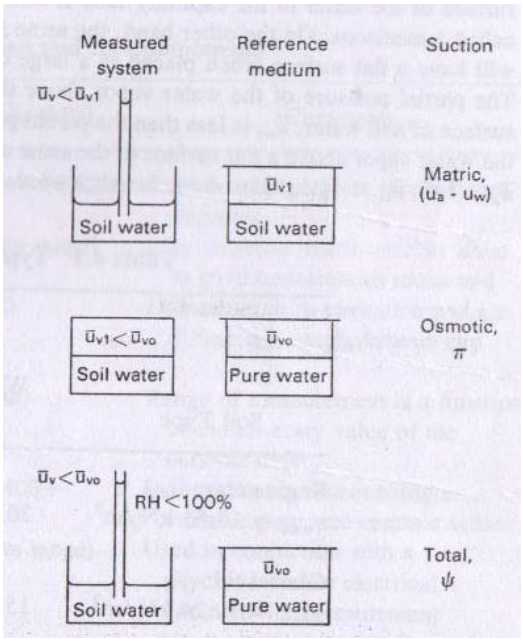

Figure 3.4 Total suction and its components: matric and osmotic suction (after Fredlund, 1993).

Consider a capillary tube filled with a soil water. The surface of the water in the capillary tube is curved and is called meniscus. On the other hand, the same soil water will have a flat surface when placed in a large container. The partial pressure of the water vapor above the curved surface of soil water, u_v, is less than the partial pressure of the water vapor above a flat surface of the same soil water, u_{v1}. In other words RH in a soil will decrease due to the presence of curved water surfaces produced by the capillary phenomenon. The water vapor pressure or RH decreases as the radius of curvature of the water surface decreases. At the same time, the radius of curvature is inversely proportional to the difference between the air and water pressures across the surface [i.e., $(u_a - u_w)$] and is called matric suction. This means that one component of the total suction is matric suction, and it contributes to a reduction in the relative humidity.

The pore-water in a soil generally contains dissolved salts. The water vapor pressure over a flat surface of solvent, u_{v1}, is less than the water vapor pressure over a flat surface of pure water, u_{v0}. In other words, the relative humidity decreases with increasing dissolved salts in the pore water of the soil. The decrease in RH due to the presence of dissolved salts in pore-water is referred to as the osmotic suction, π.

3.5 Capillarity

The capillary phenomenon is associated with the matric suction component of total suction. The height of water rise and the radius of curvature have direct implication on the water content versus matric suction relationship in soils (i.e., the soil – water characteristic curve). This relationship is different for the wetting and drying portions of the curve, and these differences can also be explained in terms of the capillary model.

3.5.1 Capillary Height

Let us consider the vertical force equilibrium of the capillary water in the tube shown in Fig. 3.5.;

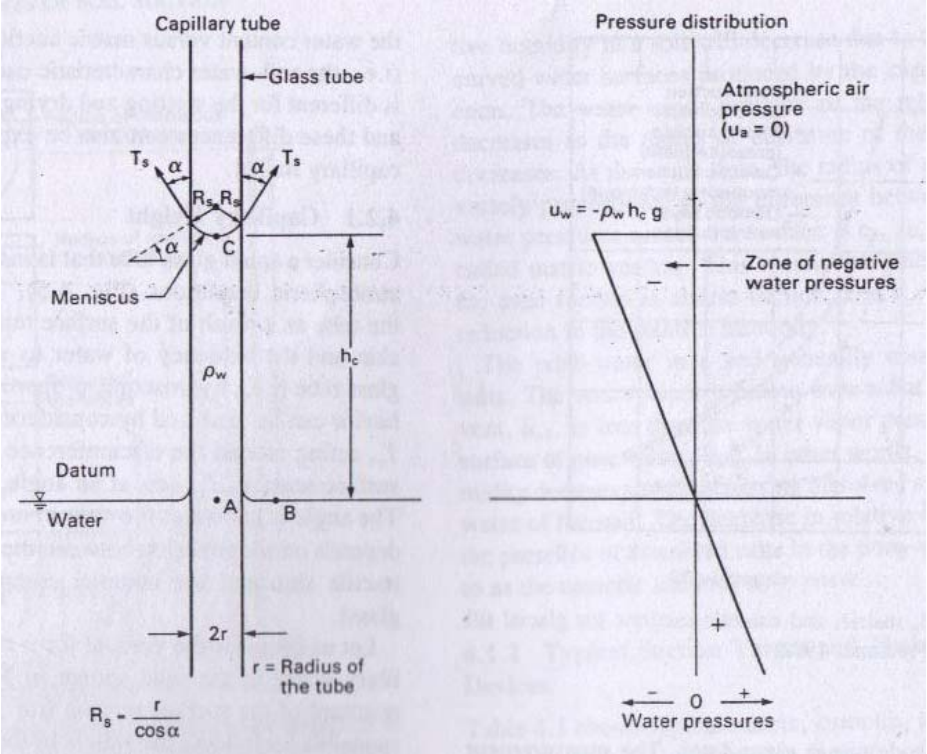

Figure 3.5 Physical model and phenomenon related to capillarity (after Fredlund, 1993).

$$2\pi r T_s \cos\alpha = \pi r^2 h_c \rho_w g \quad (3.9)$$

Where,

r = radius of the capillary tube

Ts = surface tension of water

α = contact angle

h_c = capillary height

g = gravitational acceleration.

From eq. (3.9);

$$h_c = 2T_s/\rho_w g R_s \quad (3.10)$$

Where,

R_s = radius of curvature of meniscus (i.e., r/cosα).

3.5.2 Capillary Pressure

As can be seen from the Figure 3.5, water pressures, u_w, at points A and B are atmospheric; so, they are equal and zero. Also point A and B at zero elevation and therefore their hydraulic heads also zero. The hydrostatic equilibrium among points C, B, and A requires that the hydraulic heads at all three points be equal. So, hydraulic head at C also zero. So, at point C;

$u_w = - \rho_w g h_c$ and

$u_a = 0$ (Atmospheric air pressure) (3.11)

If we subtract $u_a - u_w$;

$(u_a - u_w) = \rho_w g h_c$ (Matric Suction) (3.12)

Substitute (3.10) in (3.12)
We will get;

$(u_a - u_w) = 2T_s / R_s$ (3.13)

Eqn. (3.13) is exactly same what we get in surface tension section (Equation 3.5).

As a result, the smaller pore radius r, the higher soil matric suction. The surface tension associated with the contractile skin results in a reaction force on the wall of the capillary tube (Figure 3.6). The vertical component of this reaction force produces compressive stresses on the wall of the tube. In other words, the weight of the water column is transferred to the tube through the contractile skin. In the case of a soil having a capillary zone, the contractile skin results in an increased compression of the soil structure. As a result, the presence of matric suction in an unsaturated soil increases the shear strength of the soil.

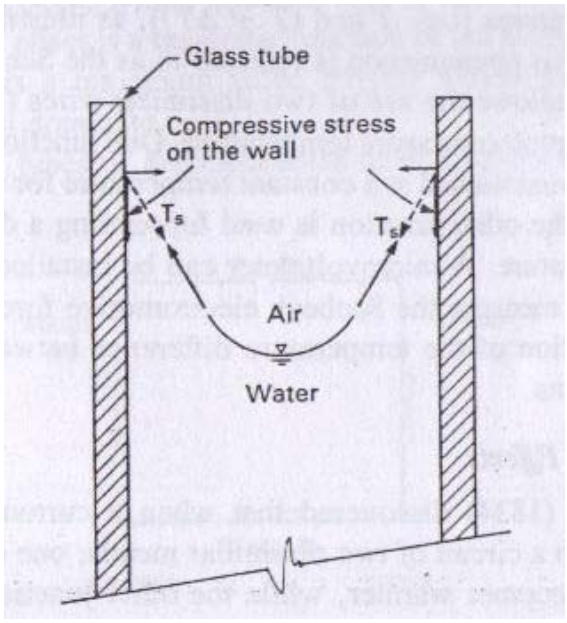

Figure 3.6 Forces acting on a capillary tube (after Fredlund, 1993).

The use of pore radius in the capillary Equation (3.13) causes the model to be impractical for engineering practice. In addition, there are other factors that contribute to being able to sustain highly negative pore-water pressures in soils, such as the adsorptive forces between the clay particles (Fredlund, 1993).

3.6 Shear Strength for Unsaturated Soils

The shear strength of an unsaturated soil can be formulated in terms of independent stress state variables (Fredlund et al. 1978). The stress state variables, $(\sigma-u_a)$ and (u_a-u_w) are the most advantageous combination for the practice. Using these stress variables, the shear strength equation is written as follows:

$$\tau_{ff} = c' + (\sigma_f-u_a)_f \tan\Phi' + (u_a-u_w)_f \tan\Phi^b \qquad (3.14)$$

where,

c'	=	Intercept of the "extended" Mohr-Coulomb failure envelope on the shear strength axis where the net normal stress and the matric suction at failure are equal to zero; it is also referred to as "effective cohesion"
$(\sigma_f-u_a)_f$	=	Net normal stress state on the failure plane at failure
u_{af}	=	Pore-air pressure on the failure plane at failure
Φ'	=	Angle of internal friction associated with the net normal stress state variable, $(\sigma_f-u_a)_f$
$(u_a-u_w)_f$	=	Matric suction on the failure plane at failure
Φ^b	=	Angle indicating the rate of increase in shear strength relative to the matric suction, $(u_a-u_w)_f$.

A comparison of Eqs. (3.14) and shear strength equation for a saturated soil reveals that the shear strength equation for an unsaturated soil is an extension of the shear strength equation for a saturated soil. For an unsaturated soil, two stress state variables are used to describe its shear strength, while only one stress state variable (i.e., effective normal stress $(\sigma_f-u_w)_f$) is required for a saturated soil.

The shear strength equation for an unsaturated soil exhibits a smooth transition to the shear strength equation for a saturated soil. As the soil approaches saturation, the pore-water pressure, u_w, approaches the pore-air pressure, u_a, and the matric suction (u_a-u_w), goes to zero. The matric suction component vanishes and Eqn. (3.14) reverts to the equation for a saturated soil.

CHAPTER 4

MEASUREMENTS OF SOIL SUCTION

The free energy of the soil water (total suction) can be determined by measuring the vapor pressure of the soil water or RH in the soil. The direct measurement of RH in a soil can be conducted using a device called a psychrometer (Fredlund and Rahardjo,1993). The RH in a soil can be indirectly measured using a filter paper as a measuring sensor. The filter paper is equilibrated with the suction in the soil.

4.1. Soil Suction Measurements with Filter Paper Method

There is a cheap and easy technique to measure soil suction, which is filter paper method. When psychrometer method compared to filter paper method, filter paper method gives more consistent results (Bulut et al., 2000).

The filter paper method is a laboratory test method, and it is inexpensive and relatively simple. It is also the only known method that covers the full range of suction. The working principle behind the filter paper method is that the filter paper will come to equilibrium with the soil either through vapor flow or liquid flow, and at equilibrium, the suction value of the filter paper and the soil will be the same.With the filter paper method, both total and matric suction can be measured.

If the filter paper is allowed to absorb water through vapor flow (non-contact method), then only total suction is measured. However, if the filter paper is allowed to absorb water through fluid flow (contact method), then only matric suction is measured.

In the filter paper method, the soil specimen and filter paper are brought to equilibrium either in a contact (matric suction measurement) or in a non-contact (total suction measurement) method in a constant temperature environment. After equilibrium is established between the filter paper and soil the water content of the filter paper disc is measured. Then, by using a filter paper calibration curve of water content versus suction, the corresponding suction value is found from the curve, so the filter paper method is an indirect method of measuring soil suction. Therefore, a calibration curve should be constructed or be adopted (i.e., the two curves presented for different filter papers in ASTM D 5298 – 94 Standard Test Method for Measurement of Soil Potential (Suction) Using Filter Paper) in soil suction measurements.

Leong et al., 2002 (after Van der Raadt et al, 1987) states that the filter paper field measurements showed that at high suctions (more than 1000 kPa) most of the movement occurs through vapor transfer than capillary transfer.

4.1.1. Required Apparatus

For Calibration Procedure and for Suction Measurements:

(a) Filter papers; the ash-free quantitative Schleicher & Shuell No. 589 White Ribbon or Whatman No. 42 type filter papers. Based on the test results of Sibley and Williams (1990) suggested that Whatman No. 42 filter paper was the most approprate for use over entire range of suction investigated (Leong et al., 2002). Therefore, in our tests Whatman No.42 type

filter paper was used.

(b) Salt solutions; sodium chloride (NaCl) solutions in a range between 0 (i.e., distilled water) to about 2.7 molality.

(c) Sealed containers; 250 ml glass jars with lids, which work nicely.

(d) Small aluminum cans; the cans with lids are used as carriers for filter papers during moisture content measurements.

(e) A balance; a balance with accuracy to the nearest 0.0001 g. is used for moisture content determination.

(f) An oven; an oven for determining the moisture contents of the filter papers by leaving them in it for 24 hours at 105 ± 5^{o}C temperature in the aluminum moisture cans (as in the standard test method for water content determinations of soils).

(g) A temperature room; a controlled temperature room in which the temperature fluctuations are kept below ±1^{o}C is used for the equilibrium period.

(h) An aluminum block; the block is used as a heat sink to cool the aluminum cans for about 20 seconds after removing them from the oven.

In addition, latex gloves, tweezers, plastic tapes, plastic bags, ice-chests, scissors, and a knife are used to set up the test.

4.1.2 Filter Paper Calibration Procedure

Two persons perform the filter paper water content measurements in order to decrease the time during which the filter papers are exposed to the laboratory atmosphere and, thus, the amount of moisture lost and gain during measurements is kept to a minimum. All the items related to filter paper testing are cleaned carefully. Gloves and tweezers are used to handle the materials in nearly all steps of the calibration. The filter papers and aluminum cans are never touched with bare hands.

The filter paper calibration curve is constructed using salt solutions as an osmotic potential source for suctions above about 2.5 pF. The procedure that is adopted for the calibration is as follows:

(a) NaCl solutions are prepared from 0 (i.e., distilled water) to 2.7 molality. The definition of molality is the number of moles of NaCl in 1000 ml of distilled water. For example, one mole of NaCl is 58.4428 g. Thus, 2 molality NaCl means 2 times 58.4428 g or 116.8856 g NaCl in 1000 ml distilled water. Table 4.1 gives the NaCl weights at different suction values.

Table 4.1 Osmotic suction values of NaCl solutions at 25°C

NaCl Concentration (in molality)	Suction in cm units	Suction in pF* units	Suction in kPa units	NaCl amount in grams (in 1000 ml distilled water)
0.000	0	0.00	0	0
0.003	153	2.18	15	0.1753
0.007	347	2.54	34	0.4091
0.010	490	2.69	48	0.5844
0.050	2,386	3.38	234	2.9221
0.100	4,711	3.67	462	5.8443
0.300	13,951	4.14	1,368	17.5328
0.500	23,261	4.37	2,281	29.2214
0.700	32,735	4.52	3,210	40.9099
0.900	42,403	4.63	4,158	52.5985
1.100	52,284	4.72	5,127	64.2871
1.300	62,401	4.80	6,119	75.9756
1.500	72,751	4.86	7,134	87.6642
1.700	83,316	4.92	8,170	99.3528
1.900	94,228	4.97	9,240	111.0413
2.100	105,395	5.02	10,335	122.7299
2.300	116,857	5.07	11,459	134.4184
2.500	128,625	5.11	12,613	146.1070
2.700	140,699	5.15	13,797	157.7956
*pF = $\log_{10}$(cm |suction|) and 1 kPa= 10,198 cm (negative head)				

(b) A 250 ml glass jar is filled with approximately 150 ml of a solution of known molality of NaCl and the glass jar is labeled with the solution molality used for that jar.

(c) Then, a small plastic cup is inserted into the glass jar. Holes are made in plastic cups in order for the filter papers to interact with and absorb water from the air in the closed jar. The configuration of the setup is shown in Figure 4.1. Two filter papers are put on the plastic cup one on top of the other in order to double check the errors in the balance readings and in a case when one of the filter paper is accidentally dropped, the other filter paper is used. The glass jar lid is sealed with plastic tapes very tightly to ensure air tightness.

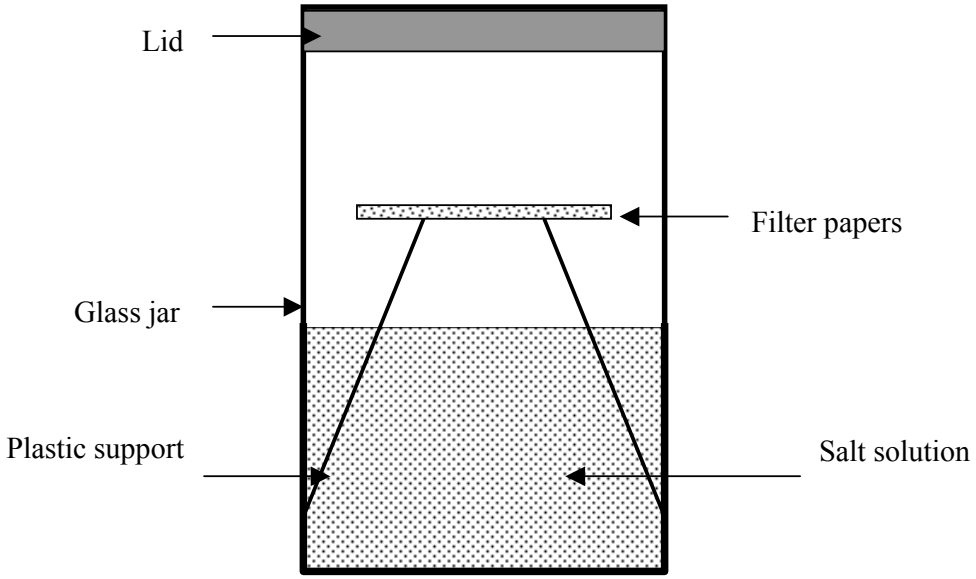

Figure 4.1 Total suction calibration test configuration

(d) Steps b. and d. are repeated for each of the different NaCl concentrations.

Then, the prepared containers are put into plastic bags for extra protection. After that, the containers are put into the ice-chests in a controlled temperature room. The suggested equilibrium period is at least one week.

After the equilibrium period, the procedure for the filter paper water content measurement is as follows:

(a) Before starting to take measurements, all the items related to the calibration process are cleaned carefully and latex gloves are used throughout the process. Before taking the glass jar containers from the temperature room, all aluminum cans that are used for moisture content measurements are weighed to the nearest 0.0001 g. accuracy and recorded on a filter paper water content measurement data sheet.

(b) After that, two persons carry out all measurements. For example, while one person is opening the sealed glass jar, the other person is putting the filter paper into the aluminum can very quickly (i.e., in a few seconds, usually less than 5 seconds) using the tweezers.

(c) Then, the weights of each can with wet filter papers inside are taken very quickly. The weights of cans and wet filter papers are recorded with the corresponding can numbers and whether the top or bottom filter paper is inside.

(d) Step (c) is followed for every glass jar. Then, all cans are put into the oven with the lids half-open to allow evaporation. All filter papers are kept at a $105 \pm 5^{o}C$ temperature for 24 hours inside the oven.

(e) Before taking measurements on the dried filter papers, the cans are closed with their lids and allowed to equilibrate for 5 minutes in the oven. Then a can is removed from the oven and put on an aluminum block (i.e., heat sinker) for about 20 seconds to cool down; the aluminum block acts as a heat sink and expedites the cooling of the can. After that, the can with the dry filter paper inside is weighed again very quickly. The dry filter paper is taken from the can and the cold can is weighed in a few seconds.

Finally, all the weights are recorded on the data sheet.

(f) Step (e) is repeated for every can.

The filter paper calibration curve of water content versus corresponding suction values is obtained from the calibration testing procedure. If suction values in pF or log (kPa) units are plotted with corresponding filter paper water content values a calibration curve for that specific type filter paper is obtained. Such a curve for Schleicher & Schuell No. 589 White Ribbon and Whatman No. 42 type filter papers is given by ASTM D 5298 (1994) and is reproduced in Figure 4.2, on which the suction values are plotted as log (kPa).

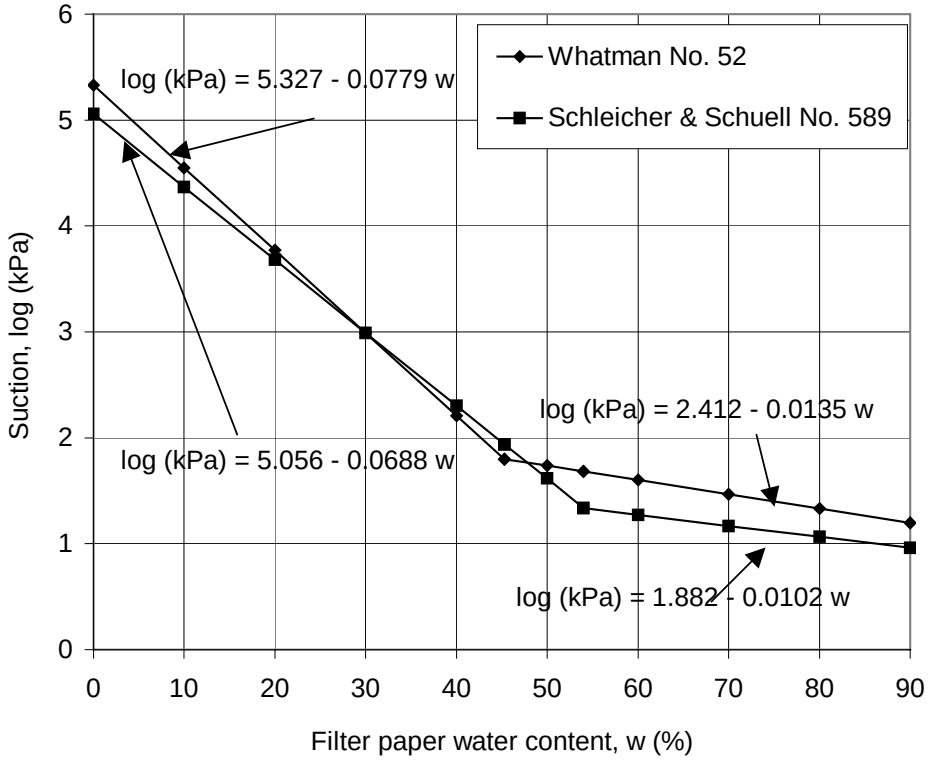

Figure 4.2 Calibration curves for two types of filter papers (reproduced from ASTM D5298).

4.1.3 Soil Suction Measurements

Both total and matric suction measurements are possible from any type of soils and soils at any conditions (i.e., natural unprocessed and uncompacted, loose, compacted, treated soils, etc.) using the filter paper method. However, care must be taken when measuring matric suction because intimate contact between the filter paper and the soil is very important. If a good contact is not provided between the filter paper and the soil, then it is possible that the result will be total suction measurement rather than matric suction measurement.

Two persons perform the filter paper water content measurements in order to decrease the time during which the filter papers are exposed to the laboratory atmosphere and, thus, the amount of moisture lost and gained during measurements is kept to a minimum. All the items related to filter paper testing are cleaned carefully. Gloves and tweezers are used to handle the materials in nearly all steps of the experiment. The filter papers and aluminum cans are never touched with bare hands. From 250 to 500 ml volume size glass jars are readily available in the market and can be adopted for suction measurements. Especially, the glass jars with 3.5" to 4" diameter in size can contain the 3" diameter Shelby tube samples very nicely. A typical setup for both the soil total and matric suction measurements is depicted in Figure. 4.3 and 4.4. The procedure that is adopted for the experiment is as follows:

4.1.3.1. Soil Total Suction Measurements

(a) At least 75 percent volume of a glass jar is filled up with the soil; the smaller the empty space remaining in the glass jar, the smaller the time period that the filter paper and the soil system requires to come to equilibrium.

(b) A ring type support (1 to 2 cm in height) is put on top of the soil to provide a non-contact system between the

filter paper and the soil.

(c) Two filter papers one on top of the other are inserted on the ring using tweezers. The filter papers should not touch the soil, the inside wall of the jar, and underneath the lid in any way.

(d) Then, the glass jar lid is sealed very tightly with plastic type electrical tape.

(e) Steps a., b., c., and d. are repeated for every soil sample.

(f) After that, the containers are put into the ice-chests in a controlled temperature room for equilibrium.

The suggested equilibrium period is at least one week. After the equilibrium period, the procedure for the filter paper water content measurement is as follows:

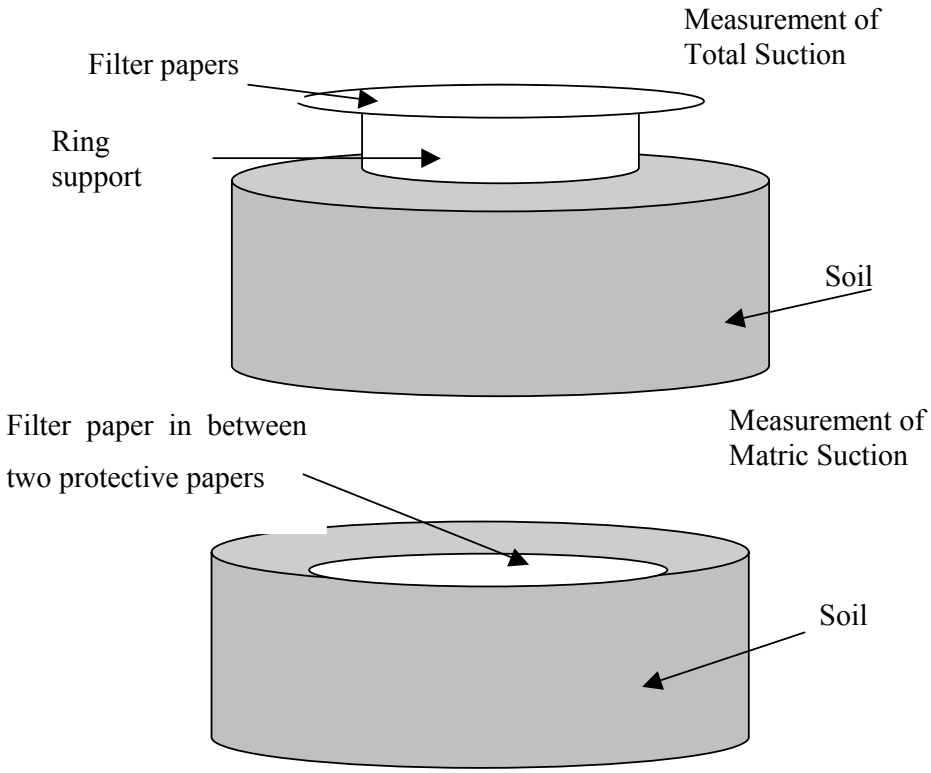

Figure 4.3 Contact and noncontact filter paper methods for measuring total and matric suction (1st Step)

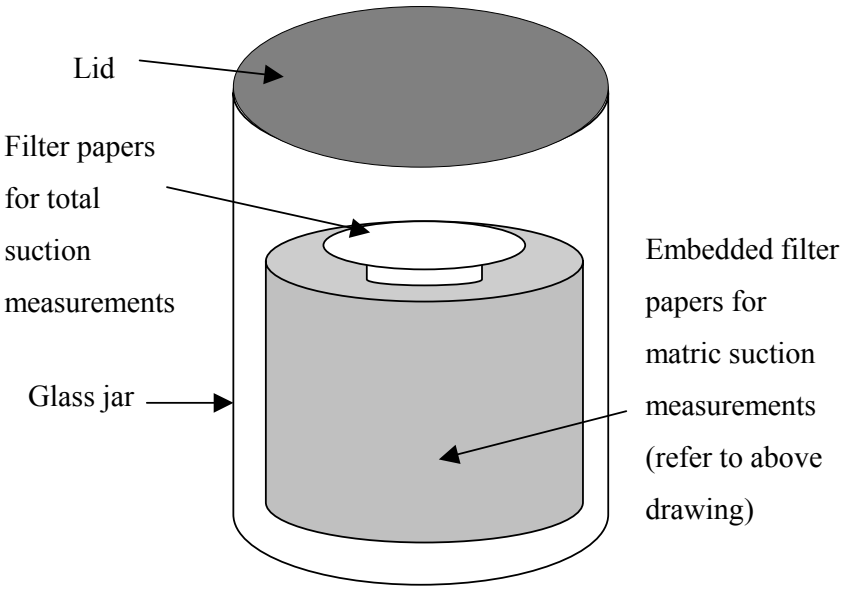

Figure 4.4 Contact and noncontact filter paper methods for measuring total and matric suction (2nd Step).

(a) Before starting to take measurements, all the items related to the measurement process are again cleaned carefully and latex gloves are used throughout the process. Before taking the glass jar containers from the temperature room, all aluminum cans that are used for moisture content measurements are weighed to nearest 0.0001 g accuracy and recorded on a filter paper water content measurement data sheet.

(b) After that, all measurements are carried out by two persons. For example, while one person is opening the sealed glass jar, the other person is putting the filter paper into the aluminum can very quickly (i.e., in a few seconds, usually less than 5 seconds) using the tweezers.

(c) Then, the weights of each can with wet filter papers inside are

taken very quickly. The weights of cans and wet filter papers are recorded with the corresponding can numbers and whether the top or bottom filter paper is inside.

(d) Step (c) is followed for every glass jar. Then, all cans are put into the oven with the lids half-open to allow evaporation. All filter papers are kept at a 105 ± 5^{o}C temperature for 24 hours in the oven.

(e) Before taking measurements on the dried filter papers, the cans are closed with their lids and allowed to equilibrate for 5 minutes in the oven. Then a can is removed from the oven and put on an aluminum block (i.e., heat sinker) for about 20 seconds to cool down; the aluminum block acts as a heat sink and expedites the cooling of the can. After that, the can with the dry filter paper inside is weighed again very quickly. The dry filter paper is taken from the can and the cold can is weighed in a few seconds. Finally, all the weights are recorded on the data sheet.

(f) Step (e) is repeated for every can.

After obtaining all of the filter paper water content values an appropriate calibration curve is employed to get total suction values of the soil samples.

4.1.3.2. Soil Matric Suction Measurements

(a) A filter paper is sandwiched between two bigger size protective filter papers. The filter papers used in suction measurements are 5.5 cm in diameter, so either a filter paper is cut to a smaller diameter and sandwiched between two 5.5 cm papers or bigger diameter (bigger than 5.5 cm) filter papers are used as protective.

(b) Then, these sandwiched filter papers are inserted into the soil sample, which can fill up the glass jar, in a very good contact manner. An intimate contact between the

filter paper and the soil is very important.

(c) After that, this soil sample with embedded filter papers is put into the glass jar container.

(d) The glass container is sealed up very tightly with electrical tape.

(e) Steps a., b., c., and d. are repeated for every soil sample.

(f) The prepared containers are put into the ice-chests in a controlled temperature room for equilibrium.

The suggested equilibrium period is 3 to 5 days. After the equilibrium period, the procedure for the filter paper water content measurement is as follows:

(a) Before starting to take measurements, all the items related to the measurement process are again cleaned carefully and latex gloves are used throughout the process. Before taking the glass jar containers from the temperature room, all aluminum cans that are used for moisture content measurements are weighed to nearest 0.0001 g accuracy and recorded on a filter paper water content measurement data sheet.

(b) After that, all measurements are carried out by two persons. For example, while one person is opening the sealed glass jar, the other person is putting the filter paper into the aluminum can very quickly (i.e., in a few seconds, usually less than 5 seconds) using the tweezers.

(c) Then, the weights of each can with wet filter papers inside are taken very quickly. The weights of cans and wet filter papers are recorded with the corresponding can numbers.

(d) Step (c) is followed for every glass jar. Then, all cans are put into the oven with the lids half-open to allow evaporation. All filter papers are kept at a $105 \pm 5^{o}C$ temperature for 24 hours inside the oven.

(e) Before taking measurements on the dried filter papers, the cans are closed with their lids and allowed to equilibrate for 5 minutes in the oven. Then a can is removed from the oven and put on an aluminum block (i.e., heat sinker) for about 20 seconds to cool down; the aluminum block acts as a heat sink and expedited the cooling of the can. After that, the can with the dry filter paper inside is weighed again very quickly. The dry filter paper is taken from the can and the cold can is weighed in a few seconds. Finally, all the weights are recorded on the data sheet.

(f) Step (e) is repeated for every can.

After obtaining all of the filter paper water content values an appropriate calibration curve is employed to get matric suction values of the soil samples.

Filter paper method can reliably be used with suctions from about 80 kPa to in excess of 6000 kPa, a much larger range than any other single technique (Chandler and Guiterrez, 1986).

4.1.3.3 Equilibration Times for Filter Paper Method

Equilibration times for filter paper method from (Leong et al., 2002) is given in Table 4.2.

Table 4.2 Equilibration times for filter paper method (after Leong, 2002)

References	Equilibration Time	Filter Paper Method
Fawcett and Collis-George (1967)	6–7 days	Contact
McQueen and Miller (1968b)	7 days	Contact
Al-Khafaf and Hanks (1974)	2 days	Contact and uncertain contact
Hamblin (1981)	Minutes–36 days	Contact
Chandler and Gutierez (1986)	5 days	Contact
Duran (1986)	7 days	Noncontact
Greacen et al. (1987)	7 days	Contact
Sibley and Williams (1990)	3 days	Contact
Lee and Wray (1992)	10 days	Noncontact
Houston et al. (1994)	14 days	Contact and noncontact
Harrison and Blight (1998)	7 days	Contact and noncontact
	7–10 days	Wetting and noncontact
	21 days	Drying and noncontact
	10 days	Wetting and contact
	25–30 days	Drying and contact

Also, suggested equilibration time from ASTM is 7 days and several filter paper suction measuremnts done by Ling and Toll (2000) shows that in seven days approximately 97% of the equilibration is completed.

Different workers have used different time periods for the equalization of the filter paper with the suction of the soil sample: usually 7 days are allowed but at least 5 days are required (Chandler and Guiterrez, 1986).

Wet samples takes longer to reach equilibrium and that takes about 7 days. Most samples reach equilibrium at 4 days to a 1% error (Swarbrick, 1995).

4.1.3.4 Properties of the Whatman No.42 Filter Paper

The typical properties of Whatman No.42 grade cellulose filter paper is given in Table 4.3.

Table 4.3 Typical properties of Whatman No.42 grade cellulose filter (from Whatman product catalogue)

Typical Properties of Whatman No.42 Grade Cellulose Filter								
Grade	Particle Retention* (Liquid) (µm)	Air flow Rate (s/100ml/in^2)	Ash (%)	Typical Thickness (µm)	Basis Weight (g/m^2)	Wet Burst (psi)	DryBurst (psi)	Tensile MD Dry (N/15mm)
42	2.5	107	0.008	200	100	0.7	25	55.8

Ash is determined by ignition of the cellulose filter at 900°C in the air.

* 98% Particle Retention Rating.

Figure 4.5 shows Whatman cellulose filter papers. Typical analytical precipitates in the Whatman cellulose filter papers include barium sulphate, metastannic acid and finely precipitated calcium carbonate.

Figure 4.5 Whatman No.42 type filter paper (from Whatman product catalogue).

CHAPTER 5

EXPERIMENTAL STUDY

5.1 Introduction

The soil sample used in this study was taken from METU Campus area and classified according to Unified Soil Classification System by using the test results of the sieve analysis, hydrometer analysis and Atteberg limits. Also specific gravity, maximum dry density and optimum moisture content of the sample were determined. The dry density versus moisture content curve of the sample was plotted by using the compaction test results in which standard proctor compaction mould and hammer was used.

After proctor compaction test, soil samples were prepared as stated in Table 5.1;

Table 5.1 Moisture contents of the samples

As Compacted Samples	-6% of OMC	-4% of OMC	-2% of OMC	OMC	+2% of OMC	+4% of OMC	+6% of OMC
Soaked Samples	-6% of OMC	-4% of OMC	-2% of OMC	OMC	+2% of OMC	+4% of OMC	+6% of OMC

Shear strength parameters of the tested samples were determined by using direct shear apparatus which is shown in Figure 5.1.

All samples were sheared under 75 kPa, 150 kPa, and 225 kPa normal pressures and after that same samples were used in filter paper suction measurements.

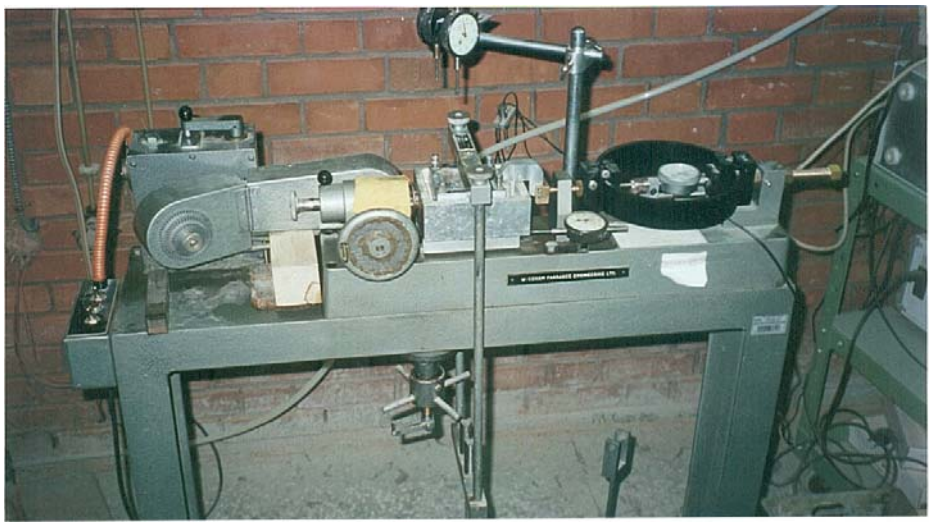

Figure 5.1 Direct shear apparatus

5.2 Procedure for Direct Shear Test

In this test program 14 sets of direct shear tests were made and each set contains 3 direct shear tests individually (moisture contents of the samples are given in the Table 5.1).

To prepare the samples, oven dried samples were mixed with appropriate mass of water and waited 24 hours in the plastic bag in the humidity room to have an homogeneous mixture.

After that samples were compacted dynamically by using proctor

compaction mould. Then samples were taken out from compaction mould by using direct shear mould and hydraulic jack.

It is very important to prevent the soil sample from moisture lost since the sheared samples were used for suction measurements after the direct shear test. Therefore, direct shear box was wrapped with nylon stretch film and covered with moisturized cloth after placing the sample in the direct shear machine.

Placed samples left one day for consolidation under normal stress of σ_n= 75 kPa, σ_n= 150 kPa, and σ_n= 225 kPa. Each set contains three stages and each stage finalized in two days. After consolidation, samples were sheared.

In order to prepare and test a soaked sample, same procedure was used but before the direct shear machine switched on, samples were soaked and left for 24 hours under weights giving normal stresses of 75 kPa, 150 kPa, and 225 kPa.

Since Consolidated Drained test procedure was followed, horizontal displacement rate was very important. Therefore after each consolidation day by using log time and root time method t_{50} and t_{90} values were determined and by using following equations (ASTM 3080) failure times were calculated for each sample.

$$t_f = 11.7\ t_{90} \quad (5.1)$$

$$t_f = 50\ t_{50} \quad (5.2)$$

And after a few calculations it was seen that 6 to 10 hours was enough for failure time and lateral displacement δ to reach the soil peak strength was in between 3mm to 5mm. So, by using following formula displacement rate was choosen as 1.0 x 10^{-4} mm/sec, which was slower than calculated, to be on the safe side.

$$V = \delta / t_f \quad (5.3)$$

After the direct shear test, tested sample was taken out from the direct shear box. After taking the samples for moisture content check, remaining sample was used for filter paper suction measurements, which will be explained in the following section.

5.3 Suction Measurements

Suction measurements were done by using filter paper method. In this study ash free Whatman No. 42 type filter papers were used.

5.3.1 Procedure for Calibration of Filter Paper

In calibration procedure instead of soil sample, salt solutions which are given in Table 4.1, were used to built up calibration curve. Also, glass jar, long supports and top and bottom filter papers were used (Figure 5.2). In calibration procedure glass jar was filled by salt solutions with known molality (Figure 5.3). Long cylindrical plastic supports, which will hold the filter papers, were immersed into the solution (Figure 5.4). After that waited for equilibration and moisture contents of the filter papers were measured in the order of 0.0001 g. So by using these filter paper moisture contents and suction values which calibration curve was drawn.

Figure 5.2 Glass jar, support and filter papers.

Figure 5.3 Glass jar filled with salt solution.

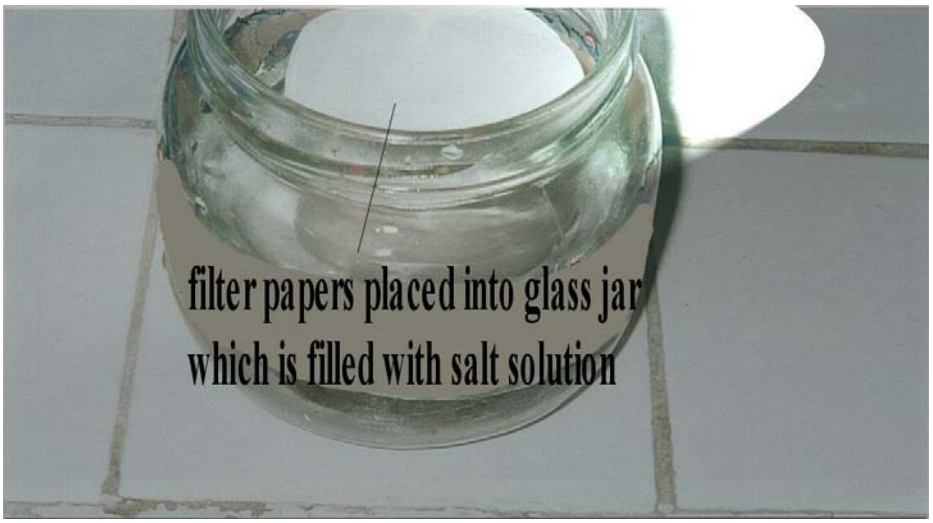

Figure 5.4 Cylindrical plastic support hold the filter papers.

The calibration curve for Whatman No.42 type filter paper is given in Figure 5.5.

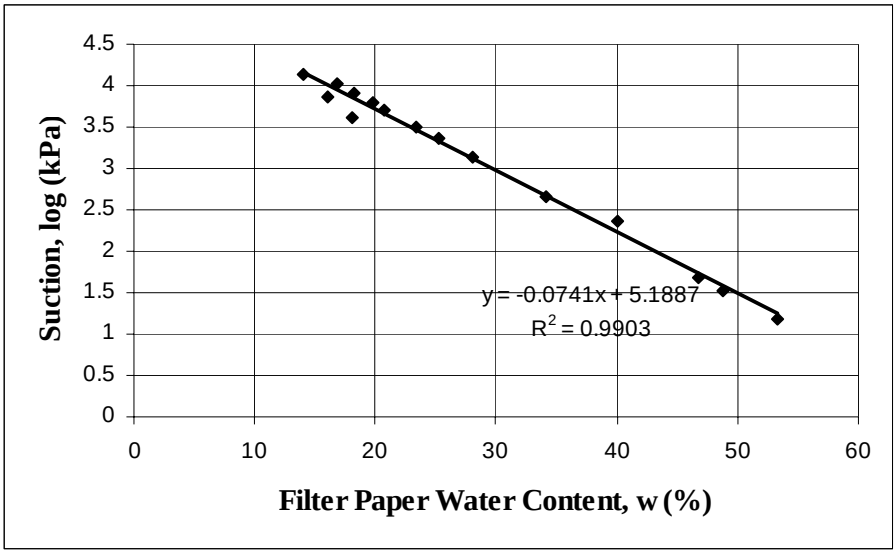

Figure 5.5 Calibration curve result for Whatman No. 42 type filter paper

5.3.2 Procedure for Soil Suction Measurements by Filter Paper

Filter paper suction measurements were done in the glass jars which were placed in the ice chest which was isolated one more time with the additional thermal isolators to minimise the temperature changes in the chest. Ice chest is shown in the Figure 5.6.

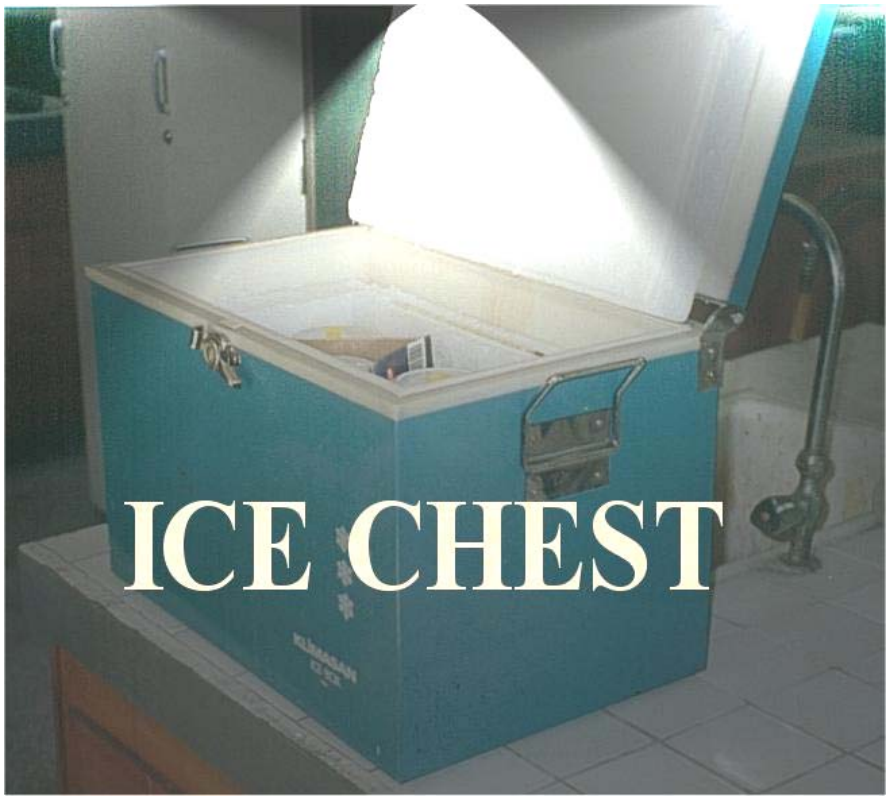

Figure 5.6 Ice chest

Samples were taken from direct shear box which were already divided into two parts from the shearing surface. Then oven dried and cooled (in the zero humidity desiccator, Figure 5.7) 3 filter papers (two protective with bigger radius (55mm), and one for measurements with smaller radius (50mm)) placed between

these two surface by using tweezers for matric suction measurements (Figure 5.8). Filter paper should be oven dried to remove moisture to be ensure that the same wetting path is followed in each case to avoid hysteresis effects (Swarbrick, 1995).

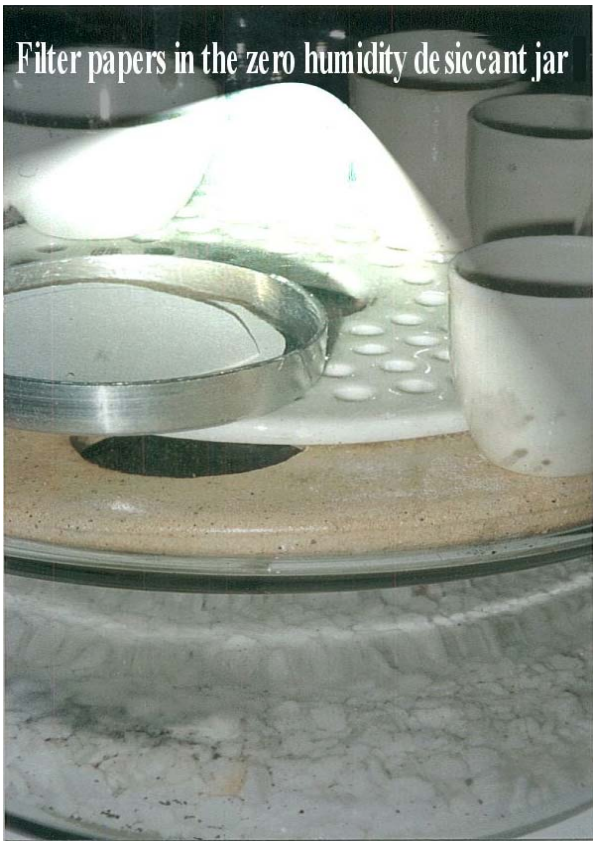

Figure 5.7 Filter papers cooled in the zero humidity desiccant jar.

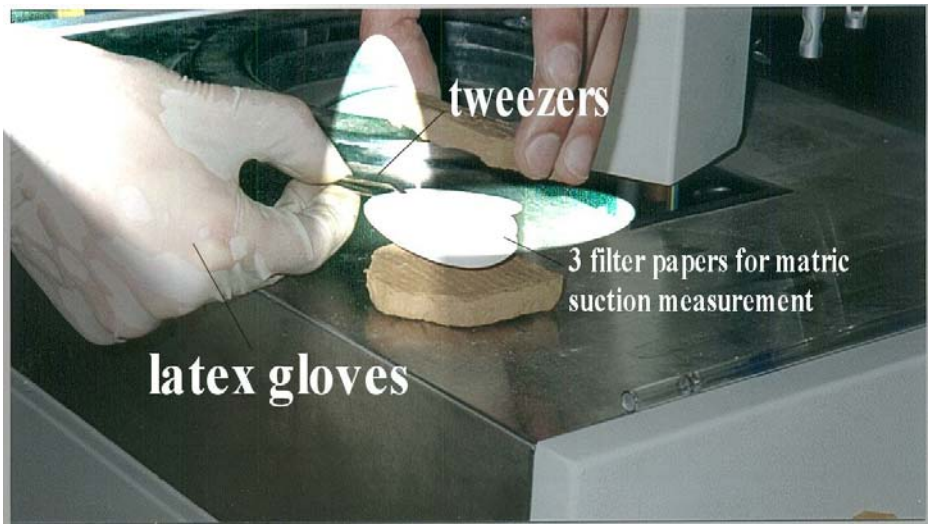

Figure 5.8 Filter papers placed for matric suction measurements.

After that, filter papers sandwiched between two surface and to protect the filter papers from vapor transfer edges of the soil sample were wrapped with plastic tape as shown in Figure 5.9.

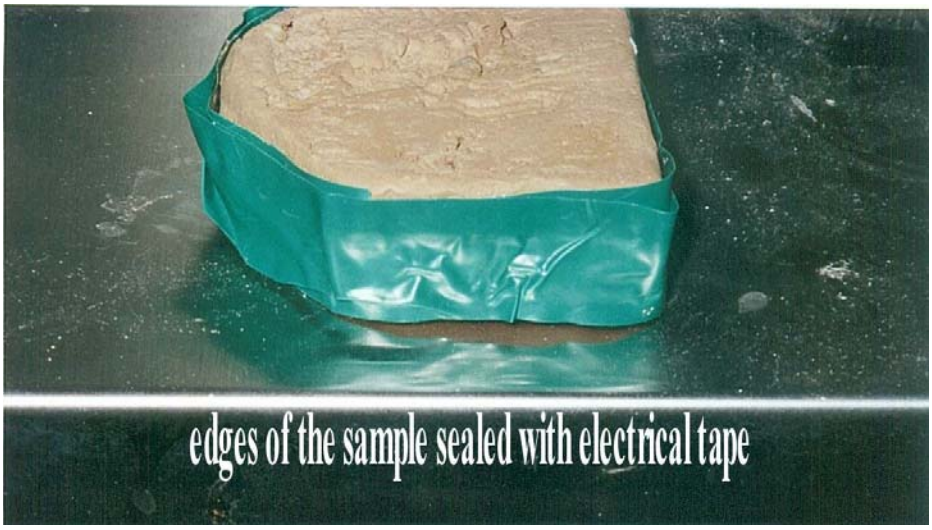

Figure 5.9 Sample wrapped with electrical tape.

Then sample was placed into glass jar and plastic ring support put over the soil sample. Then two filter papers were placed over this support for total suction

measurements (Figure 5.10).

Figure 5.10 Top and bottom filter papers placed over the plastic ring support.

After that, glass jar was closed and sealed with plastic tape and then wrapped with stretch film (Figure 5.11).

Figure 5.11 Sealed glass jar.

Then labeled jar is placed into ice chest (Figure 5.12).

Figure 5.12 Jars placed into ice chest.

After an equilibrium time of one week, jar was taken out from the chest. Before opening the glass jar, aluminum box, which would be used for moisture content, was weighed, and recorded as cold tare mass, Tc. (Figure 5.13).

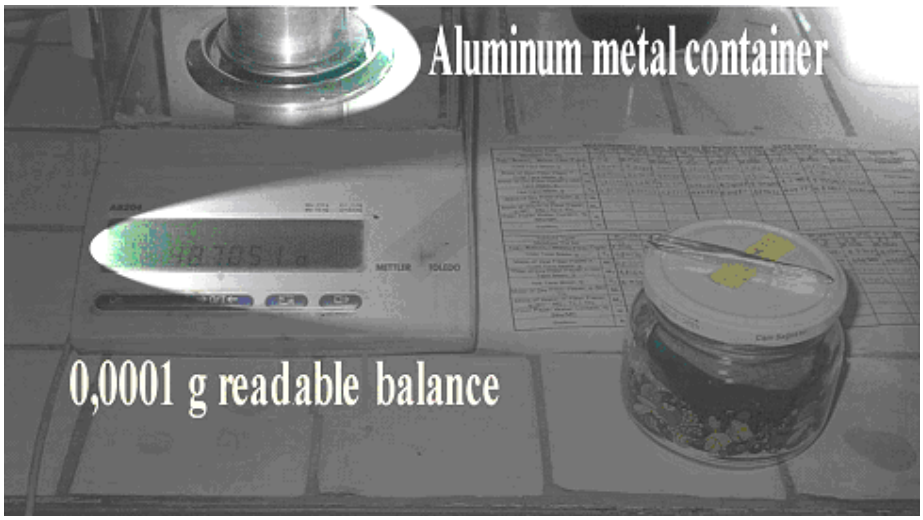

Figure 5.13 Aluminum box is weighed before filter papers taken out from the jar.

Then glass jar was opened and top and bottom filter papers were taken one by one and put into aluminum boxes quickly by using tweezers (Figure 5.14). And aluminum boxes were enclosed tightly very fast to prevent filter papers from moisture lost. After that aluminum boxes were weighed very quickly and recorded as M_1. After top and bottom filter papers, middle filter paper was taken out and quickly put into another aluminum box, which had been weighed (Figure 5.15). Then Aluminum boxes were put into oven.

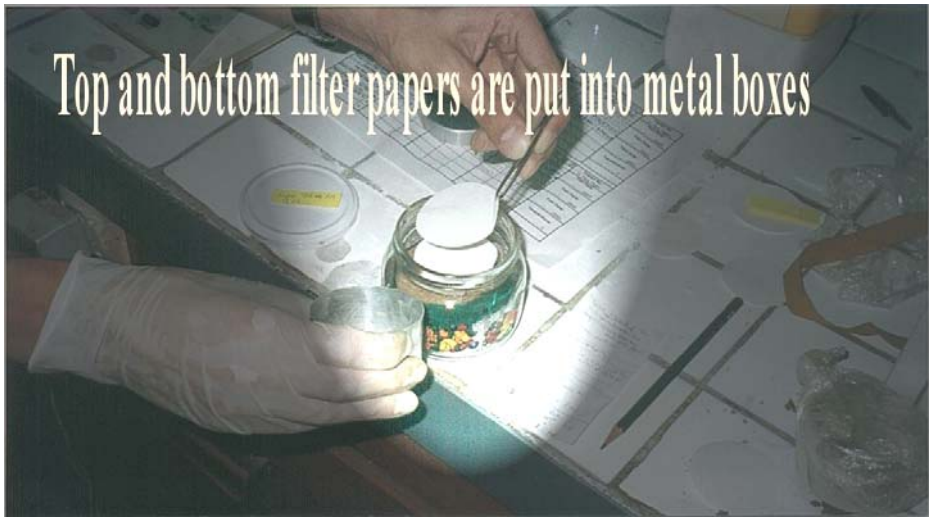

Figure 5.14 Filter papers are put into aluminum boxes for total suction.

Figure 5.15 Filter papers are put into aluminum boxes for matric suction.

After waiting overnight aluminum boxes' lids were closed and waited in the oven for 5 minutes to have an equilibrated temperature in the boxes. Then boxes were taken one by one and before weighing them, they were put over the metal mass to cool them fast (Figure 5.16). And cooled boxes were weighed in 20 seconds after taking them from the oven and this was recorded as M_2. Then aluminum box weighed without filter papers and this mass was recorded as hot tare mass, T_h.

Figure 5.16 Aluminum box put on the metal mass to cool it down fast.

Filter paper water content (w), which will give total and matric suction value is found by following formula;

$$w = \frac{Mw}{Mf} = \frac{M_1 - M_2 - Tc + Th}{M_2 - Th} \quad (5.1)$$

After that, filter paper water content value put into Equation 5.2 to get suction value.

$$\text{Log (kPa)} = 5.1887 - 0.0741w \quad (5.2)$$

A representative data sheet for filter paper measurements is given in Appendix A.

CHAPTER 6

TEST RESULTS

6.1 Soil Properties

Soil sample taken from the Middle East Technical University campus area (Ankara) and its index, compaction, swell, and suction properties are given in Tables 6.1 and 6.2.

Table 6.1 Basic properties of the clay sample

Property	Value
Specific Gravity	2.73
Liquid Limit, (LL)	48%
Plastic Limit, (PL)	21%
Plasticity Index, (PI)	27%
Clay Fraction (<2% finer than 2 μm)	67.9%
Activity, (PI / % finer than 2 μm)	0.40
Optimum Moisture Content, (w_{opt})	20.8%
Maximum Dry Density, (ρ_d)	1.67 Mg/m^3
Classification (According to Unified Classification System)	CL

Table 6.2 Swell and suction properties of the undisturbed sample

Test	Results		
Free Swell	2.4%		
Natural Water Content	21%		
Applied Normal Pressures:	75 kPa	150kPa	225 kPa
Total Suction (kPa)	3136	4110	4414
Matric Suction (kPa)	3054	3090	3042
Osmotic Suction (kPa)	81	1020	1372

Dry density versus moisture content and grain size curves of the soil sample are shown in Figure 6.1 and Figure 6.2 respectively.

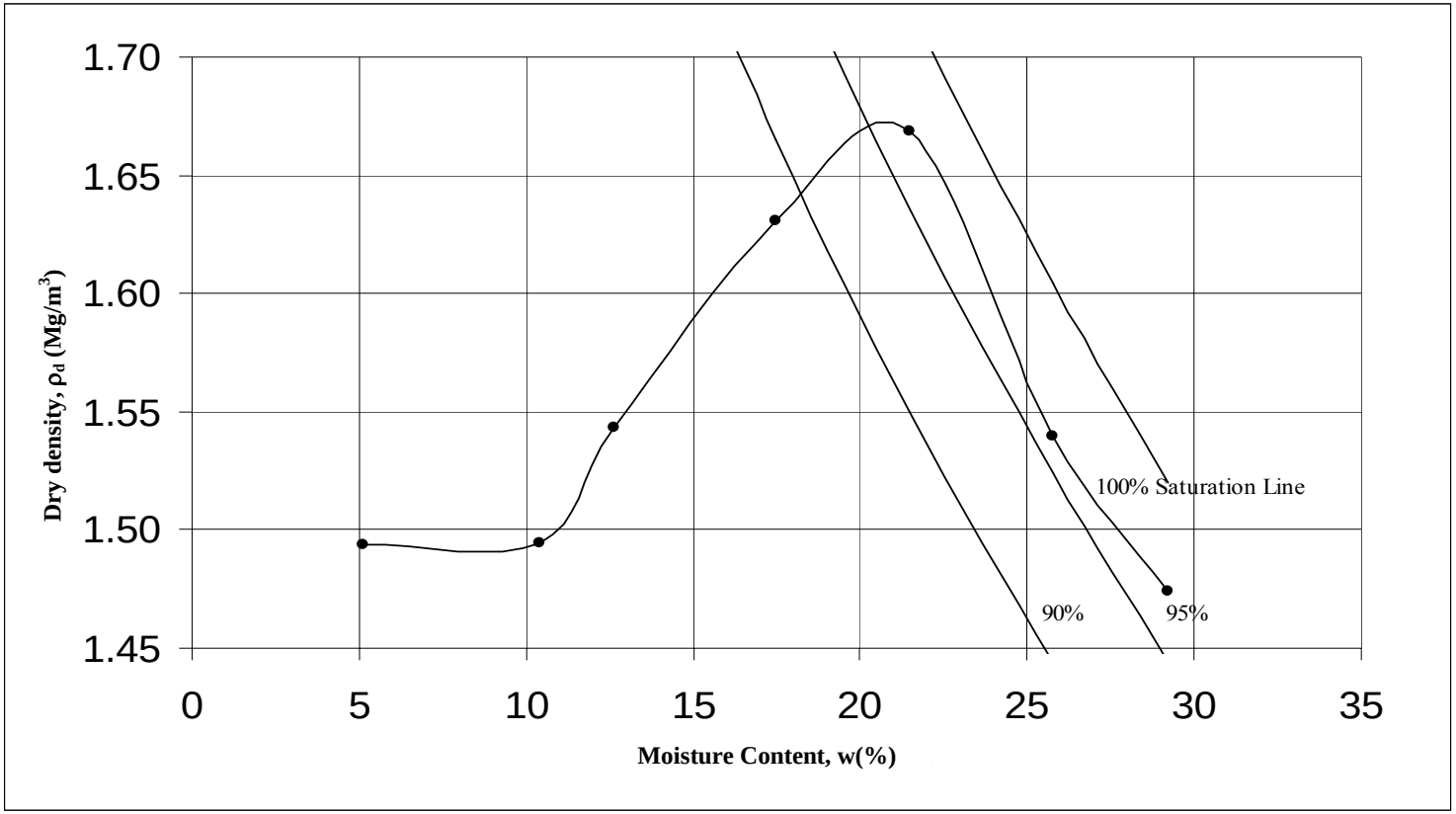

Figure 6.1 Dry density versus moisture content.

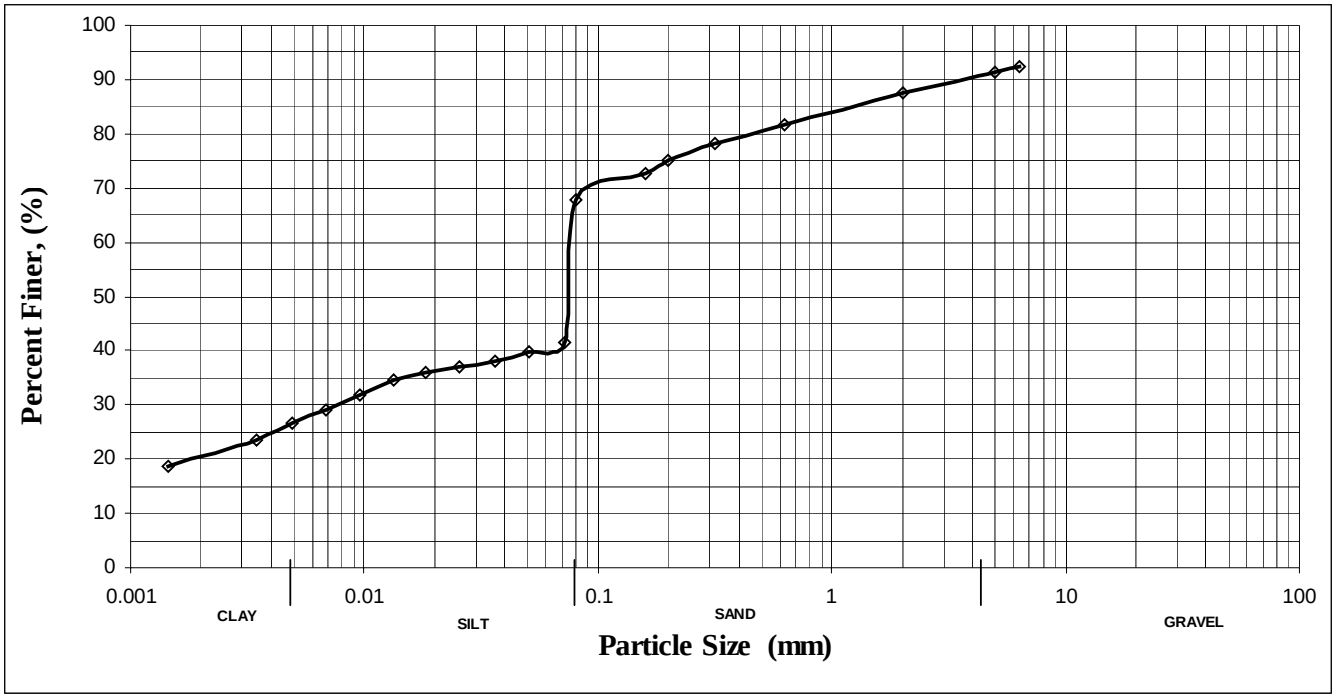

Figure6.2 Grain size curve

6.2 Shear Strength Measurements

The resulting graphics which are shear stress versus shear displacement and vertical stress versus shear strength for all moisture contents (for samples at compaction moisture content and for soaked samples) are illustrated on Figures 6.3 to 6.30.

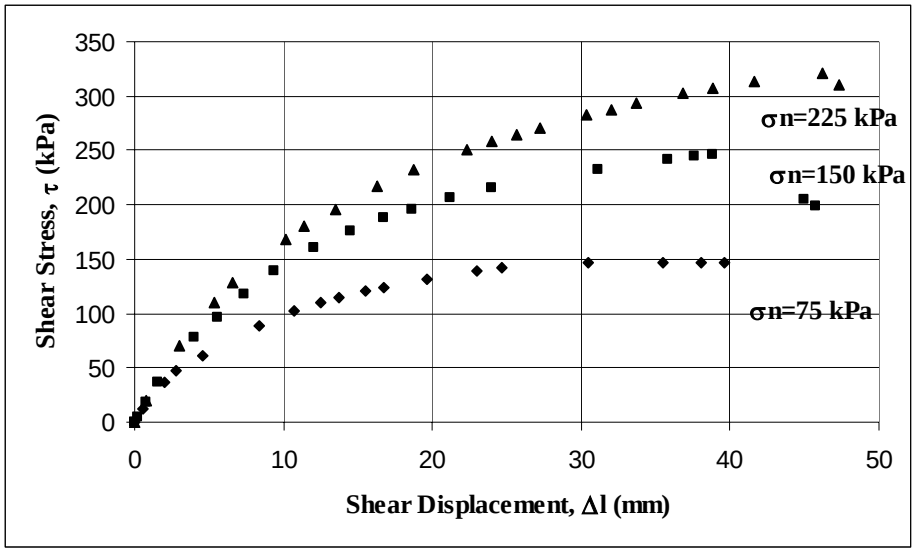

Figure 6.3 Shear stress versus shear displacement curves for -6% of OMC.

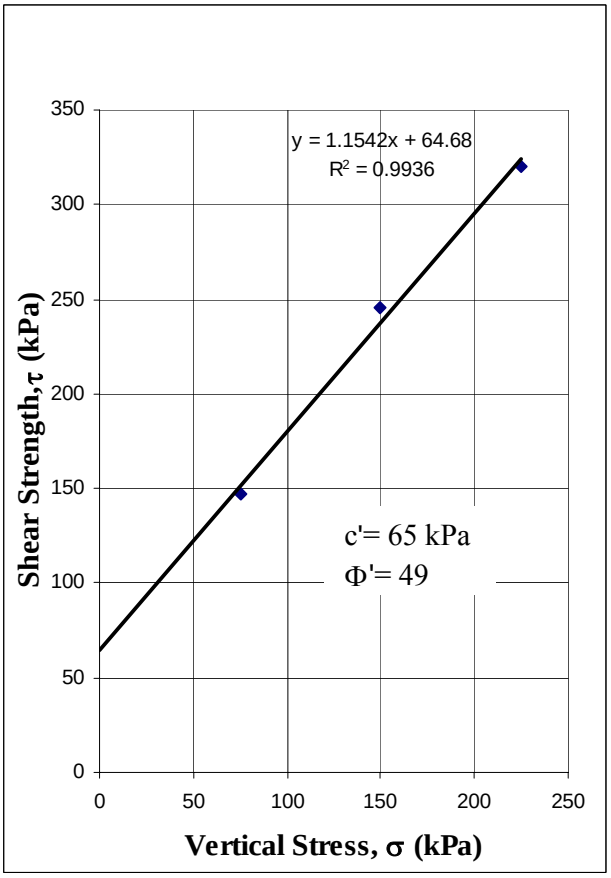

Figure 6.4 Vertical stress versus shear strength graph for -6% of OMC.

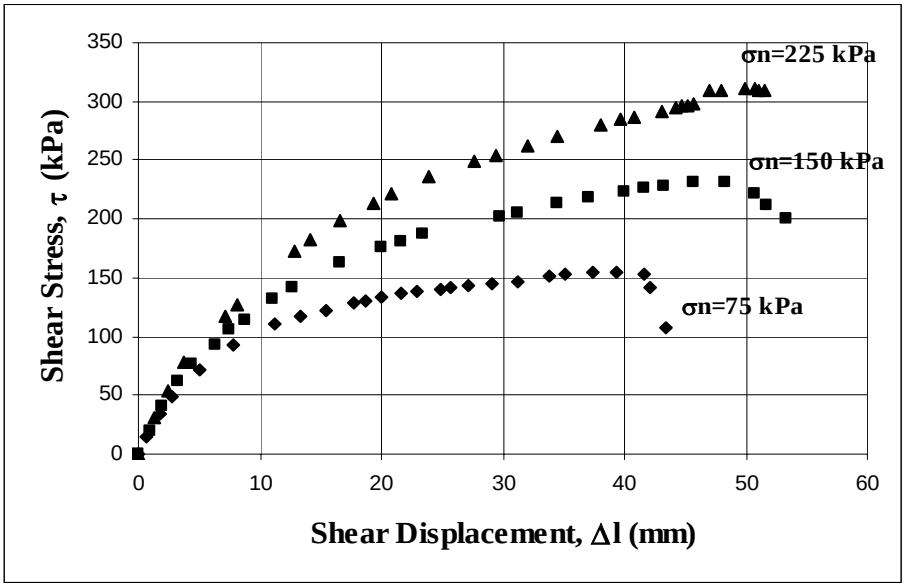

Figure 6.5 Shear stress versus shear displacement curves for -4% of OMC.

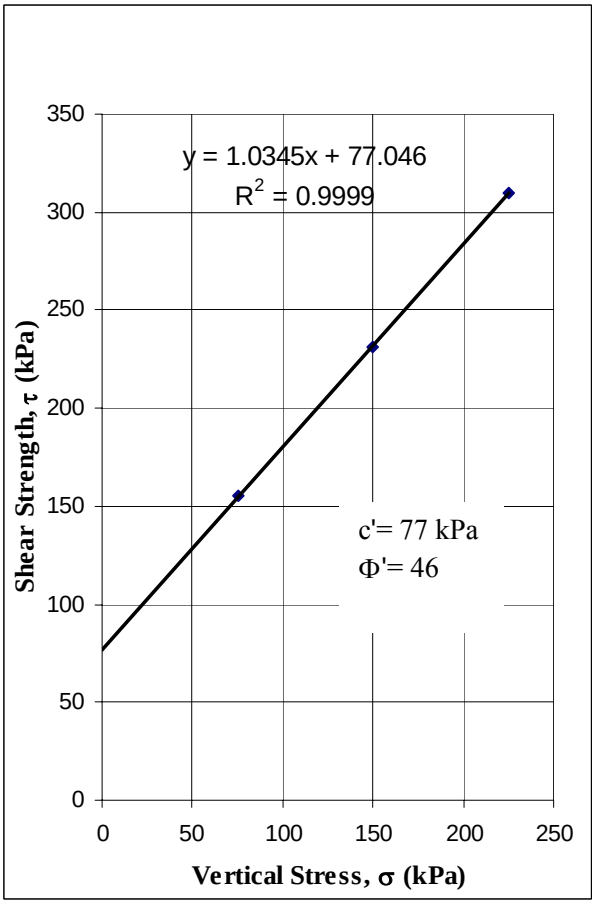

Figure 6.6 Vertical stress versus shear strength graph for -4% of OMC.

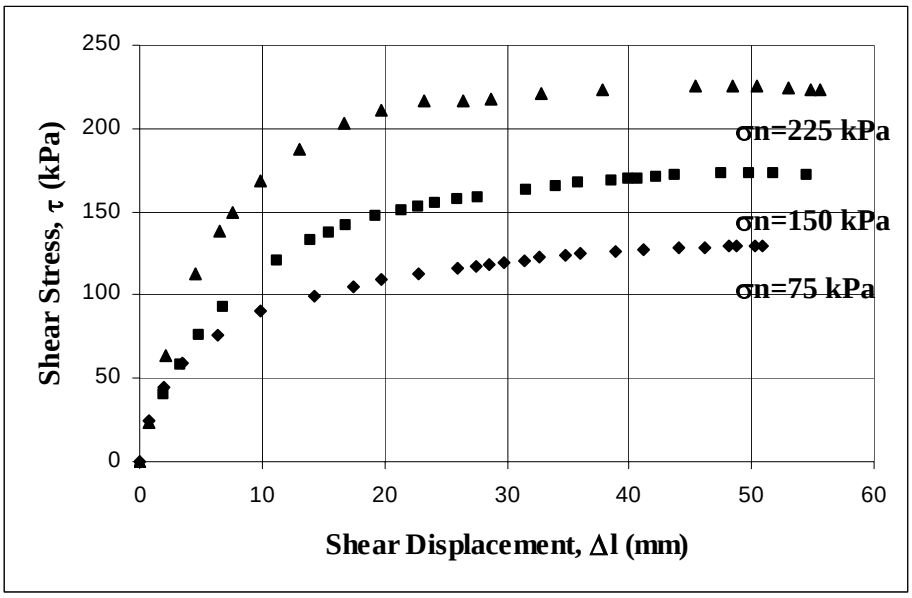

Figure 6.7 Shear stress versus shear displacement curves for -2% of OMC.

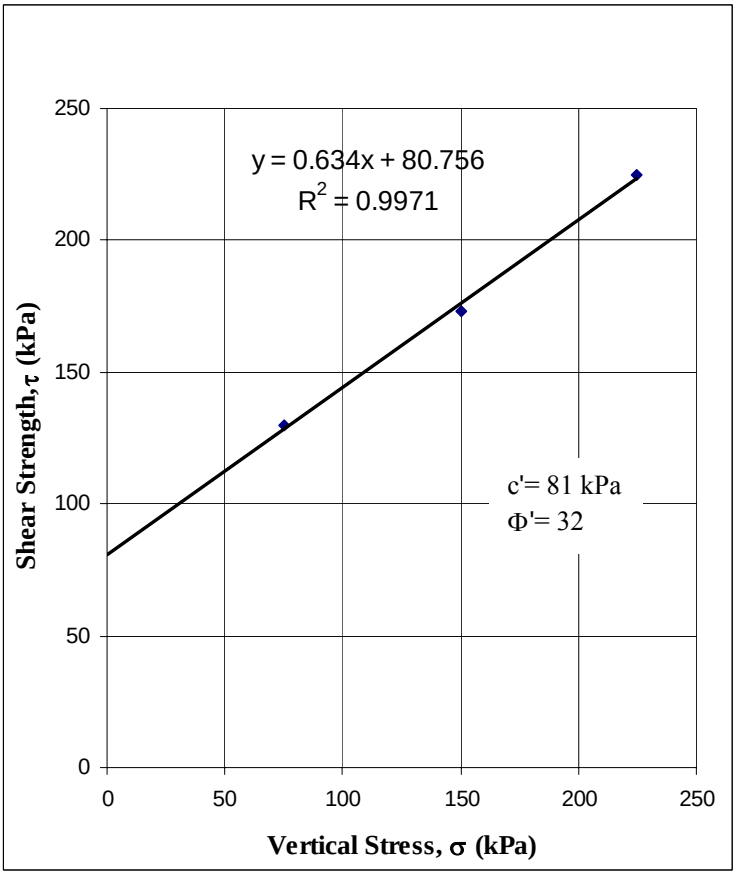

Figure 6.8 Vertical stress versus shear strength graph for -2% of OMC.

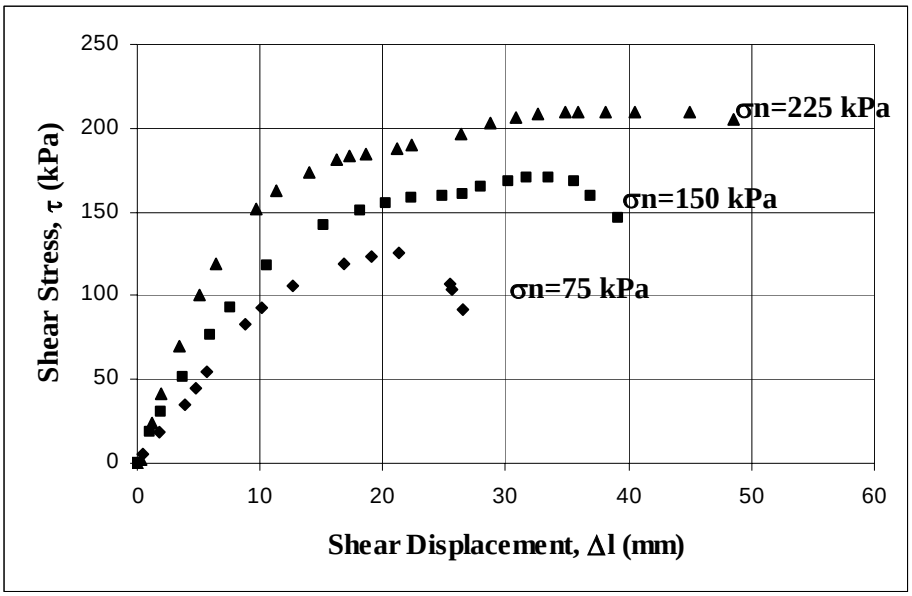

Figure 6.9 Shear stress versus shear displacement curves for OMC.

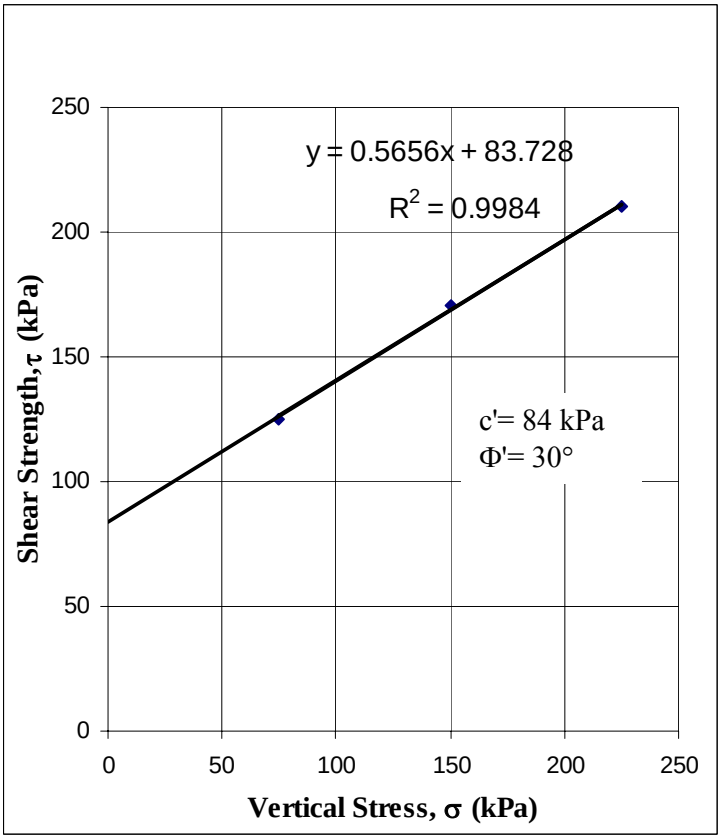

Figure 6.10 Vertical stress versus shear strength graph for OMC.

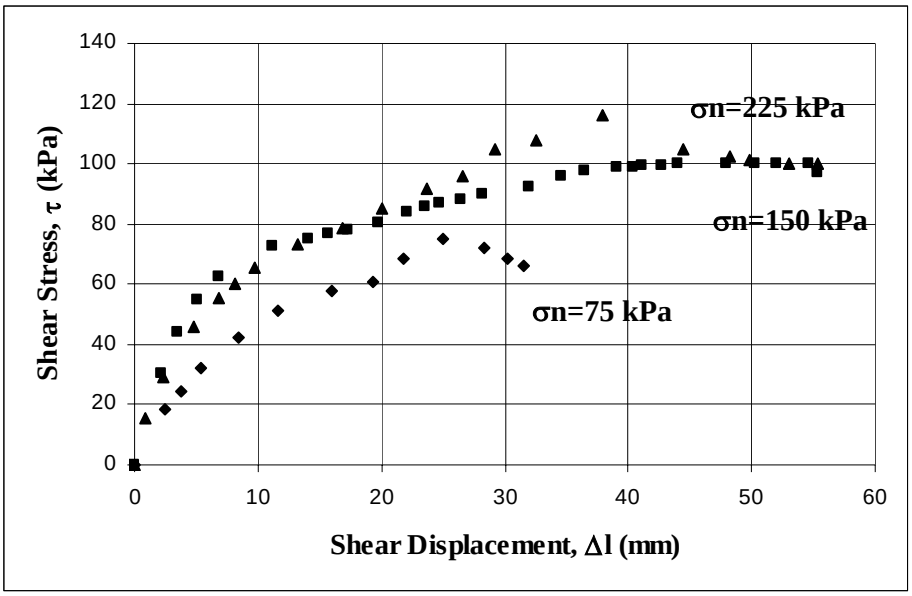

Figure 6.11 Shear stress versus shear displacement curves for +2% of OMC.

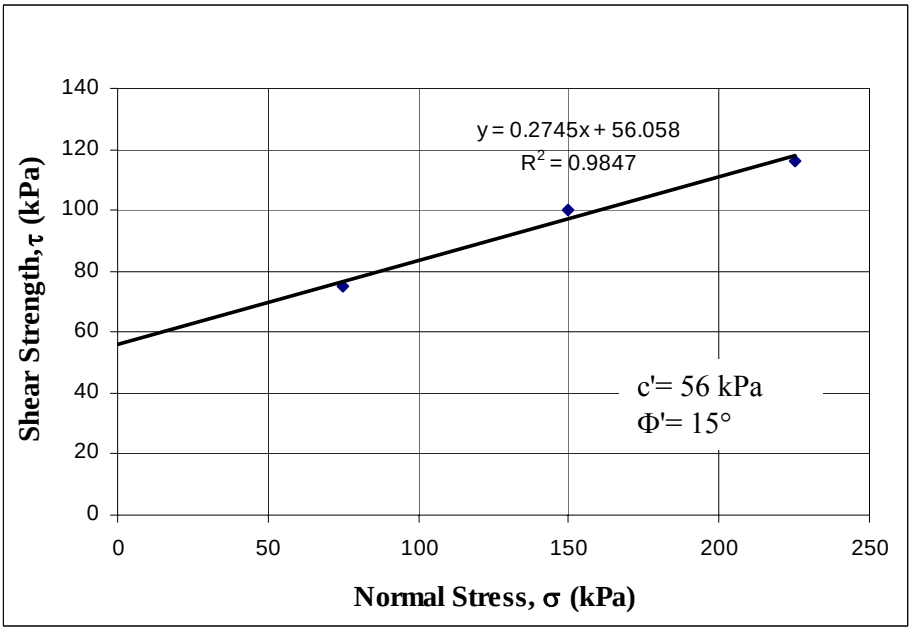

Figure 6.12 Vertical stress versus shear strength graph for +2% of OMC.

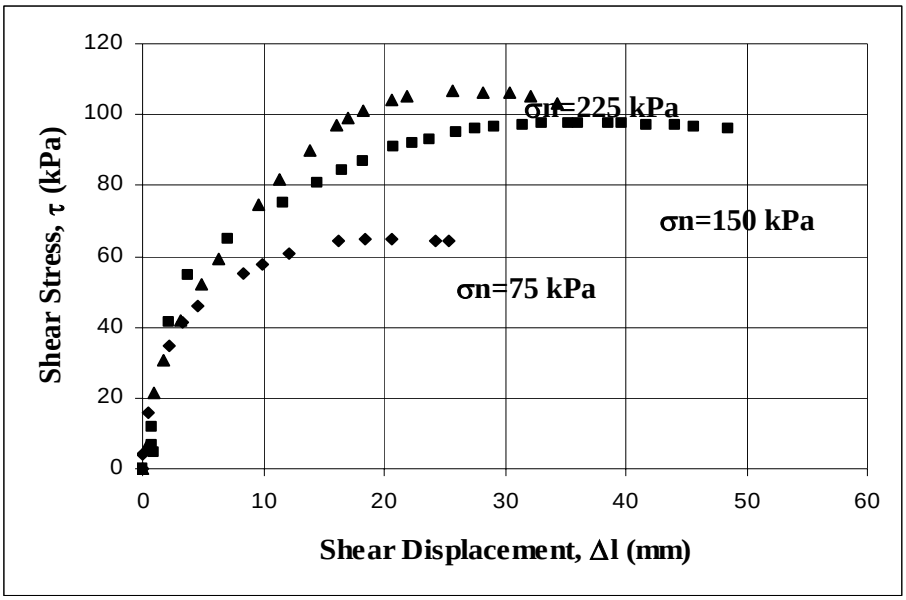

Figure 6.13 Shear stress versus shear displacement curves for +4% of OMC.

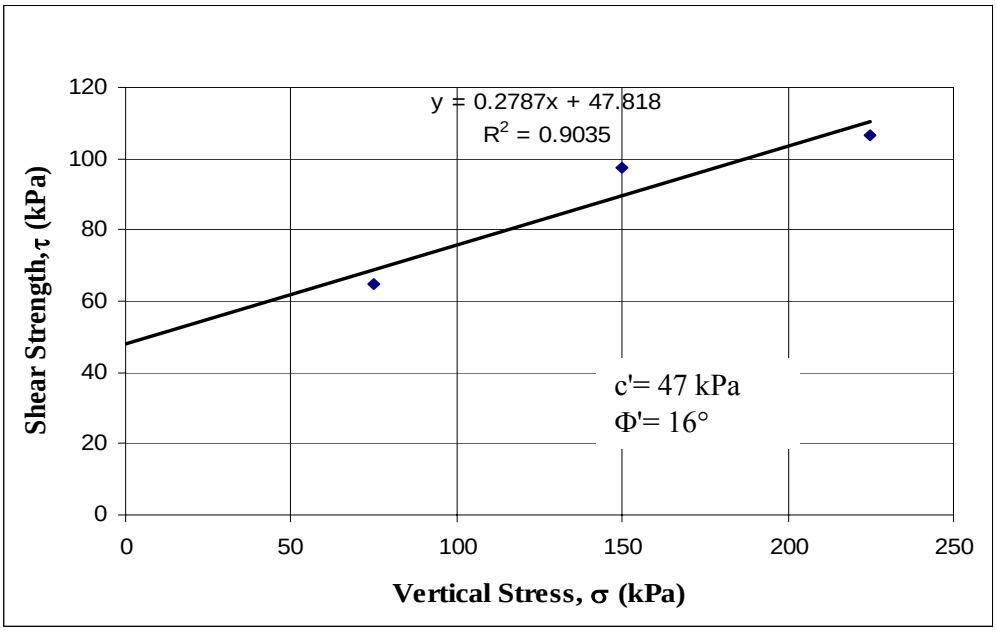

Figure 6.14 Vertical stress versus shear strength graph for +4% of OMC.

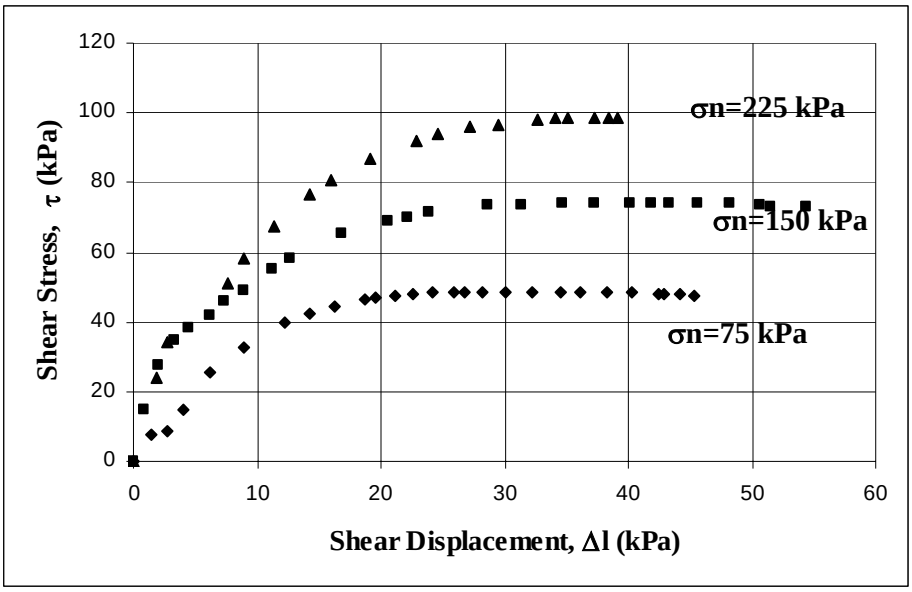

Figure 6.15 Shear stress versus shear displacement curves for +6% of OMC.

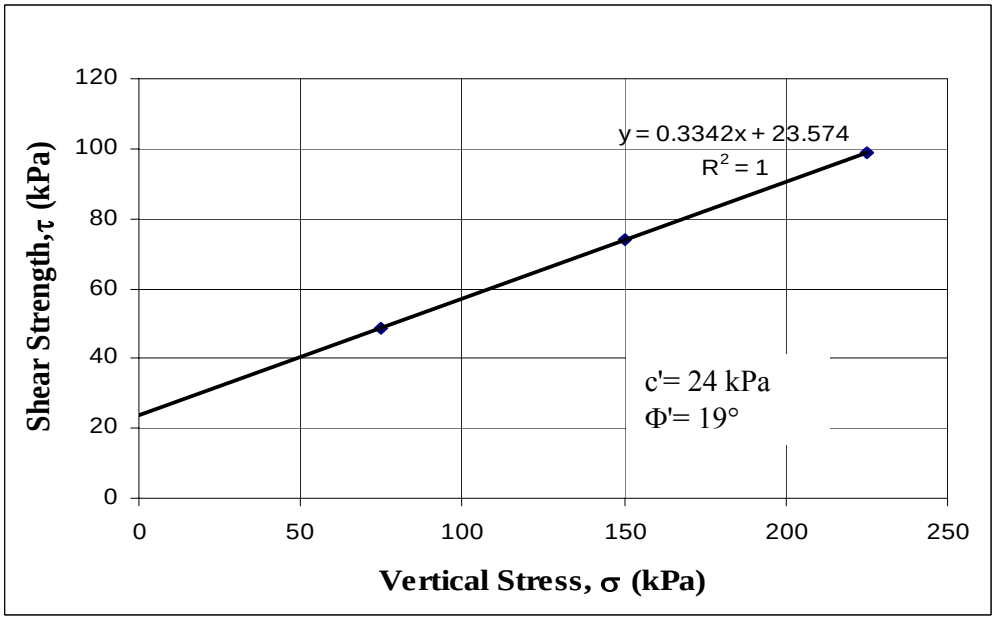

Figure 6.16 Vertical stress versus shear strength graph for +6% of OMC.

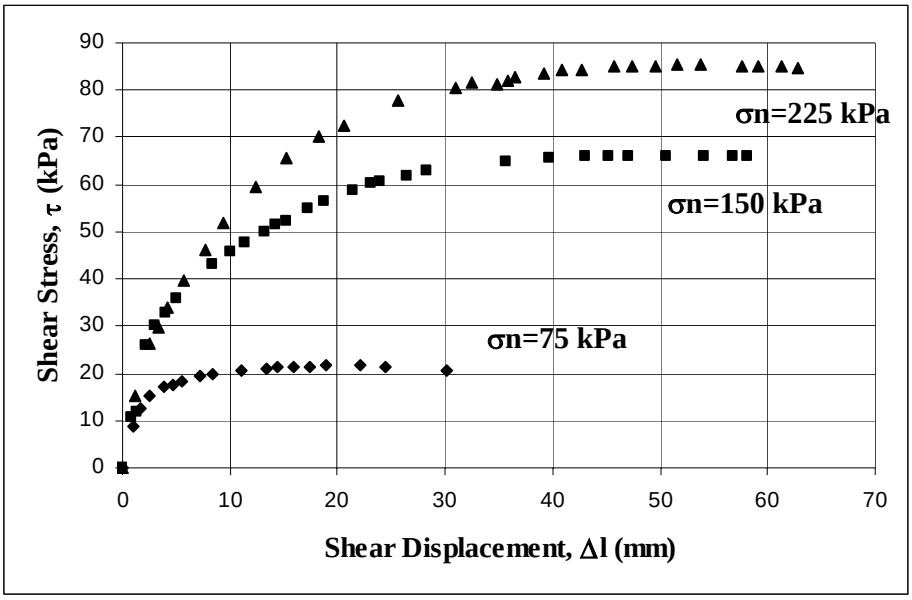

Figure 6.17 Shear stress versus shear displacement curves for -6% of OMC for soaked samples.

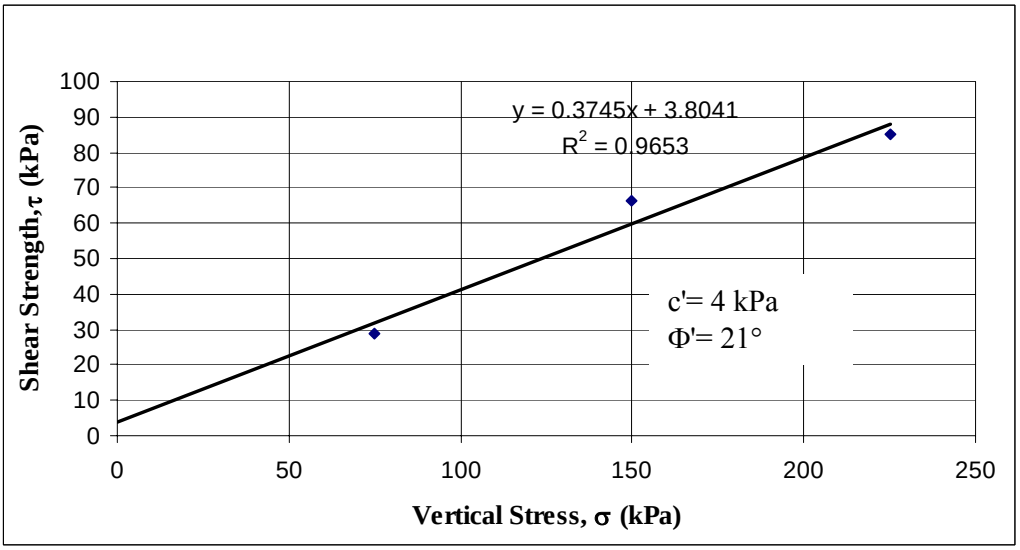

Figure 6.18 Vertical stress versus shear strength graph for -6% of OMC for soaked samples.

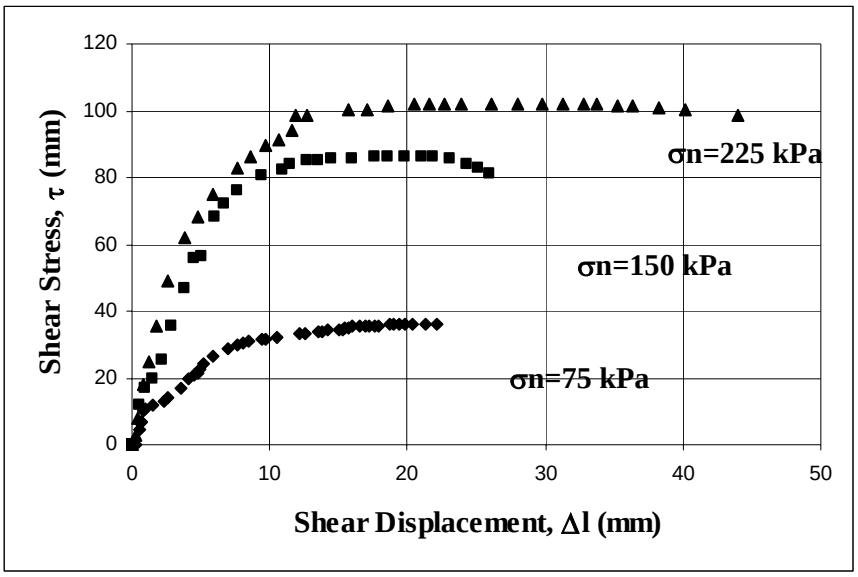

Figure 6.19 Shear stress versus shear displacement curves for -4% of OMC for soaked samples.

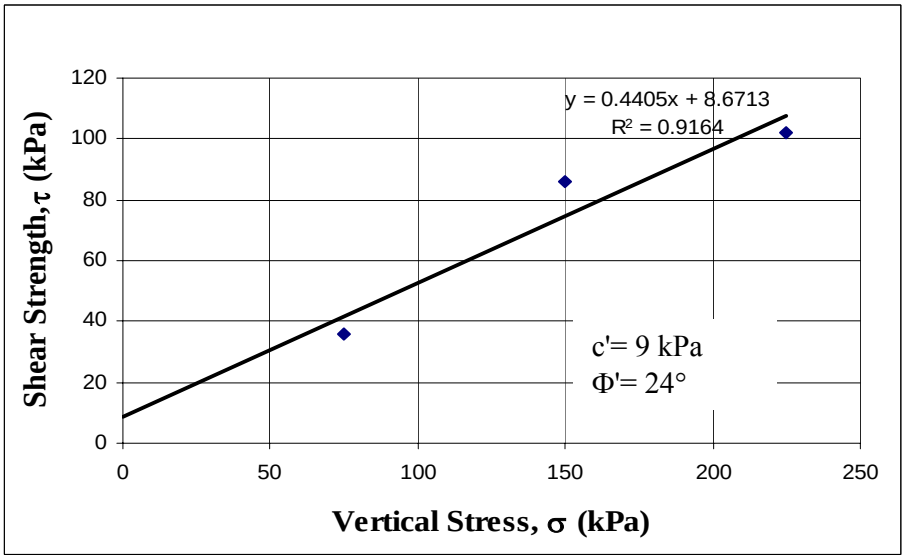

Figure 6.20 Vertical stress versus shear strength graph for -4% of OMC for soaked samples.

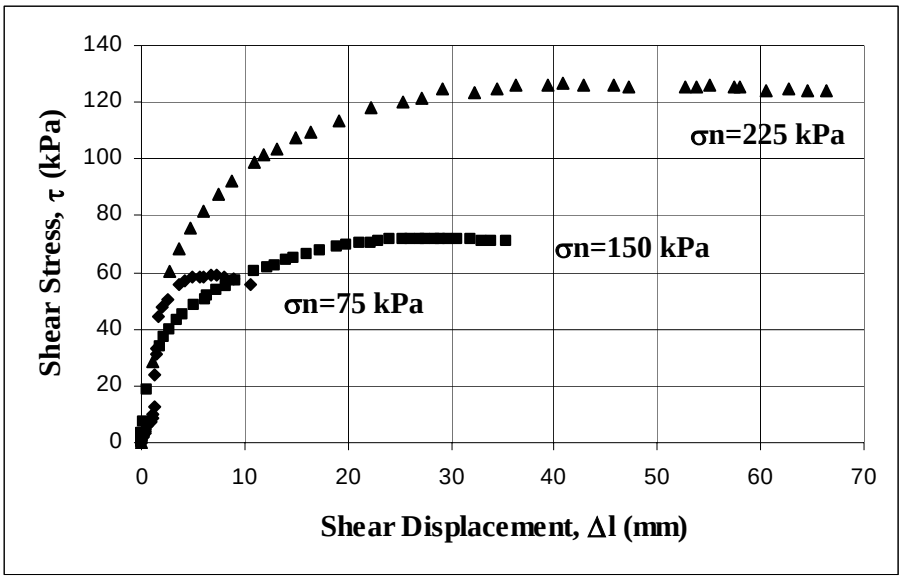

Figure 6.21 Shear stress versus shear displacement curves for -2% of OMC for soaked samples.

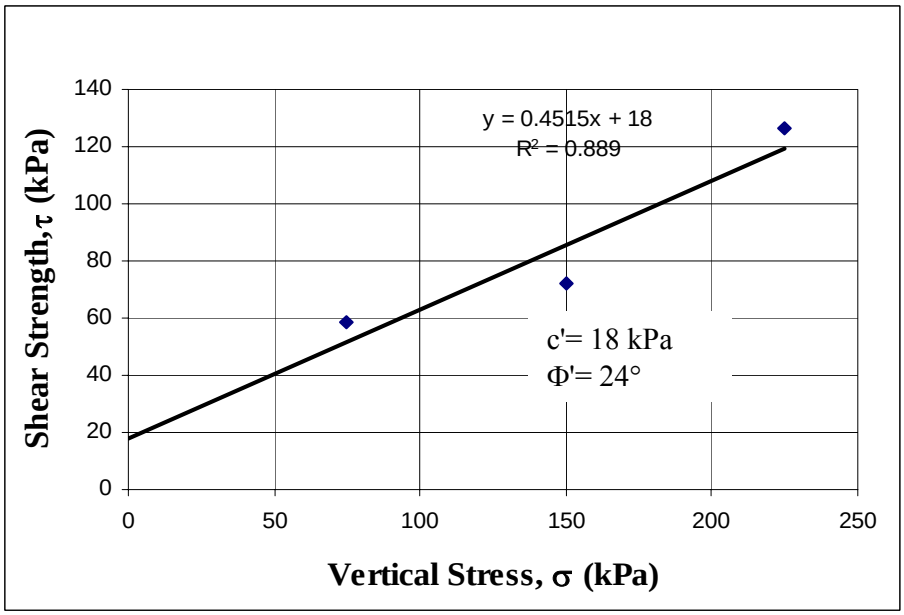

Figure 6.22 Vertical stress versus shear strength graph for -2% of OMC for soaked samples.

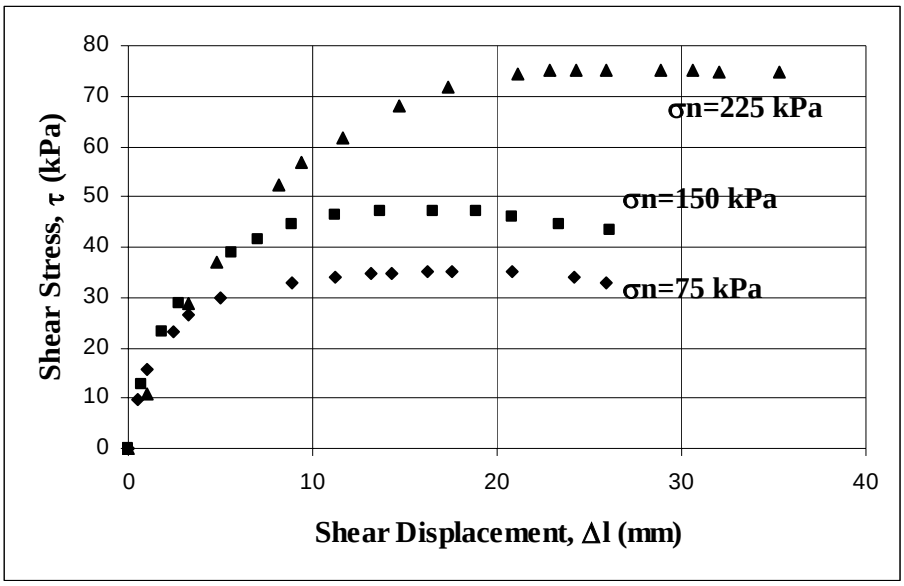

Figure 6.23 Shear stress versus shear displacement curves of OMC for soaked samples.

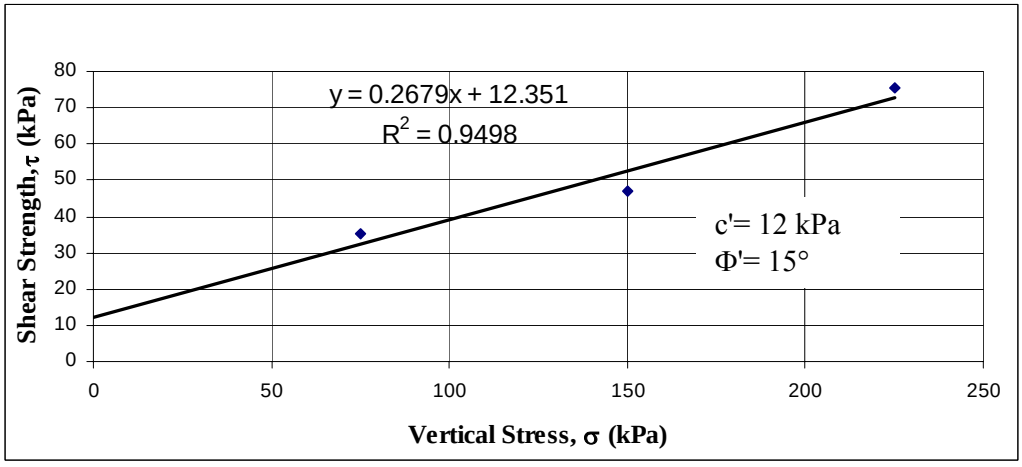

Figure 6.24 Vertical stress versus shear strength graph of OMC for soaked samples.

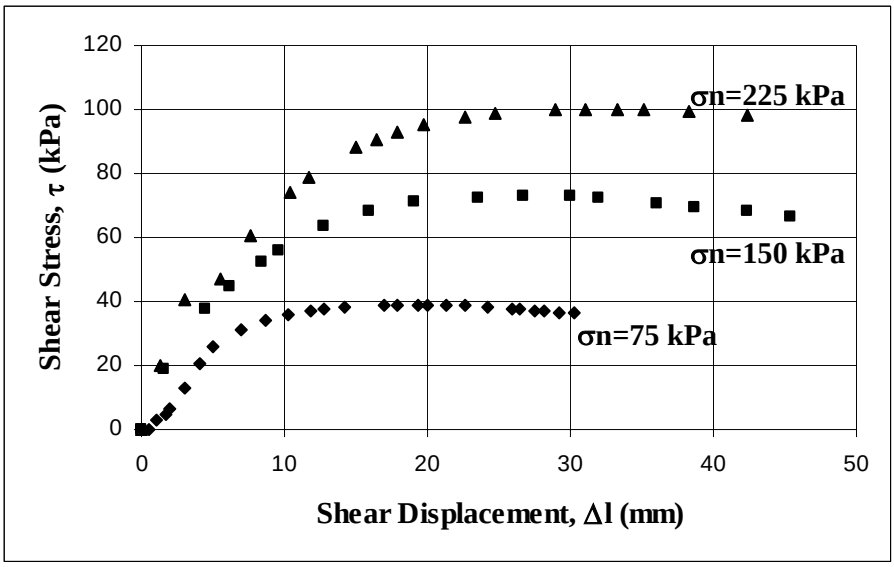

Figure 6.25 Shear stress versus shear displacement curves for +2% of OMC for soaked samples.

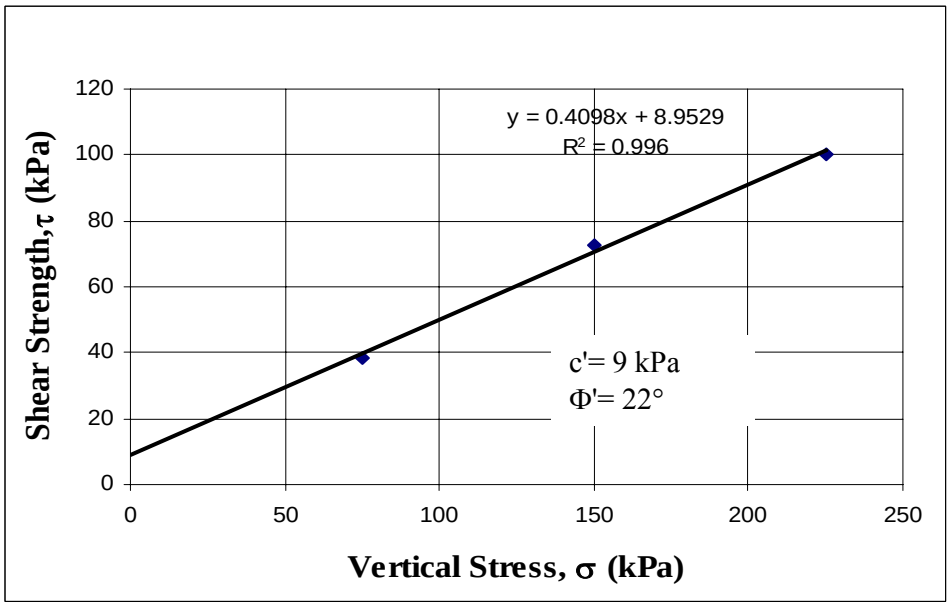

Figure 6.26 Vertical stress versus shear strength graph for +2% of OMC for soaked samples.

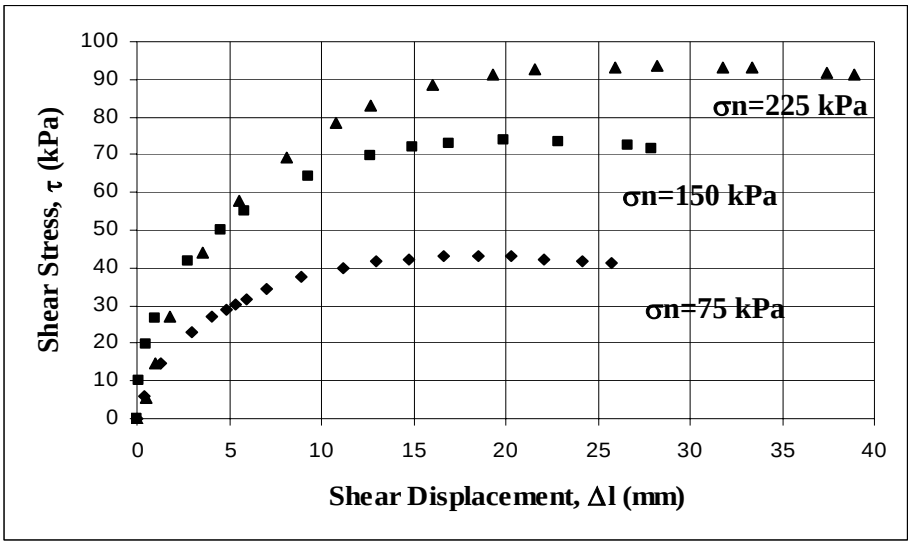

Figure 6.27 Shear stress versus shear displacement curves for +4% of OMC for soaked samples.

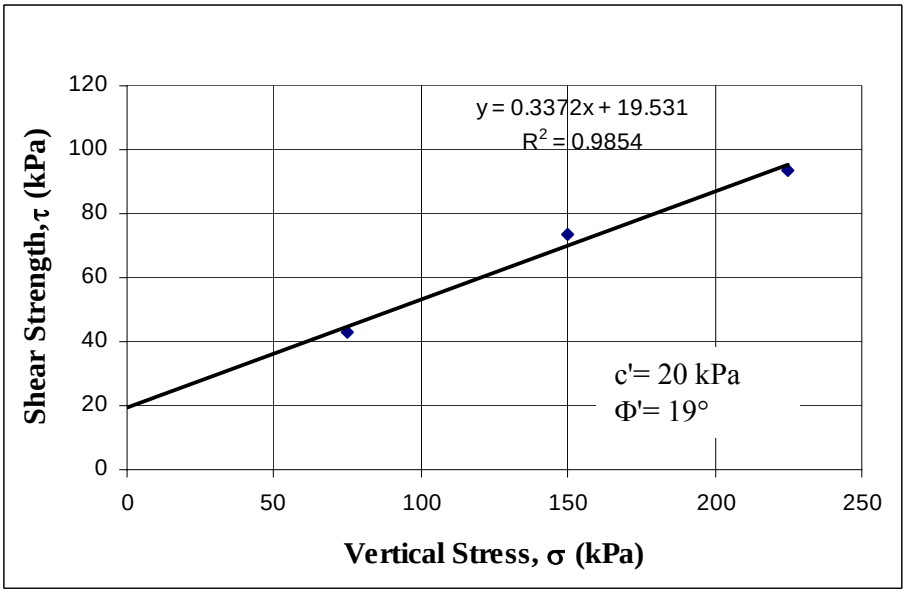

Figure 6.28 Vertical stress versus shear strength graph for +4% of OMC for soaked samples.

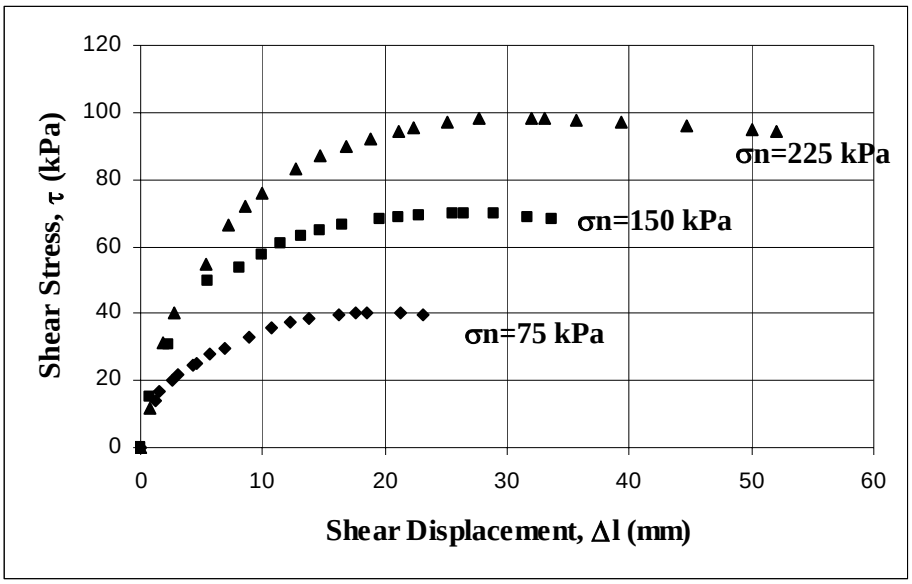

Figure 6.29 Shear stress versus shear displacement curves for +6% of OMC for soaked samples.

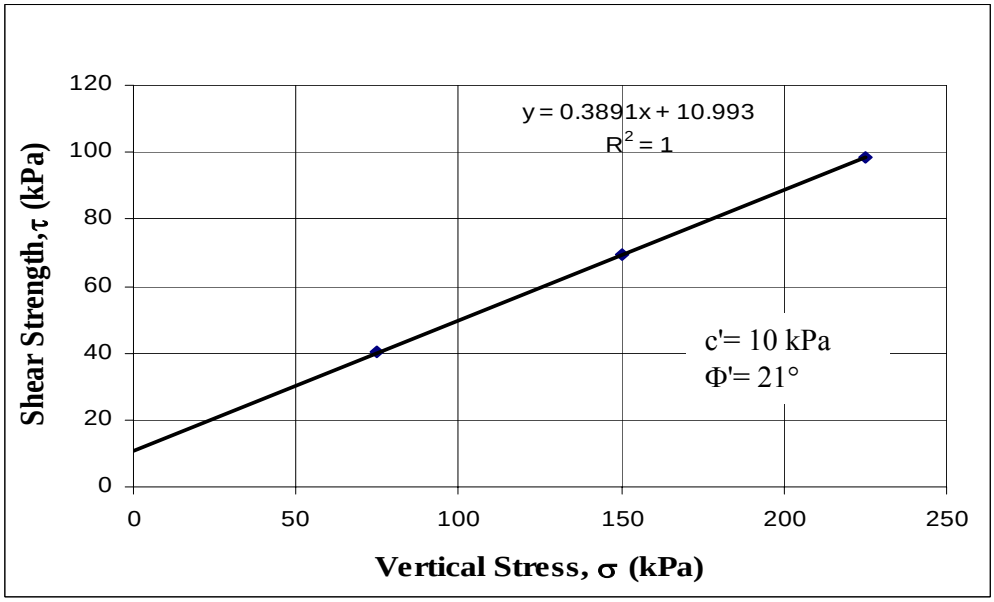

Figure 6.30 Vertical stress versus shear strength graph for +6% of OMC for soaked samples

6.3 Comparision of Direct Shear Results for As Compacted and Soaked Samples

The comparision of the shear strength parameters of the samples at compaction moisture content and for soaked samples are shown in Figures 6.31 – 6.37.

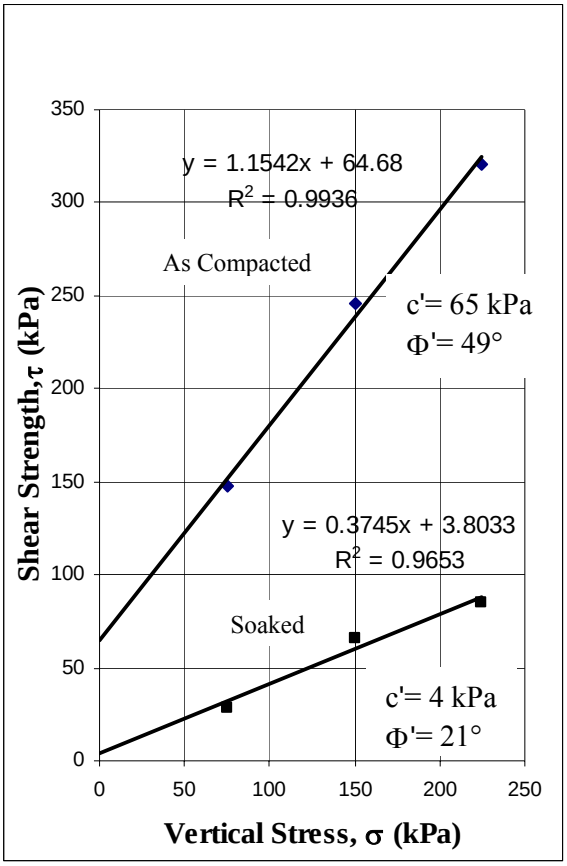

Figure 6.31 Comparison of vertical stress versus shear strength graphs of both soaked and as compacted samples for -6% of OMC.

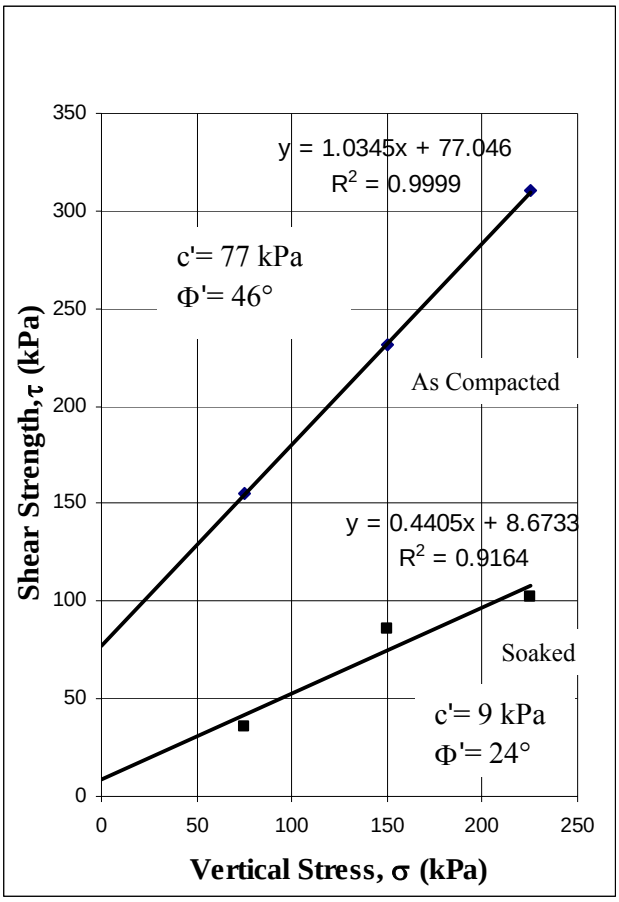

Figure 6.32 Comparison of vertical stress versus shear strength graphs of both soaked and as compacted samples for -4% of OMC.

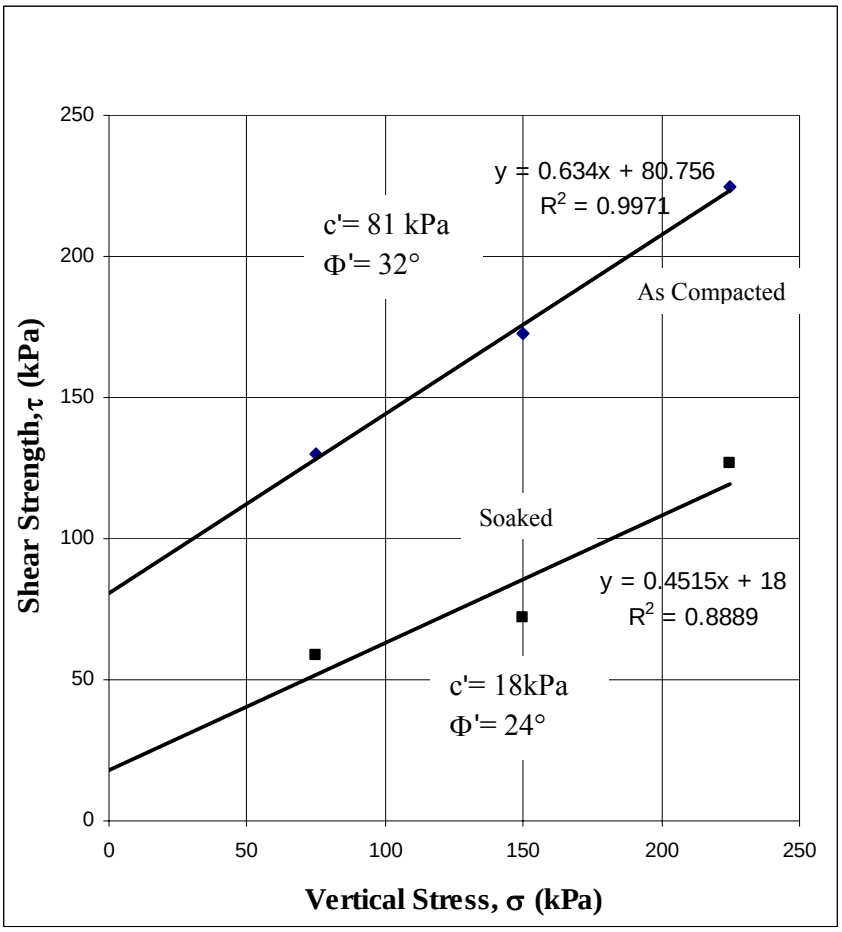

Figure 6.33 Comparison of vertical stress versus shear strength graphs of both soaked and as compacted samples for -2% of OMC.

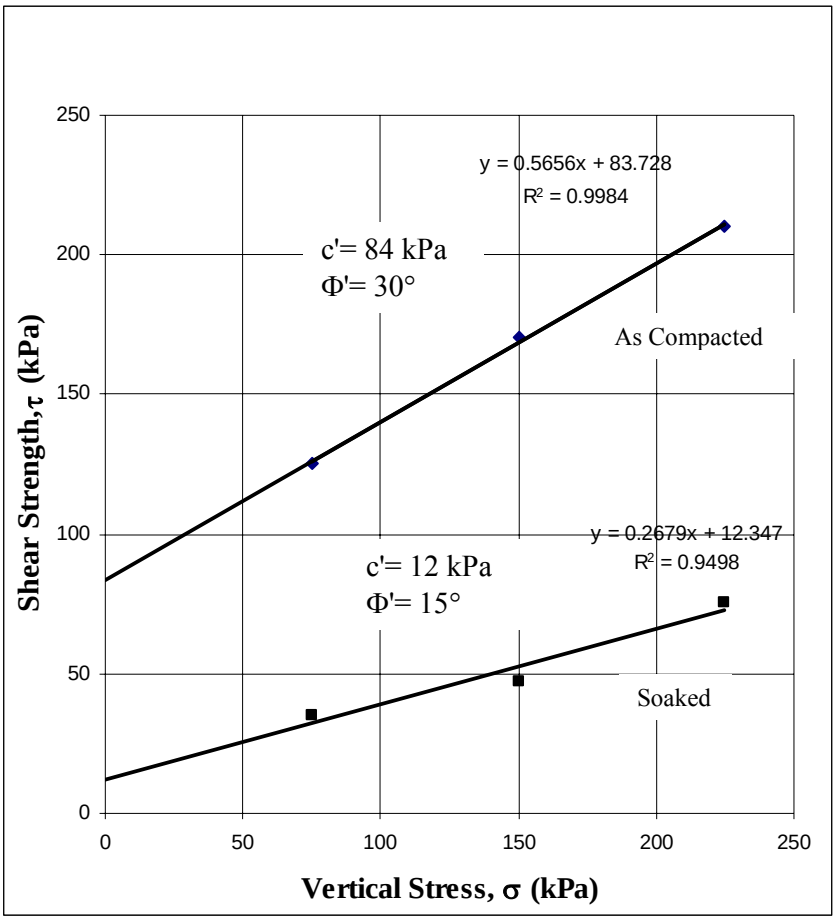

Figure 6.34 Comparison of vertical stress versus shear strength graphs of both soaked and as compacted samples for OMC.

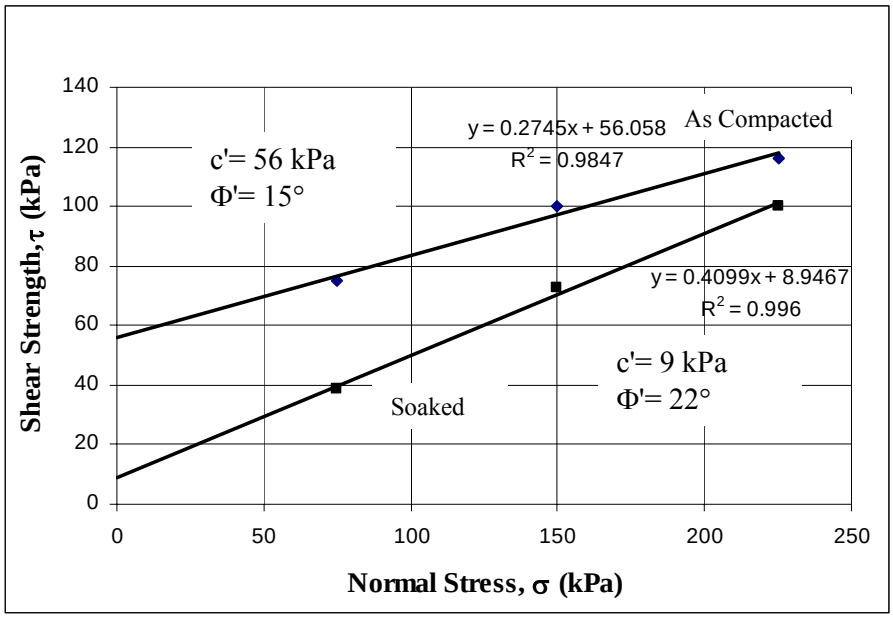

Figure 6.35 Comparison of vertical stress versus shear strength graphs of both soaked and as compacted samples for +2% of OMC.

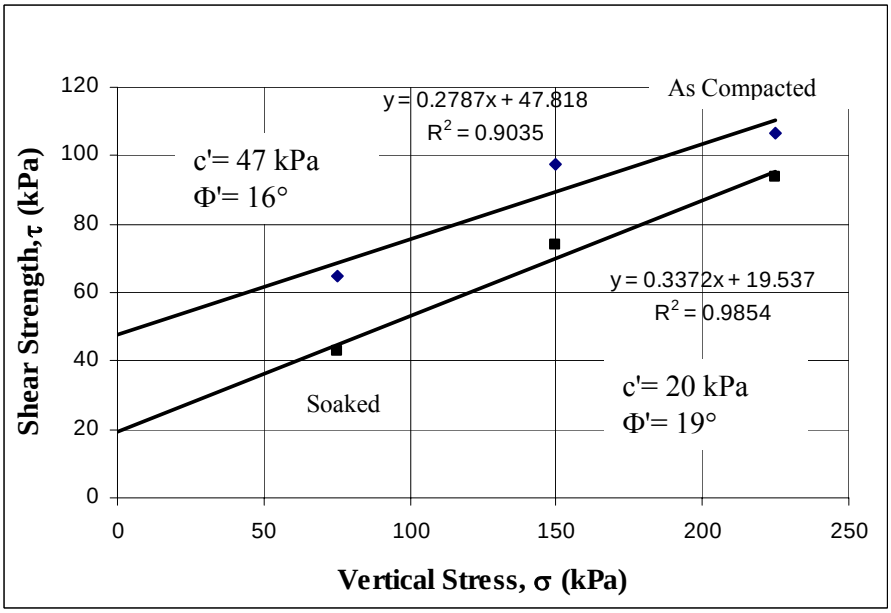

Figure 6.36 Comparison of vertical stress versus shear strength graphs of both soaked and as compacted samples for +4% of OMC.

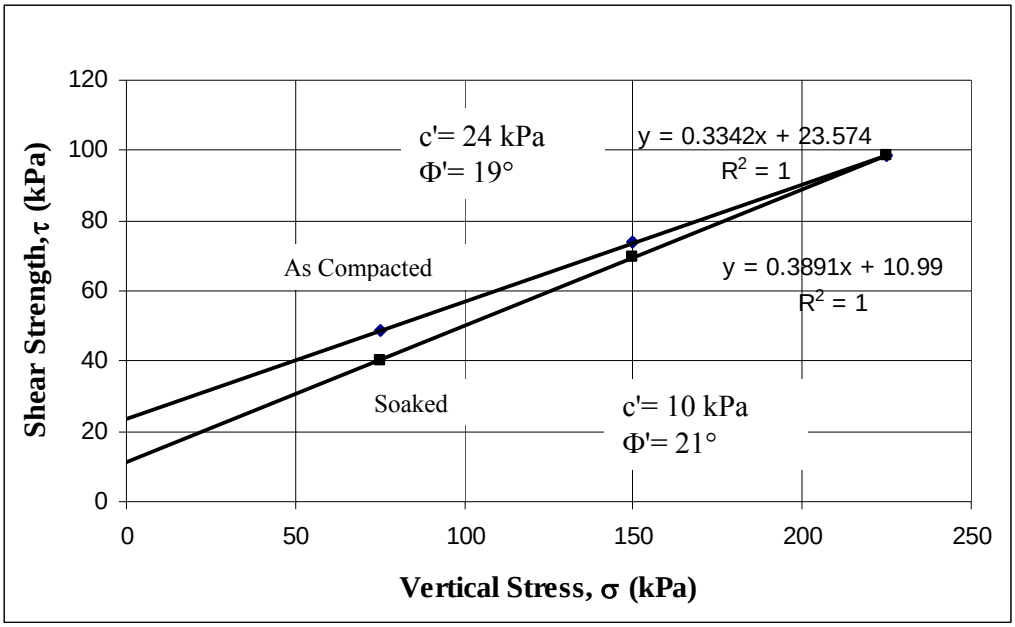

Figure 6.37 Comparison of vertical stress versus shear strength graphs of both soaked and as compacted samples for +6% of OMC.

The shear strength parameters for all cases are given in Table 6.3.

Table 6.3 Comparision of direct shear results for soaked and as compacted samples

Sample	As Compacted Parameters		Soaked Parameters	
	c' (kPa)	Φ' (°)	c' (kPa)	Φ' (°)
-6% of OMC	65	49	4	21
-4% of OMC	77	46	9	24
-2% of OMC	81	32	18	24
OMC	84	30	12	15
+2% of OMC	56	15	9	22
+4% of OMC	47	16	20	19
+6% of OMC	24	19	10	21

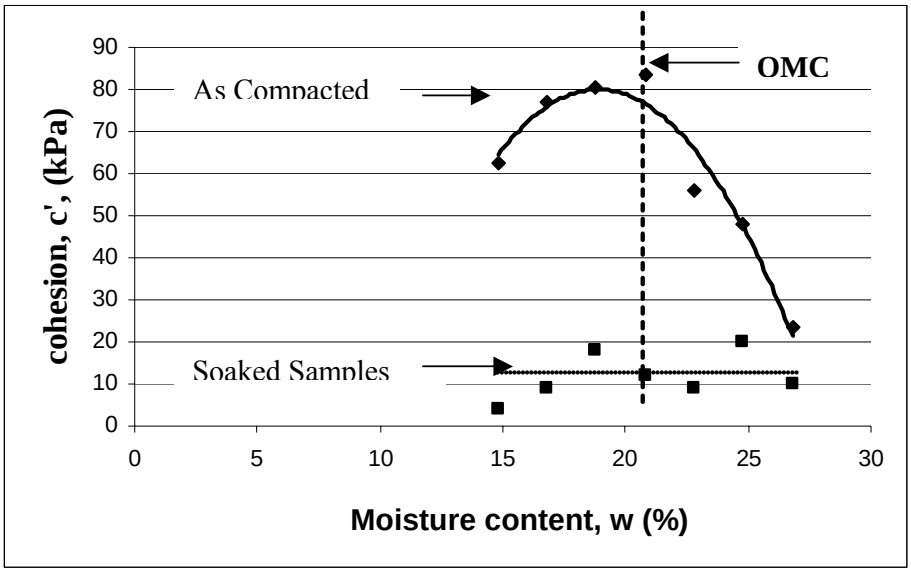

Figure 6.38 Water content versus cohesion graph for both soaked and as compacted samples

The behavior of cohesion versus moisture content is illustrated on Figure 6.38. The cohesion exhibits an increasing trend up to OMC and then drop. For soaked samples cohesion value is almost constant (c'=12 kPa).

As it can be seen from Figure 6.38 when come close to the saturation water content (27%), c' values of the as compacted samples and soaked samples come closer, and this cause a decrease in shear strength of the samples.

Micheals (1959) explained the reduction of cohesion with decreasing moisture content below OMC in unsaturated compacted clays as follows "as in conventional laboratory tests, the soil sample used in this study is air dried, before molding the necessary amount of water. The soil in this state consists of aggregates of clay particles, and the mass will be granular material. That is to say these aggregates may not be completely break down and some vestiges of their structure may remain in the compacted soil, even though there are indications that the material is dispersed in some areas. Thus lower magnitude of cohesion at dry side of optimum is due to the presence of clay aggregates that give rise to a granular character to soil mass (cited in Armangil, 1999)."

The reduction of the cohesion at wet side of optimum is attributed to the lubrication effect of excess water that give rise to thicker water films around clay particles. The result is a reduction in both the cohesion and the angle of internal friction with increasing water content above optimum (cited in Armangil, 1999).

The behavior of the angle of internal friction, Φ' versus moisture content is illustrated on Figure 6.39. The angle of internal friction decreases as moisture content increases up to OMC. On the wet side of OMC angle of internal friction has almost a constant value (Φ'=17°).

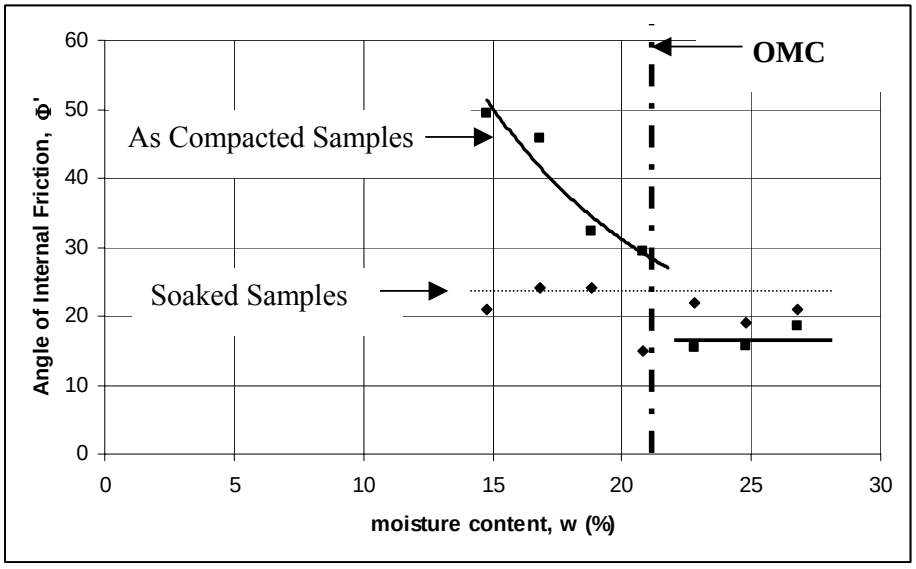

Figure 6.39 Water Content versus internal friction angle graph for both soaked and as compacted

For Φ' values, as compacted samples have a decreasing Φ' value as moisture content increase (Figure 6.39). However for soaked samples it is constant at about 22°. Also, as can be seen from Figure 6.39, on the wet side of OMC, Φ' values of as compacted and soaked samples' are close to each other.

Decreasing trend of Φ' with the increasing w is explained by Micheals (1959) as "Φ' does not depend on the moisture content but primarily depend on the particle size, when the moisture content increases the amount and size of clay aggregates is reduced, and the soil mass becomes composed of finer particles with clay phase dominating the shear strength behaviour."

6.4 Test Results of Undisturbed Samples

The shear stress – shear displacement and shear stress – normal stress relationships for undisturbed METU campus clay (at natural moisture content and for soaked samples) are given in Figures 6.40 – 6.43.

6.4.1. Shear Strength Test Results for Undisturbed Samples

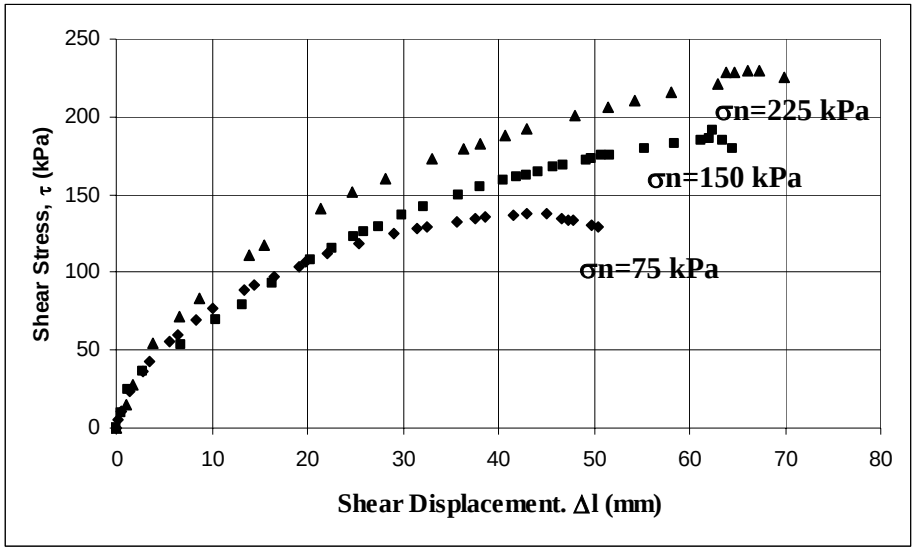

Figure 6.40 Shear stress versus shear displacement curves for undisturbed samples

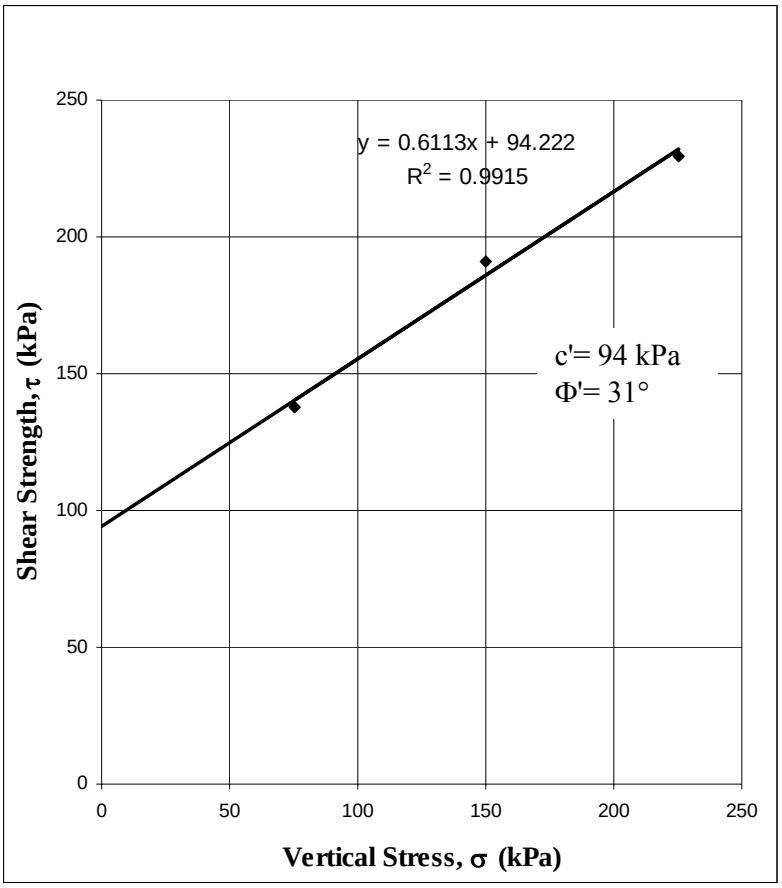

Figure 6.41 Vertical stress versus shear strength graph for undisturbed samples.

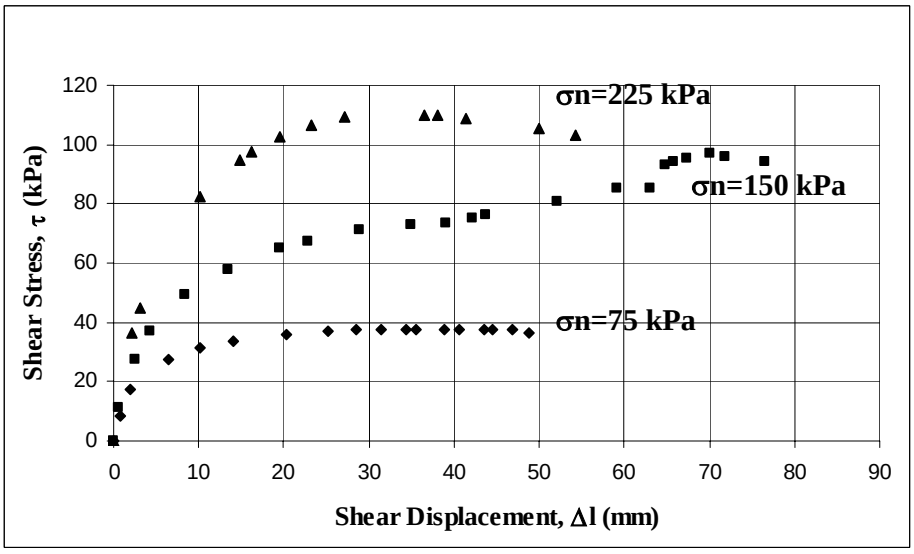

Figure 6.42 Shear stress versus shear displacement curves for undisturbed soaked samples

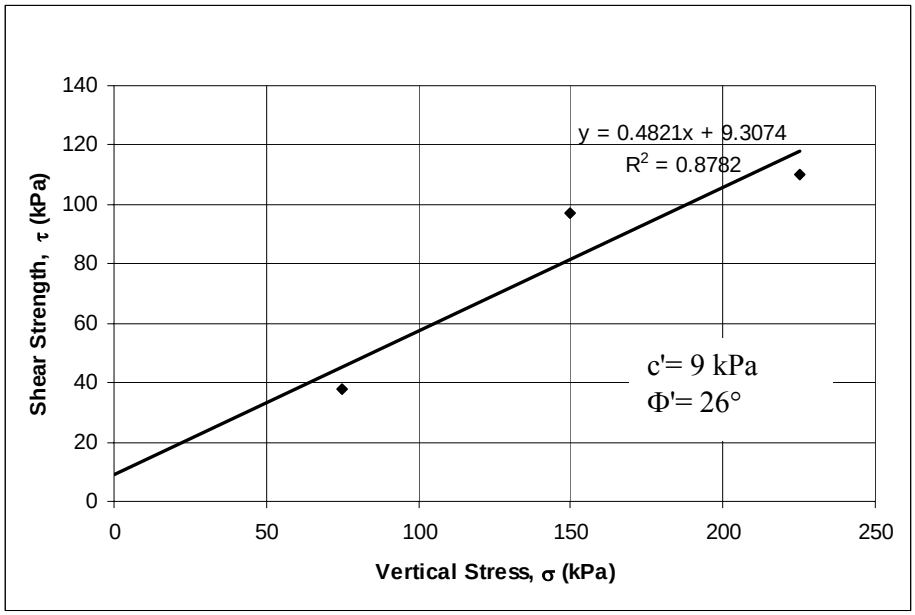

Figure 6.43 Vertical stress versus shear strength graph for undisturbed soaked samples.

Figures 6.41 and 6.43 show that for undisturbed samples Φ' and c' values are slightly higher when they are compared with remoulded samples which have almost the same inital water content and density. And when undisturbed samples soaked, they again show a behaviour similar to the remoulded samples. c' and Φ' decreases to the values for the remoulded samples.

6.5 Suction Test Results

The soil suction values (Total, matric and osmotic suction) measured by filter paper method are given in Table 6.4 and in Figures 6.44 – 6.47 (for normal stresses σ_n= 75, 150, and 225 kPa) for as compacted samples. The total suction values for soaked samples for σ_n= 75, 150, and 225 kPa are given in Table 6.5 and in Figures 6.48 – 6.50.

Table 6.4 Suction test results

Water content of the sample	Total Suction, Ψ (kPa)				Matric Suction, ($u_a - u_w$) (kPa)				Osmotic Suction, π (kPa)			
	As Compacted	After Removal of Normal Stress			As Compacted	After Removal of Normal Stress			As Compacted	After Removal of Normal Stress		
		75 kPa	150 kPa	225 kPa		75 kPa	150 kPa	225 kPa		75 kPa	150 kPa	225 kPa
-6% of OMC	2365	2596	4000	8865	1795	2020	3660	7450	570	576	340	1415
-4% of OMC	1707	1783	2816	4004	1091	1497	2400	3400	616	286	416	604
-2% of OMC	1161	1200	1400	1800	907	712	936	1292	254	488	464	508
OMC	876	1079	1200	1300	642	548	680	790	234	531	520	510
+2% of OMC	530	690	900	1010	400	275	350	403	130	415	550	607
+4% of OMC	497	658	747	792	185	372	430	480	312	286	317	312
+6% of OMC	488	634	700	780	291	384	420	520	197	250	280	260

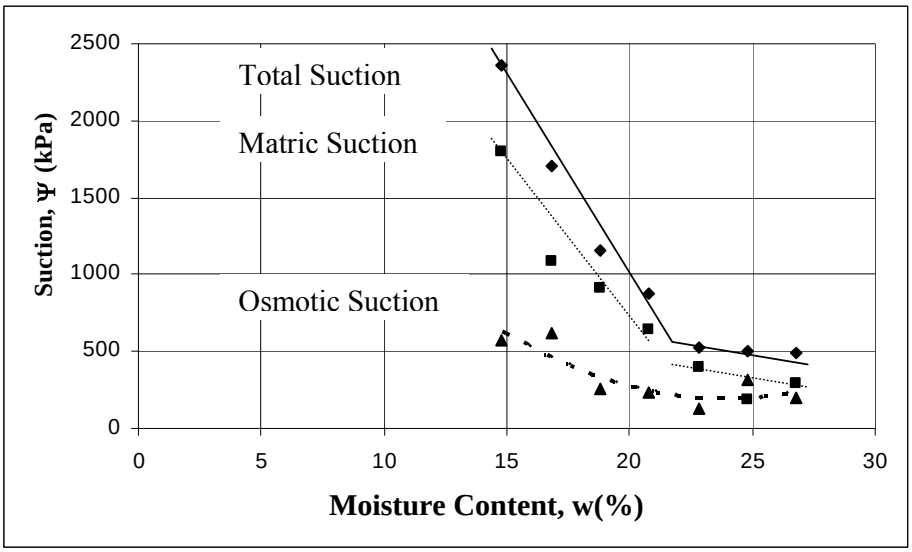

Figure 6.44 Total, matric and osmotic suction results on moisture content versus suction graph for as compacted samples.

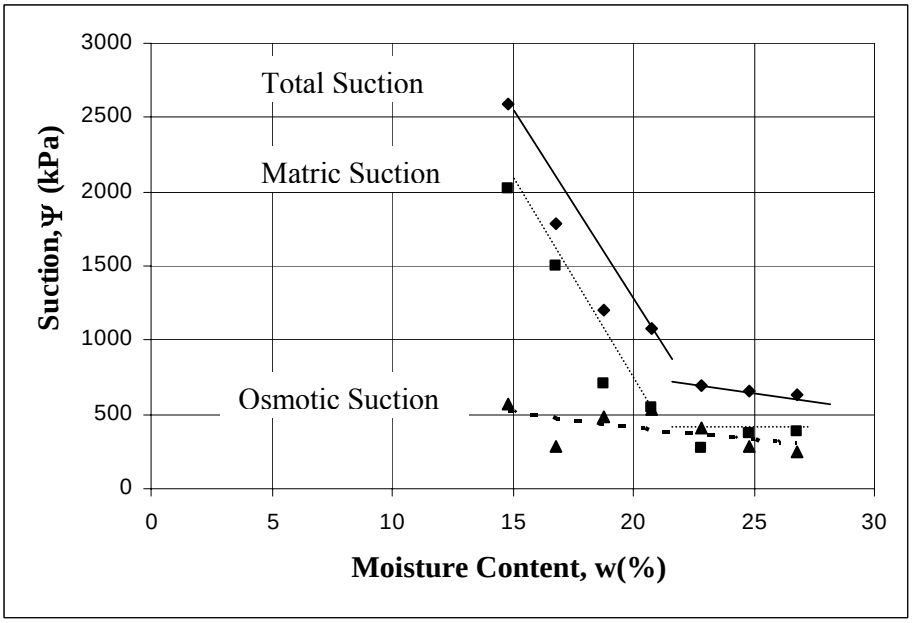

Figure 6.45 Total, matric and osmotic suction results on moisture content versus suction graph for σ_n= 75 kPa samples.

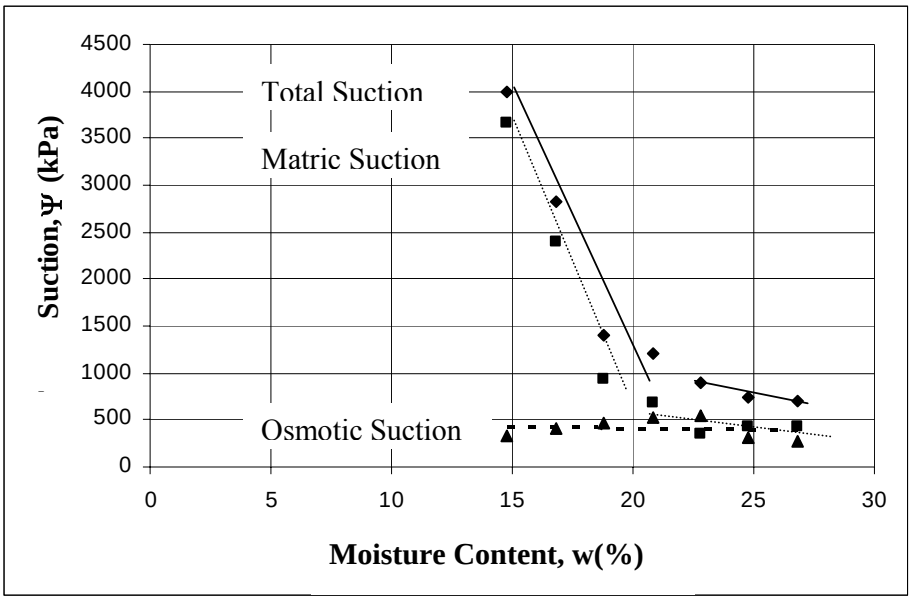

Figure 6.46 Total, matric and osmotic suction results on moisture content versus suction graph for σ_n= 150 kPa samples.

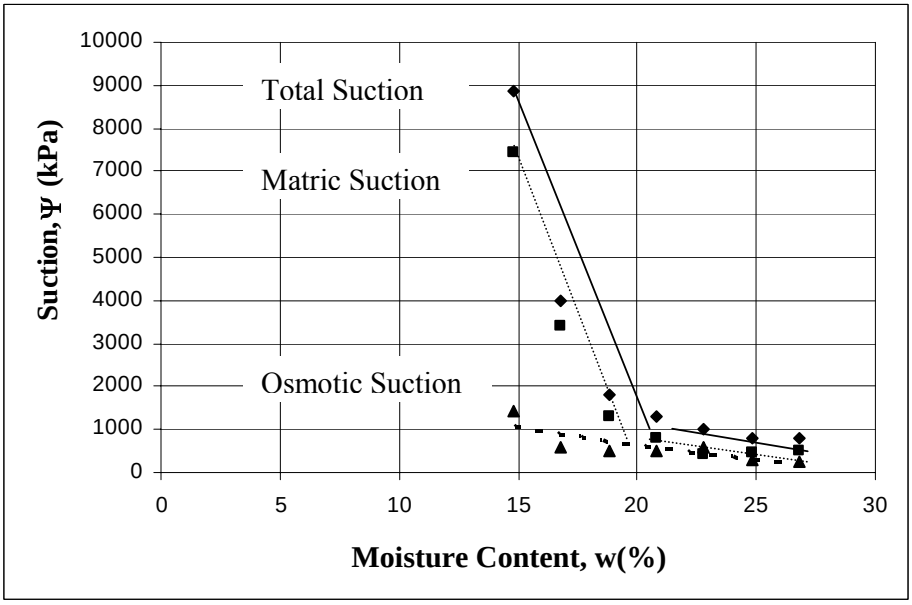

Figure 6.47 Total, matric and osmotic suction results on moisture content versus suction graph for σ_n= 225 kPa samples.

Figures 6.44-6.47 show that, for all normal pressures total, matric and osmotic suction change with moisture content are similar. Change in osmotic suction values are less than matric suction values. Also these Figures show that most of the total suction is matric suction.

Table 6.5 Suction results for soaked samples

Sample	Total Suction			Matric Suction			Osmotic Suction		
	After Removal of Normal Stress			After Removal of Normal Stress			After Removal of Normal Stress		
	75 kPa	150 kPa	225 kPa	75 kPa	150 kPa	225 kPa	75 kPa	150 kPa	225 kPa
-6% of OMC	818	988	603	188	653	391	630	335	212
-4% of OMC	602	709	810	122	223	555	480	486	255
-2% of OMC	592	712	820	90	416	400	502	296	420
OMC	492	519	803	99	389	401	393	130	402
+2% of OMC	621	725	700	105	256	159	516	469	541
+4% of OMC	497	851	1240	34	281	385	463	570	855
+6% of OMC	1012	1409	862	10	193	436	1002	1216	426

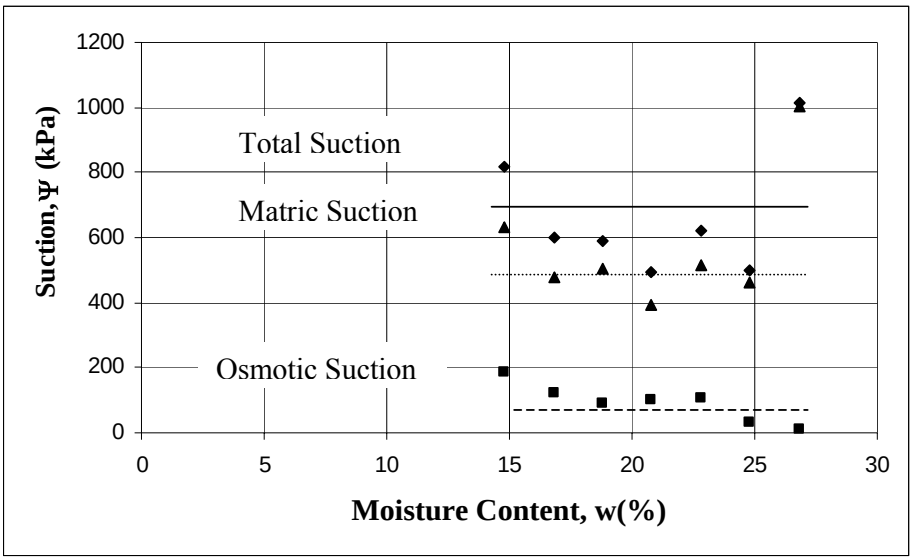

Figure 6.48 Total, matric and osmotic suction results on moisture content versus suction graph for σ_n= 75 kPa soaked samples.

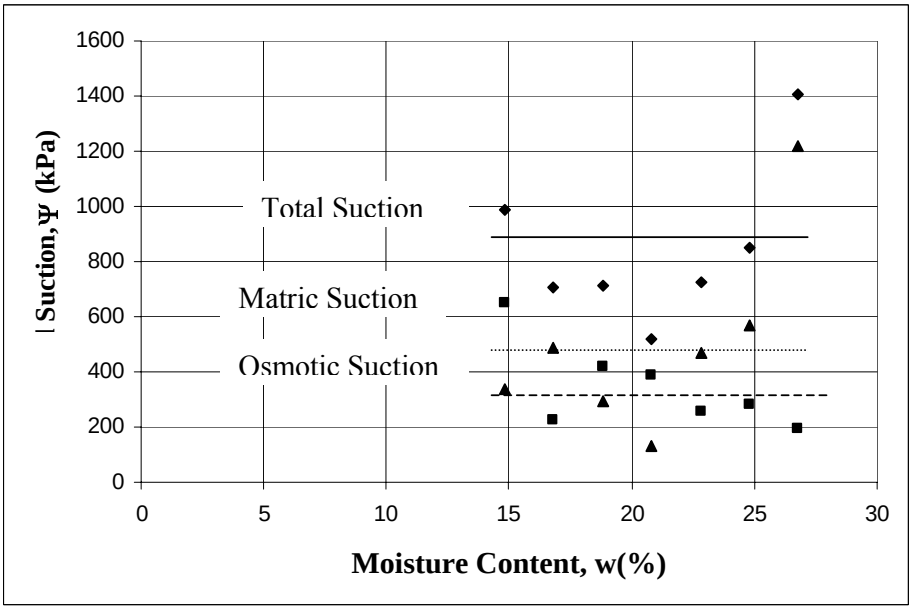

Figure 6.49 Total, matric and osmotic suction results on moisture content versus suction graph for σ_n= 150 kPa soaked samples.

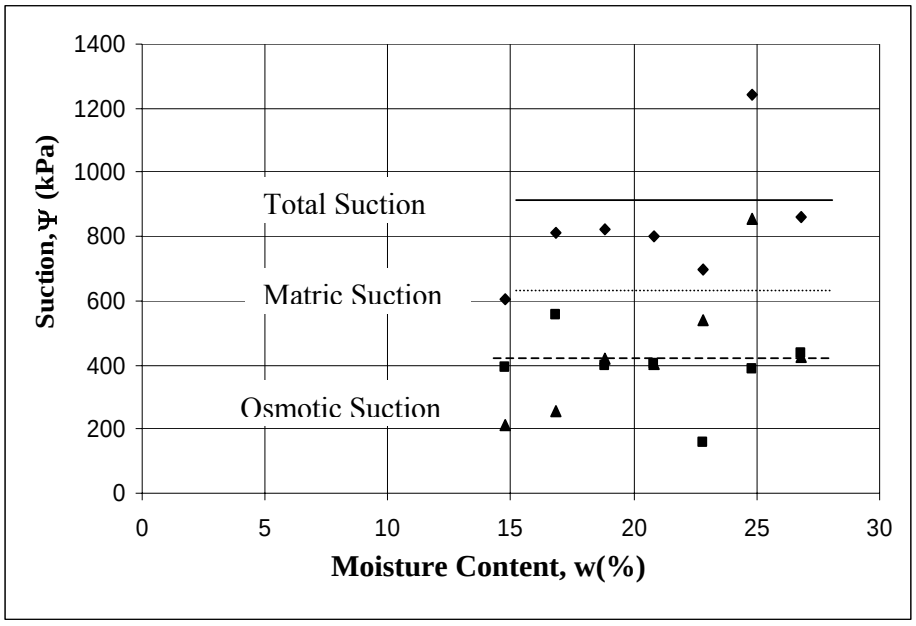

Figure 6.50 Total, matric and osmotic suction results on moisture content versus suction graph for σ_n= 225 kPa soaked samples.

When the total suction – moisture content graphs of soaked samples are compared with as compacted samples (Figures 6.44-6.47 and 6.48-6.50), the trend for compacted samples disappear due to soaking. Again there is a trend of Total suction > Matric suction > Osmotic suction. Figures 6.48 -6.50 show that, for soaked samples, total suction values are generally changing between 600 kPa and 850 kPa for all normal pressures.

6.5.1 Moisture Content and Total Suction Relationships

The moisture content versus log total suction relationships are given in Figures 6.51 – 6.54 for different σ_n values. Figures 6.51 – 6.54 indicate that the soil suction increases as the water content decreases at the dry side of optimum, and in this range of water content the moisture content versus log suction behaviour is linear (regression equations are given on the Figures).

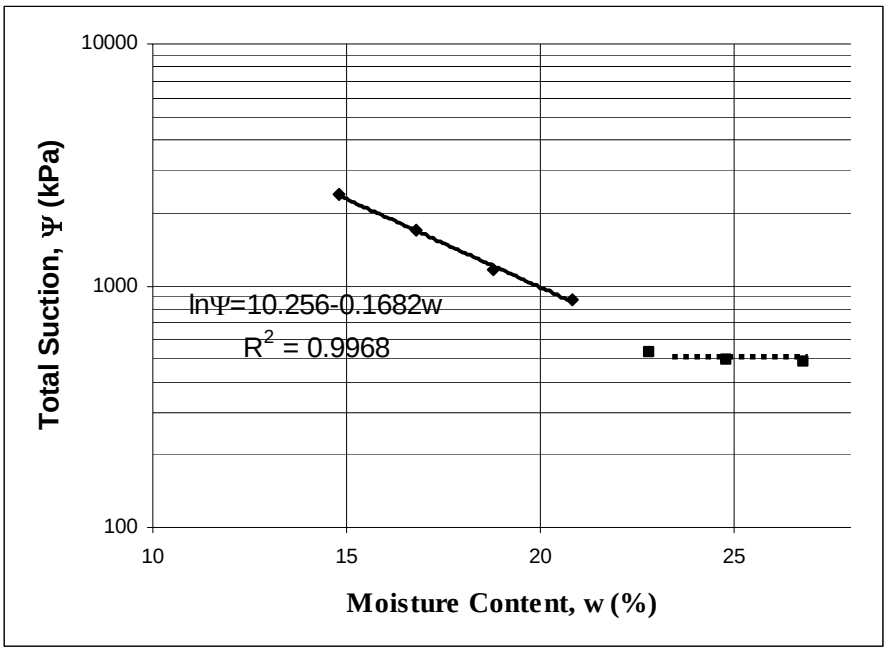

Figure 6.51 Moisture content versus total suction graph for as compacted samples.

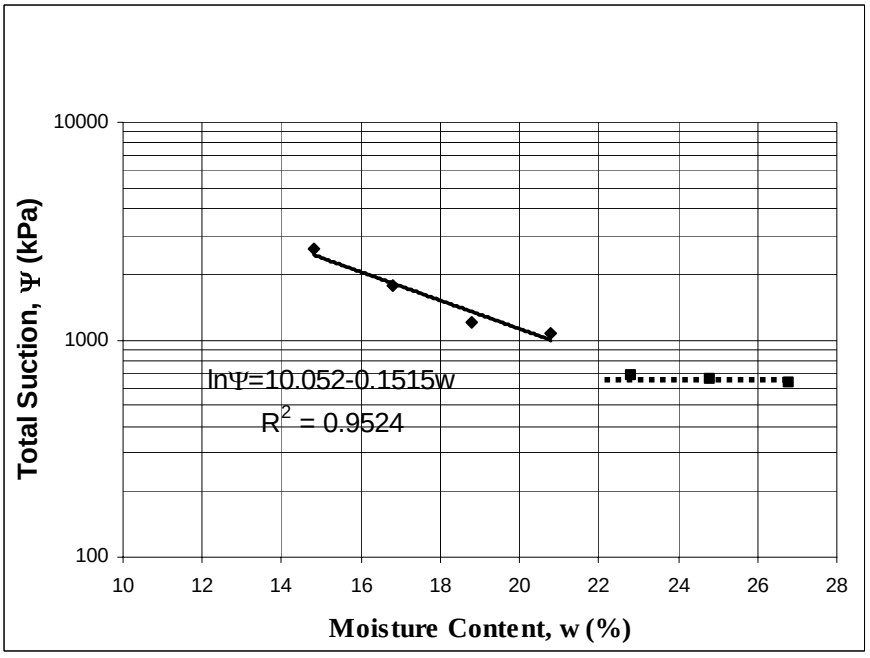

Figure 6.52 Moisture content versus total suction graph for σ_n= 75 kPa samples.

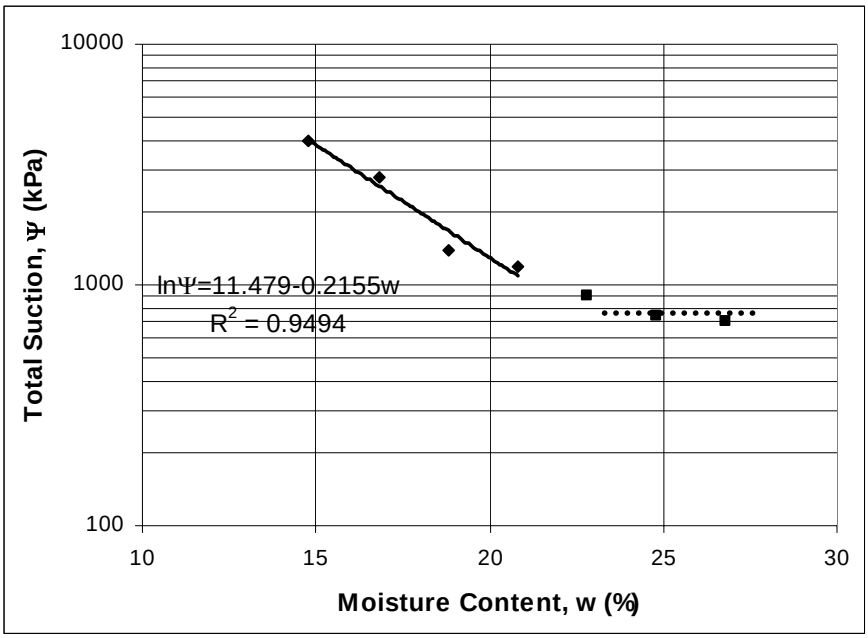

Figure 6.53 Moisture content versus total suction graph for σ_n= 150 kPa samples.

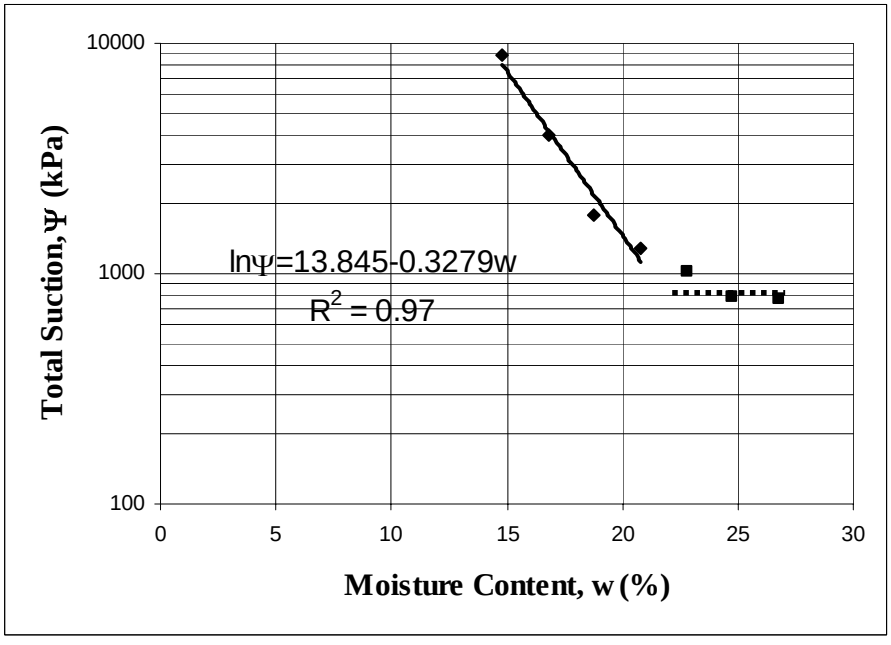

Figure 6.54 Moisture content versus total suction graph for σ_n= 225 kPa samples.

Figures 6.51 – 6.54 show that total suction decreases upto OMC and then it has an almost constant value. For the values less than OMC, change in total suction is much more than for the values on the wet side of OMC.

6.5.2 Total Suction and Shear Strength Relationships

The total suction (log) versus cohesion and total suction (log) versus angle of internal friction relationships are given in Figures 6.55-6.57 and 6.58-6.60 respectively.

Figures 6.55-6.57 show that, for all normal pressures (for as compacted samples), upto OMC, as total suction decreases, cohesion increases, at the wet side of OMC as total suction decreases cohesion decreases. Also from the graphs it can be concluded that at dry side change in cohesion is less than change in total suction.

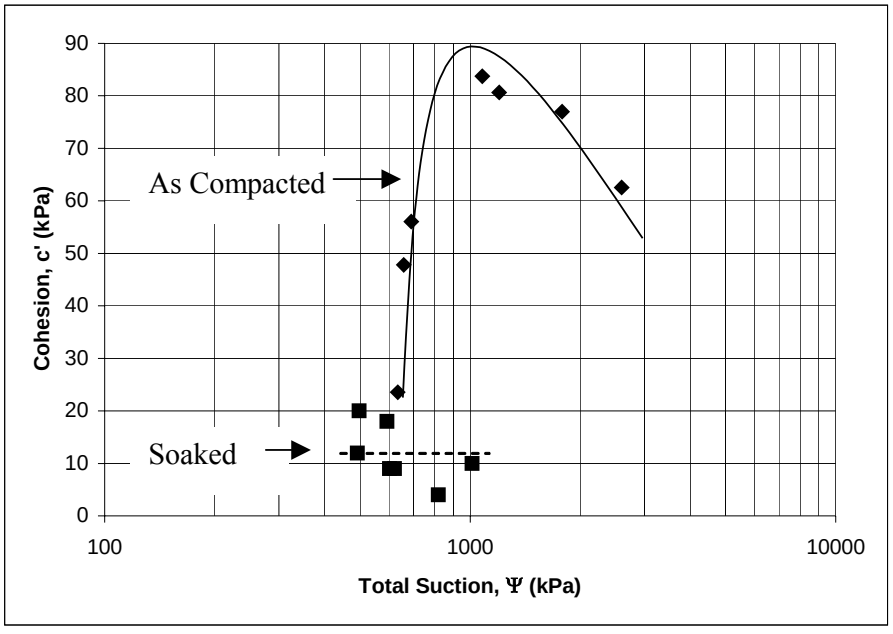

Figure 6.55 Comparison of soaked and as compacted samples' total suction vs cohesion graphs for 75 kPa.

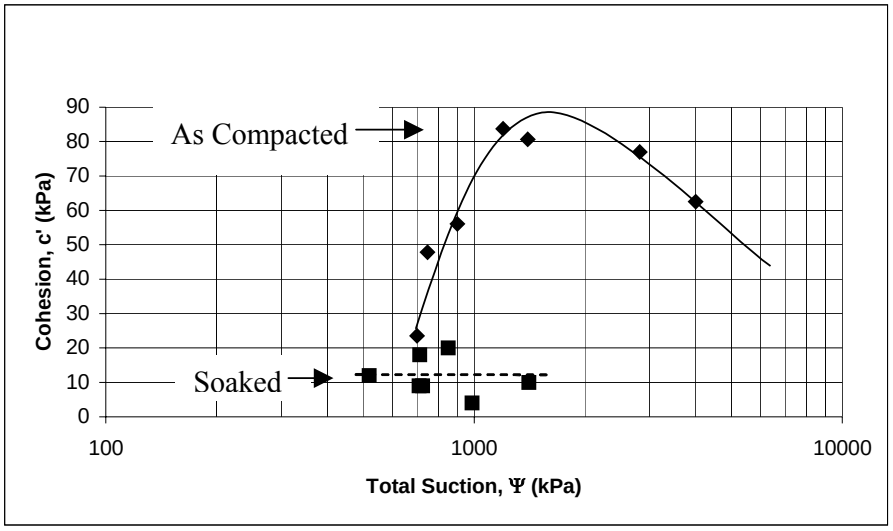

Figure 6.56 Comparison of soaked and as compacted samples' total suction vs cohesion graphs for 150 kPa.

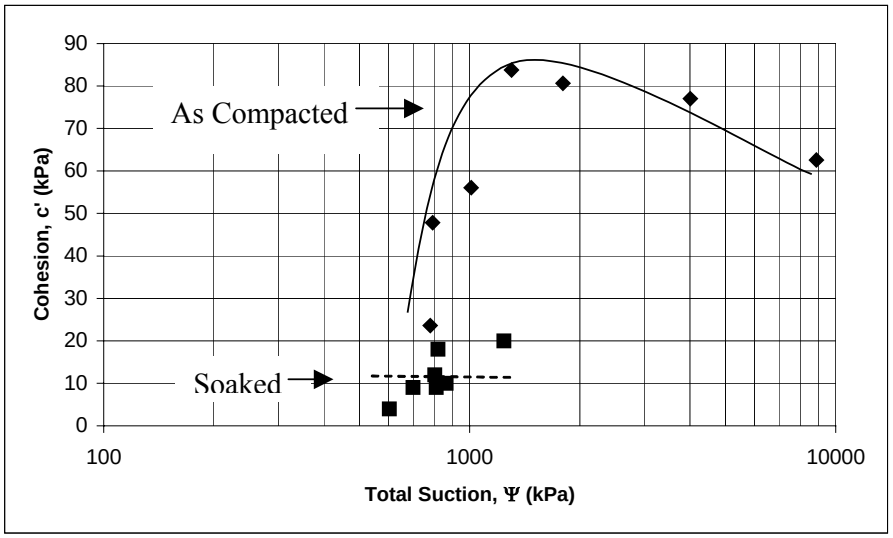

Figure 6.57 Comparison of soaked and as compacted samples' total suction vs cohesion graphs for 225 kPa.

Figures 6.58-6.60 show that, for all normal pressures (for as compacted samples) change in total suction with respect to angle of internal friction shows similar and increasing behavior from wet side to the dry side.

Figures 6.58-6.60 show that Φ' values of compacted samples at the wet side of OMC is close to the Φ' values of the soaked samples.

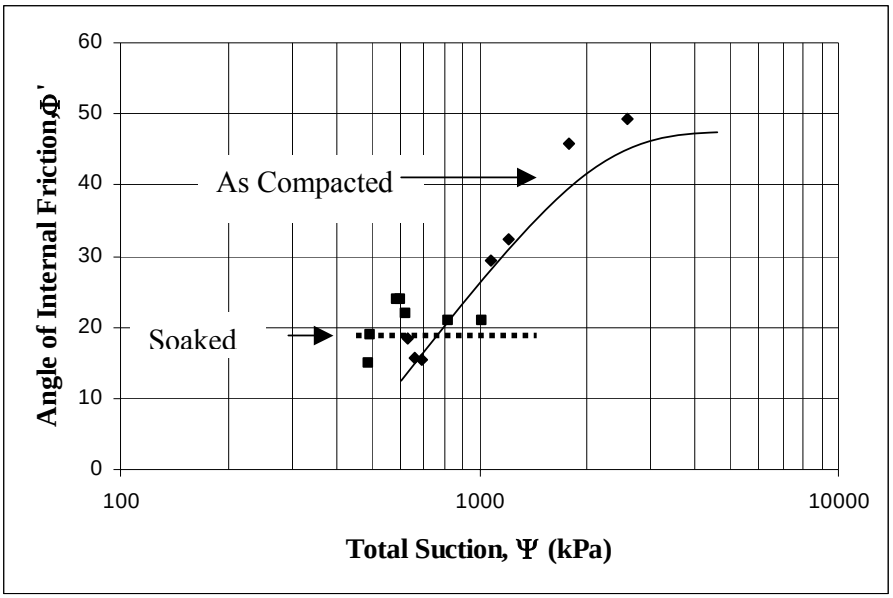

Figure 6.58 Comparison of soaked and as compacted samples' total suction vs angle of shear resistance graphs for 75 kPa.

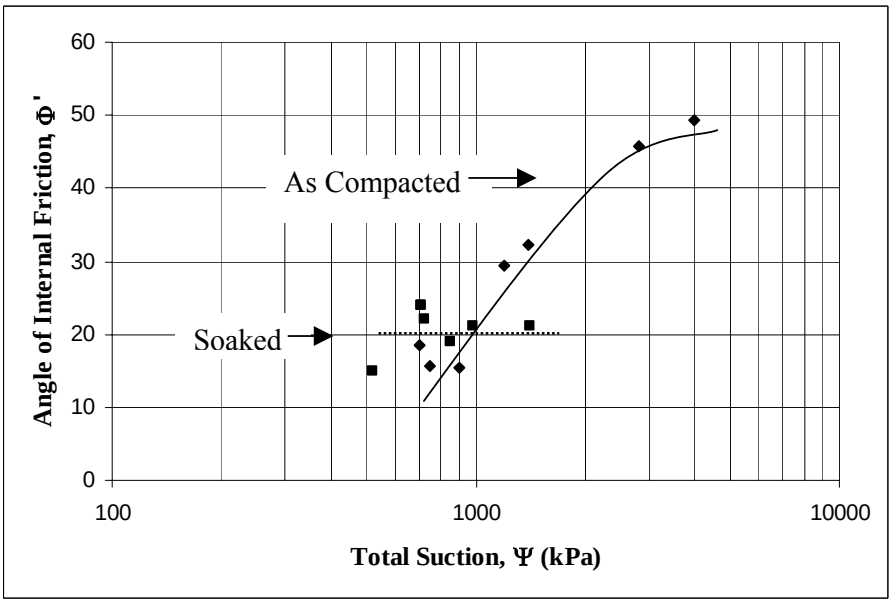

Figure 6.59 Comparison of soaked and as compacted samples' total suction vs angle of shear resistance graphs for 150 kPa.

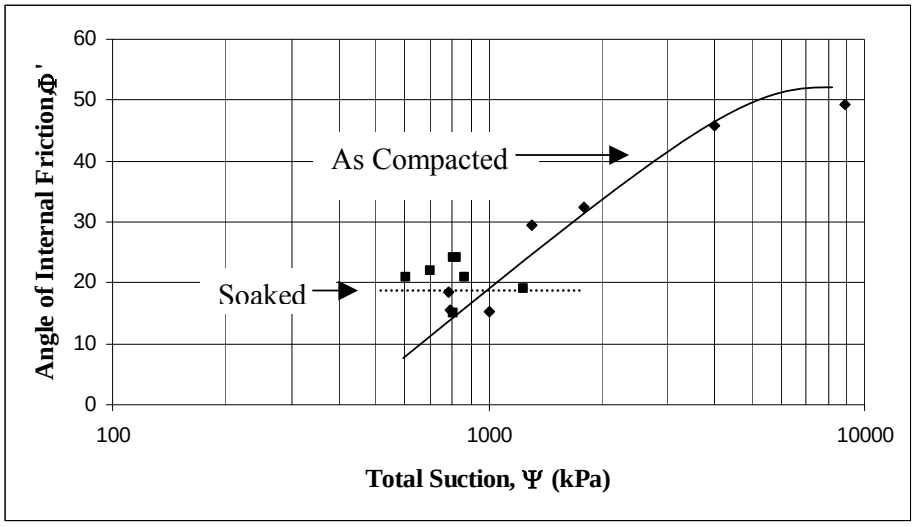

Figure 6.60 Comparison of soaked and as compacted samples' total suction vs angle of shear resistance graphs for 225 kPa.

The shear strength of the compacted samples which are defined as the maximum stress measured in the direct shear tests are plotted against total soil suction on the logarithmic scale as shown in Figure 6.61 (for as compacted samples) for the three normal stress ranges studied and for the soaked samples are given in Figure 6.62.

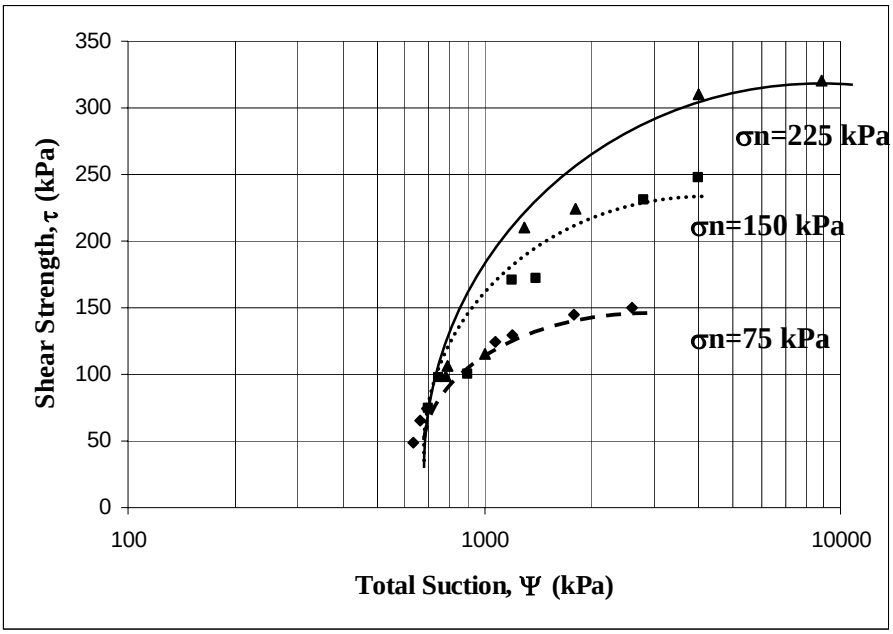

Figure 6.61 Total suction versus shear strength graph for σ_n= 75, 150, 225 kPa

Figure 6.61 shows that, for all normal pressures change in total suction with respect to shear strength shows similar behavior. Towards dry side of OMC, shear strength increases.

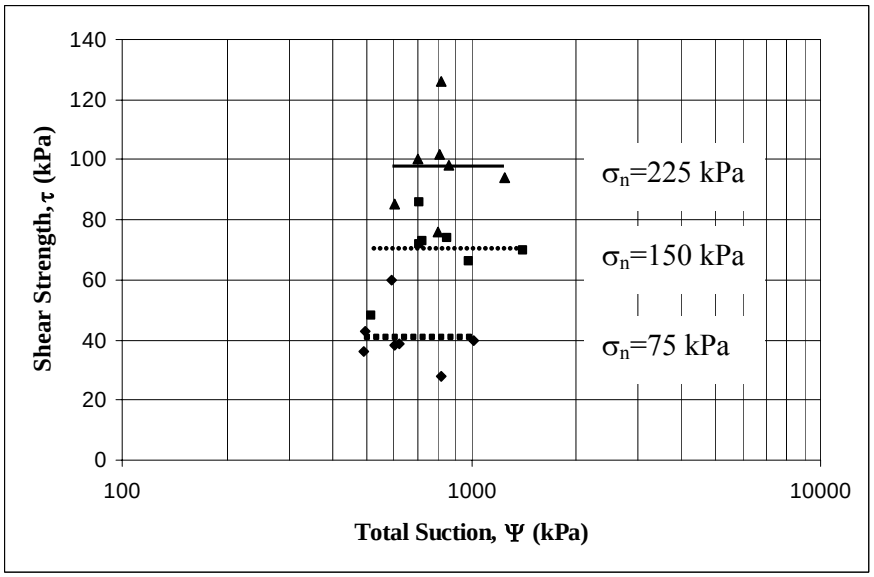

Figure 6.62 Total suction versus shear strength graph for σ_n= 75, 150, 225 kPa for soaked samples

From Figure 6.62 due to soaking, initial moisture content loose its importance for the shear strength and total suction relationship, it can be seen that as normal pressure increase, shear strength increase, too. However, this increase in normal pressure does not effect total suction values.

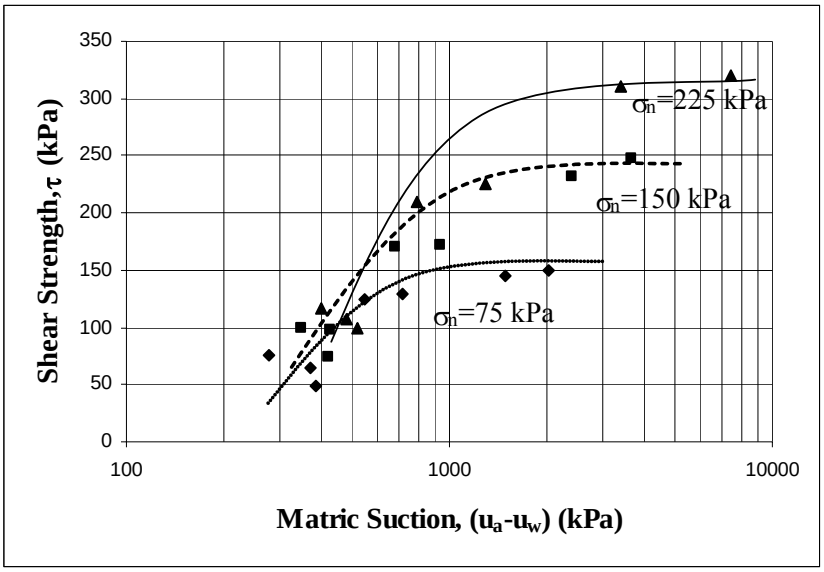

Figure 6.63 Matric suction versus shear strength graph for σ_n= 75, 150, 225 kPa.

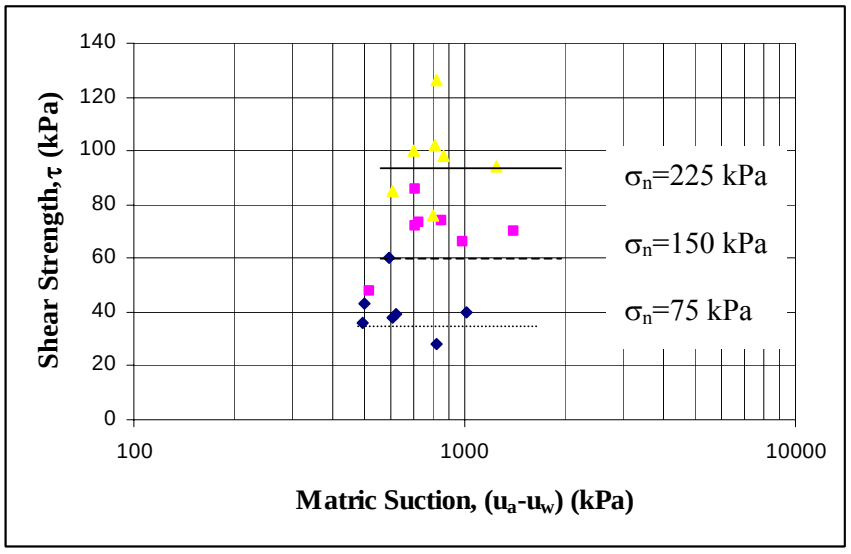

Figure 6.64 Matric suction versus shear strength graph for soaked samples (σ_n= 75, 150, 225 kPa).

CHAPTER 7

CONCLUSION

In this study, effects of compaction moisture content and soaking on the unsaturated shear strength parameters and suction of METU campus clay were investigated. Experiments were done on samples compacted at optimum moisture content (w = 20.8%), at the dry side of optimum (w = 14.8%, 16.8%, 18.8%) and at the wet side of optimum (w = 22.8%, 24.8%, 26.8%). The following conclusions were drawn from the study:

When the sample is soaked cohesion is reduced with respect to sample without soaking.

At the dry side of OMC, as moisture content increases, the cohesion exhibits an increasing trend, after the OMC it drops. For soaked samples cohesion value is almost constant (i.e. 12kPa).

For as compacted samples, Φ' values decrease as moisture content increases. However for soaked samples, it is almost constant (≈22°). On the wet side of OMC both soaked and as compacted samples have Φ' values close to each other.

For undisturbed samples Φ' and c' values are slightly higher when they are compared with remoulded samples which have almost the same inital water content and density. And when undisturbed samples soaked, they again show a behaviour similar to the remoulded samples.

For all normal pressures total, matric and osmotic suction change with water content show similar trend. Matric suction values are close to the total suction values.

The total soil suction increases as the moisture content decreases at the dry side of optimum, and in this range of moisture content the moisture content versus log suction behaviour is linear and after the OMC it has an almost constant value. For soaked samples total suction values changes between 600 – 850 kPa for all normal pressures.

For all normal pressures, at the dry side of OMC cohesion increases as total suction decreases upto OMC, and after OMC, cohesion decreases as total suction decreases. For all soaked samples c' values decrease and give values less than the c' value of the as compacted sample +6% of OMC.

For all normal pressures, at the dry side of OMC angle of internal friction decreases as total suction decreases upto OMC. Φ' values of the compacted samples at the wet of OMC is close to the Φ' values of the soaked samples.

The soil suction (total suction and matric suction affects the shear strength, and an increase in soil suction increases the shear strength.

This study shows the effect of the compaction moisture content (and total suction and matric suction) and soaking on the shear strength parameters (c' and Φ') and shear strength of the soil (shear strength decreases after soaking). Therefore, to properly study the shear strength behaviour of unsaturated compacted soils, tests should be performed on the soil in its ‘as compacted’ condition and after soaking.

REFERENCES

1. AHMED, S., LOVELL, C. W., and DIAMOND, S. (1974), "Pore Sizes and Strength of Compacted Clay", Journal of Geotech. Engineering Division, ASCE, 100, GT4, pp. 407-426.

2. ALONSO, E.E., GENS, A., and JOSA, A., (1990), "A Constitutive Model for Partially Saturated Soils," Géotechnique, Vol. 40, No. 3, pp. 405–430.

3. ARMANGİL, A.F., (1999), Suction – Shear Strength Relationships in Unsaturated Compacted Clays, Ms – Thesis (METU).

4. ASTM D5298-94, (1998) Standard Test Method for Measurement of Soil Potential (Suction) Using Filter Paper, American Society of Testing and Materials. Annual Book of ASTM Standards, pp. 156 – 161.

5. BRACKLEY, I.J.A. (1973), "Swell Pressure and Free Swell in a Compacted Clay", Proc. 3rd Int. Conf. Expansive Soils, Haifa, Vol. 1 pp. 169-176.

6. BRACKLEY, I.J.A. (1975), "A Model of Unsaturated Clay Structure and its Application to Swell Behaviour", Proc. 6th African conf. Soil Mechanics and Foundation Engineering, Durban, vol. 1 pp. 65-70.

7. BULUT R., PARK, S.W., and LYTTON, R.L., (2000), "Comparison of Total Suction Values from Psychrometer and Filter Paper", Unsaturated Soils for Asia, Rahardjo, Toll & Leong (eds), pp. 269 – 273.

8. CHANDLER, R.J., and GUITERREZ C.I., (1986), “The Filter Paper Method of Suction Measurement”, Geotechnique, Vol. 36, No.2, pp. 265–268.

9. CHATTERJI, P.K., and MORGENSTERN N.R., (1989), “A Modified Shear Strength Formulation for Swelling Clay Soils”, Symposium on Physico – Chemical Aspects of Soil, Rock and Related Materials, St. Louis, Missuri.

10. CRONEY, D., COEMAN, J.D. and BLACK, W.P.M. (1958), “Studies of the Movement and Distribution of Water in Soil in Relation to Highway Design and Performance”, HRB spec. Washington D.C. Report 40 pp. 226-250.

11. DELAGE, P., AUDIGUIER, M., CUI, Y.J., and HOWAT ,M.D. (1996), “Microstructure of a Compacted Silt”, Canadian Geotechnical Journal, Vol.33, pp. 150-158.

12. DIAMOND, S., (1970), “Pore Size Distribution in Clays, Clays and Clay Minerals”, Vol. 18, pp. 7-23.

13. ESCARIO, V., and J. SÀEZ. (1986), “The Shear Strength of Partly Saturated Soils”, Géotechnique Vol:36 pp. 453–456.

14. FREDLUND, D.G, MORGENSTERN, N.R, and WIDGER, R.A., (1978), “The Shear Strength of Unsaturated Soils”, Can. Geotech. J., 15, pp. 313 – 321.

15. FREDLUND, D.G. (1997), “An Introduction to Unsaturated Soil Mechanics”, Unsaturated Soil Engineering Practice, ASCE Geotechnical Special Publication No. 68, pp. 1-37.

16. FREDLUND, D.G., and RAHARDJO, H. (1993), Soil Mechanics for Unsaturated Soils, John Wiley & Sons, Inc. pp. 1 – 77, 247 – 258.

17. GAN,J.K.M., FREDLUND,D.G., and RAHARDJO,H., (1988), "Determination of the Shear Strength Parameters of an Unsaturated Soil Using the Direct Shear Test", Can. Geotech. J. 25, pp. 500 –510.

18. GEISER, F., (2000), "Applicability of General Effective Stress Concept to Unsaturated Soils", Unsaturated Soils for Asia, Rahardjo, Toll & Leong (eds), pp. 101– 105.

19. KONG, L.W., and TAN L.R., (2000), "Study on Shear Strength and Swelling – Shrinkage Characteristic of Compacted Expansive Soil", Unsaturated Soils for Asia, Rahardjo, Toll & Leong (eds), pp. 515 – 519.

20. KOS, J., PACOVSKY, J., and TRAVNICEK, R., (2000), "Shear Strength and Swelling of Compacted Partly Saturated Bentonite.", Unsaturated Soils for Asia, Rahardjo, Toll & Leong (eds), pp. 521 – 526.

21. LEONG, E.C., HE L., RAHARDJO, and H. (2002), "Factors Affecting the Filter Paper Method for Total and Matric Suction Measurements", J. Geotechnical Testing, Vol:25, No. 3.

22. LEROUEIL S., and BARBOSA P.S. DE A., (2000), "Combined Effect of Fabric, Bonding and Partial Saturation on Yielding of Soils", Unsaturated Soils for Asia, Rahardjo, Toll & Leong (eds), pp. 527-532.

23. LEROUEIL S., and VAUGHAN P. R. (1990), "The General and Congruent Effects of Structure in Natural Soils and Weak Rocks", Géotechnique, Vol. 40(3), pp.467-488.

24. LING, N.L., and TOLL, D.G., (2000), "Suction and Strength Behaviour of Unsaturated Calcrete", Unsaturated Soils for Asia, Rahardjo, Toll & Leong (eds), pp. 533-538.

25. MANCUSO, C., VASSALO, R., and VINALE, F., (2000), "Effects of Moulding Water Content on the Behaviour of Unsaturated Silty Sand", Unsaturated Soils for Asia, Rahardjo, Toll & Leong (eds), pp. 545 – 550.

26. MICHEALS, A.S. (1959), Discussion to "Physical-Chemical Properties of Soils: Soil – Water Systems", by I. Th. Rosenqvist, ASCE Proceedings Paper 2010.

27. MITCHELL J.K. (1993), Fundamentals of soil behaviour, Wiley & Sons, New York 1993.

28. NISHIMURA, T., and FREDLUND, D.G, (2000), "Relationship Between Shear Strength and Matric Suction in an Unsaturated Silty Soil.", Unsaturated Soils for Asia, Rahardjo, Toll & Leong (eds), pp. 563 – 568.

29. ROSENQVIST, O. TH. (1955), "Physico – Chemical Properties of Soils: Soil Water Systems", Journal of the Soil Mechanics and Foundations Division, Proceedings of the American Society of Civil Engineers, pp.31-53.

30. SEED, H. B., MITCHELL, J.K. and CHAN, C.K. (1961), The Strength of Compacted Cohesive Soils", Conf. Shear Strength of Soils, Colorado, pp. 879-961.

31. SIBLEY, J.W., and WILLIAMS, D.J., (1990), A New Filter Material for Measuring Soil Suction, Geotechnical Testing Journal, Vol:13, No:4 pp. 381 – 384.

32. SRIDHARAN, A., RAO, A.S., MAKAN, S., (1983), "Shear Strength Behaviour of Expansive Clays", Proc. 7th.Asian Conference on Soil Mechanics and Foundation Engineering, Haifa, Vol 1, pp. 80 – 83.

33. SWARBRICK, G.E., (1995), "Measurement of Soil Suction Using the Filter Paper Method", 1st Int. Conf. on Unsaturated Soils, Paris paper no: 246.

34. T.W.LAMBE and R.V.WHITMAN, Soil Mechanics, NewYork:Wiley,1979.

35. TOLL, D.G. (2000), "The Influence of Fabric on the Shear Behaviour of Unsaturated Compacted Soils", Advances in Unsaturated Soils, Geotechnical Special Publication No. 99 American Society of Civil Engineers, pp. 222-234.

36. VANAPALI, S.K., FREDLUND, and D.G., PUFAHL, D.E., "The Relationship Between the Soil – Water Characteristics Curve and the Unsaturated Shear Strength of a Compacted Glacial Till", Geotechnical Testing Journal, GTJODJ, Vol. 19, No. 3 September 1996, pp. 259 – 268.

37. VANAPALI, S.K., FREDLUND, D.G., PUFAHL, D.E, and CLIFTON, A.W., (1996), "Model for the Prediction of Shear Strength with Respect to Soil Suction", Can. Geotech. J .33, pp. 379 – 392.

38. WHEELER, S.J. and SIVAKUMAR, V. (1995), "An Elasto-Plastic Critical State Framework for Unsaturated Soil", Geotechnique; Vol. 45 pp. 35-53.

39. ZEIN,A.K.M. (1985), Swelling Characteristics and Microfabric of Compacted Black Cotton Soil, Phd. thesis, University of Strathclyde, Glasgow.

APPENDIX A

Table A.1 Measurement of soil suction by filter paper – data sheet.

MEASUREMENT OF SOIL SUCTION BY FILTER PAPER - DATA SHEET											
Sample Type		W_{opt}....%	.....kPa	N.S. / S.	W_{opt}....%	.....kPa	N.S. / S.	W_{opt}....%	.....kPa	N.S. / S.	**Tested By:**
Moisture Tin No											H. Pars Tilgen
Top / **B**ottom / **M**iddle Filter Paper		**T** (Tot)	**B** (Tot)	**M** (Mat)	**T** (Tot)	**B** (Tot)	**M** (Mat)	**T** (Tot)	**B** (Tot)	**M** (Mat)	**Test Date:**
Cold Tare Mass, g	T_c										...../...../2003
Mass of Wet Filter Paper + Cold Tare Mass, g	M_1										**Test Date:**
Mass of Dry Filter Paper + Hot Tare Mass, g	M_2										...../...../2003
Hot Tare Mass, g	T_h										**Test Date:**
Mass of Dry Filter Paper, g (M2 - Th)	M_f										...../...../2003
Mass of Water in Filter Paper, g (M1 - M2 - Tc + Th)	M_w										**Temperature:**
Filter Paper Water Content, % (Mw/Mf)	**w**										C
Suction	**h**										